EXPLORING SYNTHETIC FUNCTIONAL DNA MOLECULES FOR BIOSENSOR DEVELOPMENT

EXPLORING SYNTHETIC FUNCTIONAL DNA MOLECULES FOR BIOSENSOR DEVELOPMENT

By

Kha Tram

B. Sc. Brock University, St. Catharines, Ontario, 2008

M. Sc. Brock University, St. Catharines, Ontario, 2010

A Thesis

Submitted to the School of Graduate Studies

In Partial Fulfillment of the Requirements

For the Degree

Doctor of Philosophy

McMaster University

DOCTOR IN PHILOSOPHY (2015) McMaster University

(Chemical Biology) Hamilton, Ontario

TITLE: Exploring Synthetic Functional DNA Molecules for Biosensor Development

AUTHOR: Kha Tram, M. Sc., B. Sc. (Brock University)

SUPERVISOR: Dr. Yingfu Li

NUMBER OF PAGES: XVIII, 129

Abstract

The development of the *in vitro* selection technique permits the creation of synthetic DNA molecules with ligand-binding capabilities (DNA aptamers), or abilities to catalyze chemical reactions (DNAzymes), or both (aptazymes). Significant research efforts in this field over the past two decades have led to the creation of a large array of DNA aptamers and DNAzymes and ever-increasing interests in taking advantage of these molecular species for diverse applications. One area of remarkable potential and development is the exploration of functional DNA molecules for bioanalytical applications. The work described in this dissertation aims to pursue innovative concepts and technologies that expand utility of functional DNA molecules for biosensing applications. I have focused on two functional DNA species: RNA-cleaving DNAzymes and protein-binding DNA aptamers. My key interest is to develop simple but effective colorimetric assays that employ these functional DNA molecules and to establish an effective strategy that makes functional DNA biosensors highly functional in biological samples.

My first research project focuses on the development of a simple colorimetric detection platform that takes advantage of RNA-cleaving DNAzyme probes. The key goal is to develop a simple test that is suited for point-of-care applications. This test should be easy to use, cost-effective, able to produce a sharp color change, has broad target applicability, and does not require expensive equipment. I have developed a platform technology that employs magnetic beads immobilized with an aptazyme-urease conjugate where the RNA-cleaving aptazyme serves as molecular recognition element,

urease functions as signal transducer, and magnetic beads mediate the translation of the aptazyme action to the activity of urease. In the presence of the target of interest, the aptazyme cleaves the RNA linkage, liberating urease from beads into solution. The released urease can then be used to hydrolyze urea, resulting in significant pH increase that can be easily detected using litmus dyes or papers. To prove the concept, I have developed a litmus test for the detection of *Escherichia coli* (*E. coli*) using an *E. coli*-specific RNA-cleaving aptazyme previously reported by our laboratory. However, this technology can be used for any target for which an RNA-cleaving aptazyme can be created.

My second project aims to solve a critical issue faced by RNA-cleaving DNAzyme biosensors: their vulnerability with biological samples. Since all biological samples contain RNases that can efficiently hydrolyze RNA and all efficient RNA-cleaving DNAzymes utilized for biosensor development use RNA substrates that are susceptible to RNases, we must develop an effective strategy to overcome the issue of RNA degradation by RNases. My strategy was to switch the RNA substrate from its natural D-configuration to its mirror image L-configuration, which is known to be completely inert to RNases. For this reason, I have developed a highly efficient DNAzyme that cleaves a chimeric DNA/RNA substrate that contains a single L-RNA unit as the cleavage site. Interestingly, I have discovered that this DNAzyme uses a functionally essential kissing loop to engage the substrate, a structural motif that has never been observed any D-RNA-cleaving DNAzymes. I have also engineered a stimuli-response aptazyme using our new L-RNA-cleaving DNAzyme and a well-studied ATP-

binding DNA aptamer, and have demonstrated that this aptazyme is fully functional in human serum, a complex sample matrix with strong RNA-degrading activity.

The final project of my work concerns the exploration of an unexpected observation for biosensing applications. It has been known that certain DNA polymerases, such as phi29 DNA polymerase, can make round-by-round copying of a circular single-stranded DNA template, producing extremely long single-stranded DNA molecules with repetitive sequence units. This process is widely known as rolling circle amplification or RCA. It represents an excellent DNA amplification strategy that is very attractive for point-of-care or field applications because RCA can be conducted isothermally without a thermal cycler. Interestingly we have observed that when a protein-binding DNA aptamer is incorporated into a circular DNA template, the protein target for the aptamer can arrest the RCA process. I have subsequently devised a colorimetric assay that exploits this novel observation for the detection of two different protein targets: human thrombin and platelet-derived growth factor (PDGF).

In summary, I have investigated novel ways to productively explore synthetic functional DNA molecules for biosensor development. Each strategy I have developed can be further expanded for targets beyond what I have used in my studies, namely *E. coli*, ATP and thrombin and PDGF. For example, the litmus test demonstrated for *E. coli* detection can be easily extended to the detection of other targets through the use of other ligand-responsive RNA-cleaving DNAzymes. With our ability to develop functional DNA probes for virtually any target of interest, I hope my work serves a springboard for

the development of practical DNA aptamer/DNAzyme biosensors that can eventually improve our quality of life.

To my teachers who gave me knowledge: Mrs. Adams, Mrs. Dean, Ms. Tiberio

To my mentors who gave me wisdom: Gabor Katai, Tony Yan, Yingfu Li

And to my parents who told me to use it.

Acknowledgements

These past four years at McMaster University have created experiences that I will remember for the rest of my life, both professionally and personally. Even with all its ups and downs, I have learned a great deal and owe my appreciation to many.

I'd like to first express my gratitude to my supervisor, Dr. Yingfu Li. Under his guidance, I was given many opportunities to work on my weaknesses and develop my skills through writing journal articles, attending conferences, and mentoring students. His frequent and spontaneous suggestions of new project ideas are often filled with quirky enthusiasm and spirit. It is not only a constant reminder of why we do science, but also how we should do it – with passion.

In addition, I would also like to thank my committee members, Dr. Fred Capretta and Dr. John Brennan, for their support, constructive criticisms, and suggestions during our meetings.

I would also like to thank my peers and friends in the Li Lab. Our coffee breaks and lengthy impromptu discussions have been both insightful and entertaining. I am privileged to have formed these relationships that have supported me throughout my time here.

Last but not least, I would like to acknowledge my parents for their love and support. They have given me an opportunity to create a great life so long as I work hard and stay grounded.

Table of Contents

List of Figures

Chapter 1

Chapter 2

List of Tables

List of Abbreviations

ATP	adenosine 5'-triphosphate
AuNPs	gold nanoparticles
BSA	bovine serum albumin
CEM	crude extracellular mixture
CNT	carbon nanotubes
DABCYL	4-(4-dimethylaminophenylazo)benzoic acid
dATP	deoxyadenosine 5'-triphosphate
dCTP	deoxycytidine 5'-triphosphate
dGTP	deoxyguanosine 5'-triphosphate
ddH2O	double-distilled water
$DiSC_2(5)$	diethylthiadicarbocyanine
DMSO	dimethyl sulphoxide
DNA	deoxyribonucleic acid
DNAzyme	deoxyribonucleic acid enzyme
dNTPs	dATP, dTTP, dGTP and dCTP
dTTP	deoxythymidine 5'-triphosphate
dsDNA	double stranded DNA
EDTA	ethylene diamine tetraacetic acid
FNA	functional nucleic acid
GO	graphene oxide
GNR	gold nanorods

LRD	L-RNA-cleaving DNAzyme
MB	magnetic bead
MBS	maleimidobenzoic acid N-hydroxysuccinimide ester
MRE	molecular recognition element
NAE	nucleic acid enzymes
nt	nucleotide
PAGE	polyacrylamide gel electrophoresis
PDGF	platelet-derived growth factor
φ29DNAP	phi29 DNA polymerase
PNA	peptide nucleic acid
PNK	T4 polynucleotide kinase
RCA	rolling circle amplification
RCAP	rolling circle amplification product
RNA	ribonucleic acid
SELEX	systematic evolution of ligands by exponential enrichment
ssDNA	single stranded DNA

Chapter 1

Introduction to Functional Nucleic Acids and Biosensors

1.1 Nucleic acids: beyond genetic storage

Nucleic acids are the genetic blueprint for all life on Earth. It is responsible for storing and passing on critical information from one generation to the next. This hereditary material was first recognized for its passive role in faithfully transferring the template of life, as it is the starting point of molecular biology's central dogma. However, with the discovery of RNA molecules that are capable of catalyzing reactions at a rate comparable to that of protein enzymes,[1,2] many believed that this would change how we fundamentally perceive nucleic acids.[3] DNA and RNA molecules functioning beyond their intended role as genetic carriers have shaped our understanding of modern biology.

In the 1990s, pioneering research for probing DNA or RNA molecules that can serve purposes beyond information storage has led to the development of a technique known as *in vitro* selection or SELEX (Systematic Evolution of Ligands by Exponential Enrichment).[4-6] It is a combinatorial approach that begins with a large randomized library of $10^{14} – 10^{16}$ DNA or RNA molecules. These pools of sequences are subjected to successive rounds of selection whereby sequences that express the desired function are enriched while inactive sequences are discarded (Figure 1-1). The result of this 'test-tube evolution' approach will favor synthetic molecules that can either catalyze chemical

reactions (termed DNAzymes or ribozymes) or function as molecular receptors (aptamers). Collectively, these unique molecules are referred to as functional nucleic acids (FNAs).

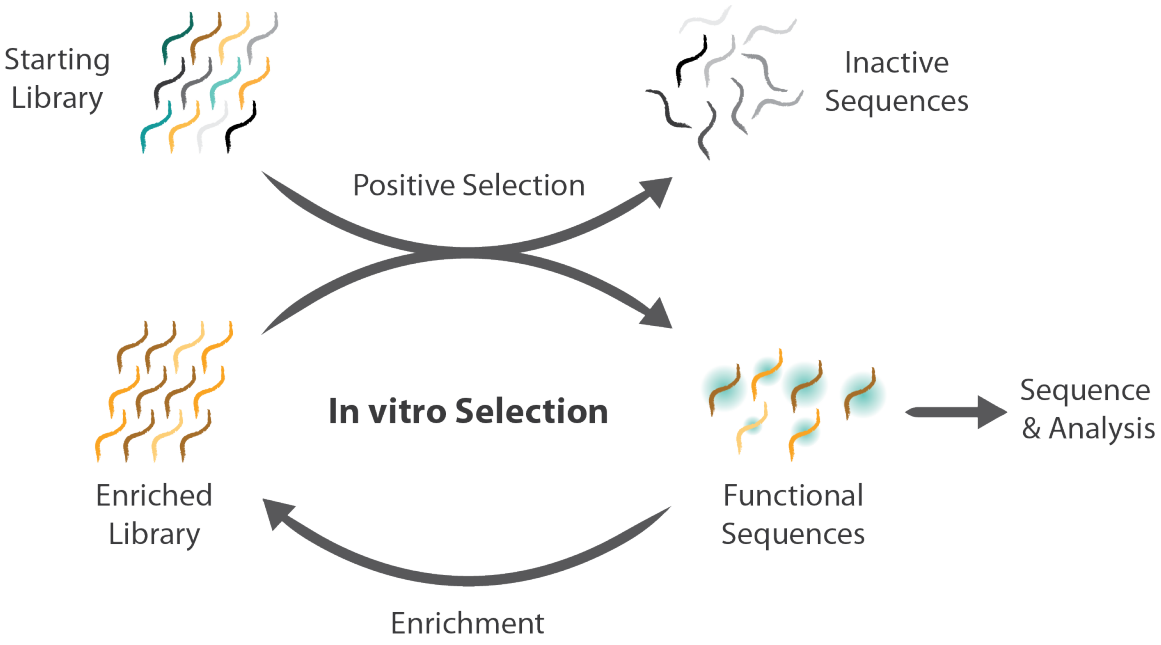

Figure 1-1. In vitro selection scheme. A starting library of 10^{14} – 10^{16} unique sequences is subjected to a positive selection step to isolate a sequence with a desired function. The inactive sequences are removed from the system while the favored sequences are enriched. This process is repeated until the library is sequenced. The sequences are then chemically synthesized and tested for activity.

The invention of *in vitro* selection has led to the generation of many FNAs with fascinating properties. It has sparked the interest of the scientific community and has recruited researchers from different disciplines to answer various fundamental questions ranging from the origins of life to chemistry and biology. The contributions made by

these communities have been very productive over the past 25 years. We have witnessed the discoveries of several naturally occurring ribozymes and RNA aptamers[7-10] (e.g. riboswitches) in biology and the discovery of a substantial number of man-made FNAs. Also during this time, significant efforts were made towards employing FNAs to a broad spectrum of applications, most notably in therapeutics and biosensing.

FNAs have increasingly been explored for developing therapeutics and biosensors for several reasons. First, FNAs are chemically synthesized. This process is readily scalable, produces excellent batch-to-batch consistency, and eliminates biological contaminations from viruses and bacteria. Second, FNAs can be chemically modified to increase their stability and bioavailability. Introducing functional groups also allows access to interesting conjugation chemistries such as linking nucleic acids to small molecules (dyes, carbohydrates, amino acids), proteins, and various nanomaterials. Third, they are non-immunogenic. Lastly, FNAs are stable at high temperatures and are able to refold into its native structure. These attractive features offered by FNAs are the principal motivation behind many innovative FNA-based therapeutics and FNA-based biosensors.

From a pharmaceutical perspective, developing FNA-based therapeutics are inherently challenging due to poor pharmacokinetics and delivery mechanisms. Consequently, very few candidates have been made into drugs. Regardless, the optimism for developing FNA-based therapeutics continues to be high and several review articles and books detail the progress made thus far.[11-14] In this thesis, I will focus on FNA-based biosensors. The field of biosensors has been extremely fruitful and has grown to be

a multi-billion dollar industry. However, there are still areas of deficiencies that need to be addressed. FNA-based biosensors have emerged as a new player in the field of diagnostics and have the potential to further contribute to this exciting subject. In the following chapters, I will outline the significance and impact of traditional biosensors and why so much research effort has been invested in this particular area. I will discuss the current trends, progress, and deficiencies in the current state of biosensors and how they can be resolved using FNA.

1.2 Biosensors

1.2.1 History of traditional biosensors

Biosensors are analytical devices that rely on a biological component for the detection of a specific analyte. Leland Clark first conceptualized this idea in 1962 with the world's first biosensor described as "enzyme electrode".[15] The prototype used an oxygen electrode to detect the electrochemical signal generated by a thin layer of immobilized glucose oxidase. Although this invention was initially developed to monitor oxygen in blood during surgery, what Clark also observed was that the concentration of glucose was decreasing in proportion to oxygen levels.[16] He had inadvertently created a method to monitor glucose. Following this, Yellow Springs Instrument Company made this technology commercially available in 1975. Medisense later brought this technology to market in 1987 under the name "ExacTech Glucose Meter" as a personal point-of-care device.[17] The glucose biosensor system today is a staple point-of-care device and

accounts for the largest stake in the biosensor market.[18] The discovery of this biosensing platform laid the foundation for exploring alternative biological components to recognize different analytes. One such component is antibodies.

Two decades after the discovery of the enzyme electrode, optical transducers were coupled with antibodies to create a subfield known as bioaffinity sensors. It is believed that these immunosensors pioneered a new generation of biosensing technology.[18] This category of biosensor was far more sophisticated and costly. These instruments were originally designed to rapidly measure complex biological interactions in a high-throughput manner. They were not engineered for personal use. Consequently, the field of biosensors can be broadly categorized into two types of design: 1) simple - portable devices that could be operated by non-specialists; 2) complex - highly sensitive instruments used for screening. The glucose biosensor is a great example of a simple system that has revolutionized personal medical assistance for monitoring diabetes. Conversely, bioaffinity sensors that uses equipment based on surface plasmon resonance to probe antibody-antigen interactions are examples of a complex system that are utilized only in research laboratories. Nevertheless, the invention of the enzyme electrode and bioaffinity assay was a major step forward. Both technologies, each offering their own specific advantages, have been miniaturized to allow in-home testing. They have contributed tremendously to the success of biosensors and have captured the attention of major diagnostic companies.

1.2.2 Limitations of traditional biosensors

Demand for biosensor technology has been steadily rising every year and this growth is reflected in the global biosensor market (Figure 1-2).[19] Collaborative efforts made by research institutions, universities, and various industrial sectors strive to develop more advanced biosensors that are highly accurate, sensitive, and portable. As a result, biosensing technologies have begun to penetrate other markets aside from medical point-of-care devices. The next generation biosensors have been increasingly adopted into various sectors such as environmental monitoring, biodefense, food quality control and other processing industries (Figure 1-3).[19] As the diversity of the market continues to expand, biosensors are faced with new challenges of targeting more complex analytes sensitively and accurately.

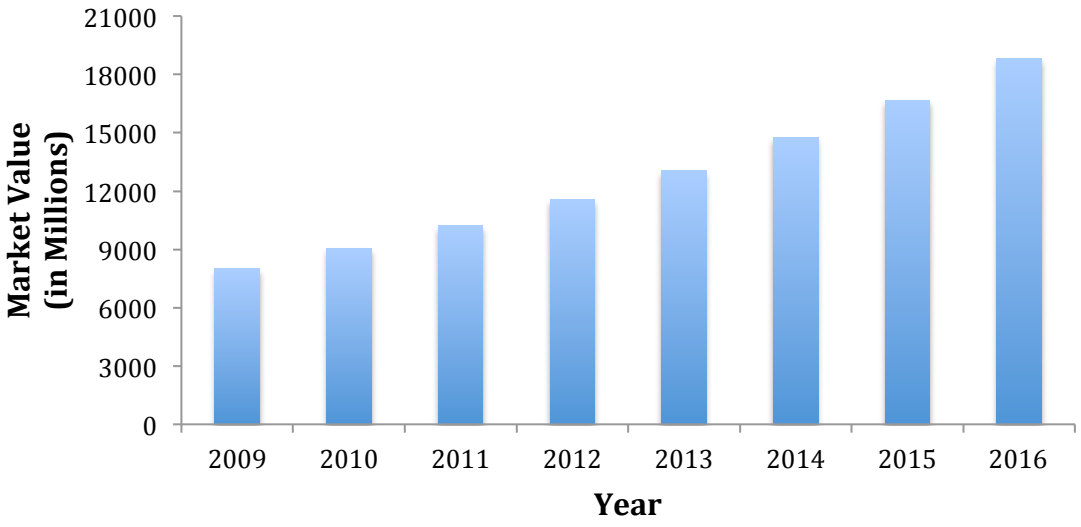

Figure 1-2. Total current and predicted market value of the biosensors

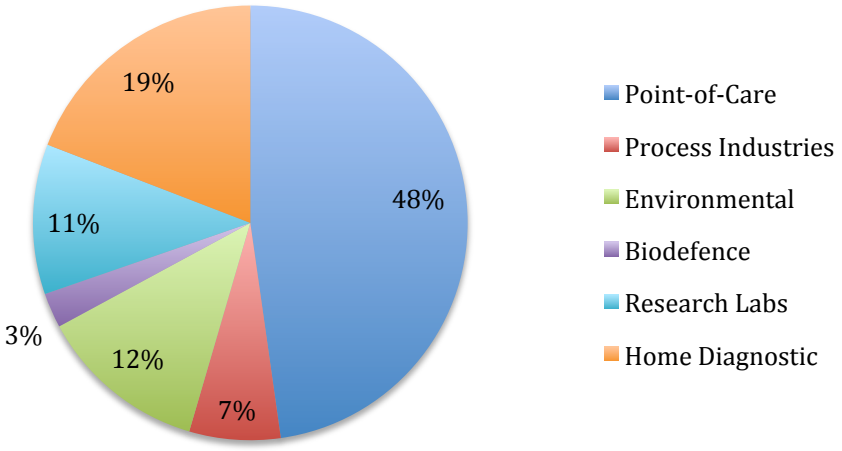

Figure 1-3. Market distribution of the biosensor industry

To date, the majority of commercially available biosensors utilize proteins as their biological component for catalysis or recognition.[20] This proven model continues to be a major driving force for new biosensor development. However, relying on protein enzymes and antibodies comes with limitations. Enzymes are evolved biological machineries that are limited to their cognate ligand. Consequently, this leaves very little room for adaptability and modifications. Alternatively, antibodies are more flexible because they can be isolated to target new analytes. However, the process of isolating antibodies is expensive and difficult to scale for mass production.[21] Even with current advances to enhance stability, reduce cost, and optimize production of protein-based biosensors, there is a need for alternative biological platforms that could fulfill the demands of this rapidly growing sector. One such alternative is Functional Nucleic Acids.

1.2.3 FNAs as an alternative to antibodies and enzymes

Over the past decade, there has been a paradigm shift in biotechnology, particularly in biosensor development. The most successful biosensors to date rely on using proteins, however in the past few years, we have seen more intensive uses of FNAs. Every year, the number of research publications for FNA-based biosensor continues to grow (Figure 1-4).[18] There are major efforts being made towards understanding the fundamental structure of FNAs and how they could be used to replace proteins for developing biosensors. Currently, the FNA equivalent of protein enzymes and antibodies are DNAzymes (or ribozyme if it is composed of RNA) and aptamers, respectively. Although FNA-based biosensors are still in its infancy, researchers are beginning to understand how to manipulate and modify FNAs to engineer the most ideal biosensor.

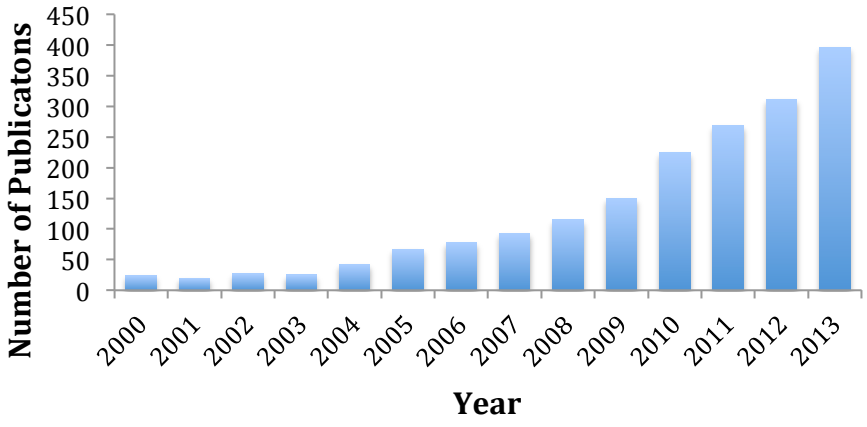

Figure 1-4. Number of related functional nucleic acid sensor publications. PubMed search for: (Sensor AND Biosensor) AND (deoxyribozymes OR ribozyme OR DNAzyme OR aptamer OR aptazyme)

1.3 Exploring functional nucleic acids for developing biosensors

1.3.1 Nucleic acid enzymes

A diverse number of nucleic acid enzymes (NAEs) have been isolated from *in vitro* selection experiments. The starting libraries for these experiments can be made of either DNA or RNA. However, there is a growing interest in using DNA over RNA for creating biosensors. From the perspective of stability, DNA is chemically more stable than RNA due to the lack of a 2′-OH. The presence of a 2′-OH in RNA can spontaneously undergo hydrolysis. Consequently, biosensors that rely on RNA-based NAE will have limited shelf life. Although loss of this 2′-OH may seem to restrict the functionality of a DNA-based NAE, a substantial number of existing DNA-based NAE have proven to be as effective as their RNA counterparts. This is due to structural and chemical similarities that DNA and RNA share. Similar to RNA, DNA is capable of forming intricate tertiary structures through hydrogen bonding, charge-charge and π-stacking interactions. With so few negative drawbacks from using DNA over RNA, future biosensors that consider adopting NAE for engineering biosensors should preferentially use DNA-based enzyme if possible.

Current DNA-based NAEs, also referred to as DNAzymes, have been isolated to carry out a wide array of chemical transformations, some of which are listed in Table 1-1. Among them, the RNA-cleaving DNAzymes have been broadly explored for developing biosensors. There are a few reasons why RNA-cleaving DNAzymes are the preferred catalyst over other NAEs. First, the RNA transesterification reaction carried out by

DNAzymes has been extensively studied over the past 20 years. Their structural and catalytic properties are well characterized. As a result, the available information on this class of DNAzymes significantly facilitates biosensor development. Second, the rates of RNA cleavage performed by these DNAzymes are among the best of all chemical reactions catalyzed by NAEs. One of the key traits of an ideal biosensor is to generate results as quickly as possible, thus, a faster catalyst is able to process more substrates, which results in a quicker response time. Lastly, RNA cleavage results in two shorter strands that can be easily monitored using various separation techniques. The mechanism of two departing strands can be coupled to various transduction platforms to generate an electrochemical, colorimetric, or fluorescent signal.

Table 1-1. Artificial FNA catalysts

Artificial Ribozymes	
Reactions Catalyzed	Reference
RNA cleavage	[22-24]
RNA ligation	[32-35]
RNA branching	[39]
RNA phosphorylation	[42,43]
RNA capping	[45-47]
RNA polymerization	[49]
Diels-Alder	[52-54]
Amino acylation	[56-58]
Peptide formation	[60]
Porphyrin metalation	[62]

Artificial Deoxyribozymes	
Reactions Catalyzed	Reference
RNA cleavage	[25-31]
RNA ligation	[36-38]
RNA branching	[40,41]
DNA phosphorylation	[44]
DNA capping	[48]
DNA ligation	[50,51]
DNA deglycosylation	[55]
Thymine dimer repair	[59]
Phosphoramidate cleavage	[61]
Porphyrin metalation	[63]

1.3.2 RNA-cleaving DNAzymes

Given nucleic acids' natural affinity for metal ions, many early RNA-cleaving DNAzymes rely these cofactors to accelerate the transesterification reaction. Thus, a wide

variety of RNA-cleaving DNAzymes have been isolated through *in vitro* selection to respond to different metal cofactors (Table 1-2). From a historical perspective, the first catalytic DNA isolated was a Pb^{2+}-dependent RNA-cleaving DNAzyme by the Joyce group in 1994. After five cycles of *in vitro* selection, a DNA sequence that could cleave the RNA with a rate enhancement of 10^5 over the uncatalyzed reaction was isolated. From Figure 1-5A, the DNAzyme makes two point of contact with the substrate through the formation of two short helical motifs that flank the cleavage site. The remaining 15-nucleotide loop between these two binding sites facilitate the RNA cleavage reaction with a turn-over rate of 1 min^{-1}. Since then, a variety of DNAzymes have been isolated to cleave RNA substrates, or chimeric DNA-RNA substrates under a wide range of conditions.[25,29,64-67]

Table 1-2. Cofactors for RNA-cleaving DNAzyme

Metal Ion Cofactors	Reference
Pb^{2+}	[22,25,68]
Mg^{2+}	[23,29,30]
Ca^{2+}	[64]
Zn^{2+}	[26]
Cu^{2+}	[44]
Co^{2+}	[69,70]
Mn^{2+}	[67]
UO^{2+}	[71]
Hg^{2+}	[72,73]
Cd^{2+}	[73]
Ce^{3+}	[74]
Nd^{3+}	[75]

With the demonstration of DNA cleaving a single ribonucleotide in an all DNA substrate, the Joyce group followed up with a DNAzyme that could cleave an all-RNA substrate under physiological conditions.[30] Isolating DNAzymes that could function under these conditions would have applications in RNA centered therapeutics or developing biosensors for targeting RNA substrates. By slightly modifying their previously established protocol, two classes of DNAzymes were isolated with distinct structural features. These two DNAzymes were named 8-17 and 10-23 after the 8^{th} and 10^{th} cycle of *in vitro* selection, respectively, and the second number represented their cloned isolates (Figure 1-5B, C). These DNAzymes have been very well studied ever since. Under physiological conditions, 10-23 was able to cleave any RNA substrate that contains a cleavage site with a purine-pyrimidine junction. Many variants of 10-23 have been made to target messenger and viral RNA targets.[76] The second DNAzyme that was isolated from the same selection experiment, 8-17, has proven to be a versatile catalyst for biosensor development. Mutagenesis and structural analysis of 8-17 revealed a catalytic core that consists of a small 3-base pair stem and 8 conserved nucleotides. 8-17 has been well documented in literature because it was isolated in multiple independent *in vitro* selection experiments.[77,78] The coincidental isolation of the same 8-17 motif suggests that this could be the simplest structure for DNA to cleave RNA.

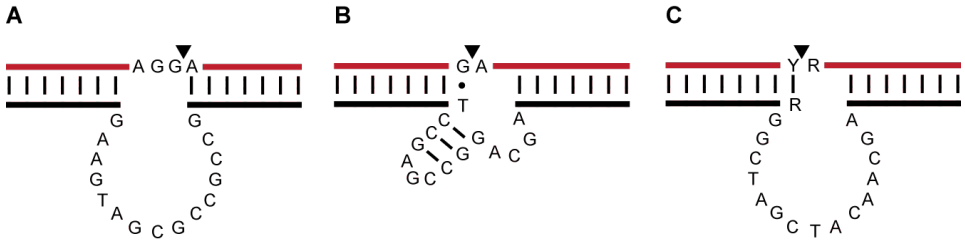

Figure 1-5. RNA-cleaving DNAzymes. A) The first Pb^{2+}-dependent DNAzyme; B) the "8-17" DNAzyme C) the "10-23" DNAzyme. The filled triangle represents the cleavage site, the R is purine-based nucleotide, and Y is a pyrimidine-based nucleotide.

1.3.3 Other RNA-cleaving DNAzymes

Biochemical studies of the RNA cleavage reaction play an integral part of understanding the versatility and utility of this chemical transformation. Uncovering alternative mechanisms for RNA cleavage will not only provide more options for engineering biosensors, but also give greater insight into the full potential capabilities of nucleic acid catalysts as a whole. Early examples of RNA-cleaving DNAzymes have relied on divalent metal ion cofactors to facilitate catalysis. To investigate if RNA cleavage could be performed without any divalent metal ions, the Perrin group appended imidazoles and amines directly to DNA in order to mimic RNase A activity, a protein enzyme that cleaves RNA without any cofactors.[79] This resulted in a His-dependent DNAzyme that was able to cleave an RNA substrate with a catalytic rate of 0.045 min^{-1}. Even though RNA cleavage was carried out in the absence of metal ions, the reaction still required additional assistance, in this case by imidazoles, to facilitate the transesterification reaction.

In a recent study by the Holliger group, four synthetic nucleic acid-derived polymers (termed XNA) were used for *in vitro* selection of RNA cleavage.[80] As illustrated in Figure 1-6, the FANAzyme, ANAzyme, HNAzyme, and CeNAzyme, were capable of cleaving RNA with a catalytic rate of 0.058 min^{-1}, 0.0012 min^{-1}, 2.2×10^{-5} min^{-1}, and 1×10^{-4} min^{-1}, respectively. From an academic perspective, these XNAzymes have major implications for defining the chemical boundaries that may have existed during the emergence of life on earth. The theory for the origins of life named RNA as the principal genetic polymer for the first catalyst. However, under different circumstances, it is hypothesized that alternative biopolymers other than RNA could function as the catalyst in the key transition for the origin of life. Nevertheless, use of nucleic acid-derived biopolymers to mimic the RNA cleavage reaction continues to broaden the scope of biosensor development. Modifications of nucleic acids are routinely introduced to enhance chemical stability and functional effectiveness, however, using a completely different biopolymer that can go through the rigorous process of *in vitro* selection can be an exciting new area of research for applications in diagnostics.[81]

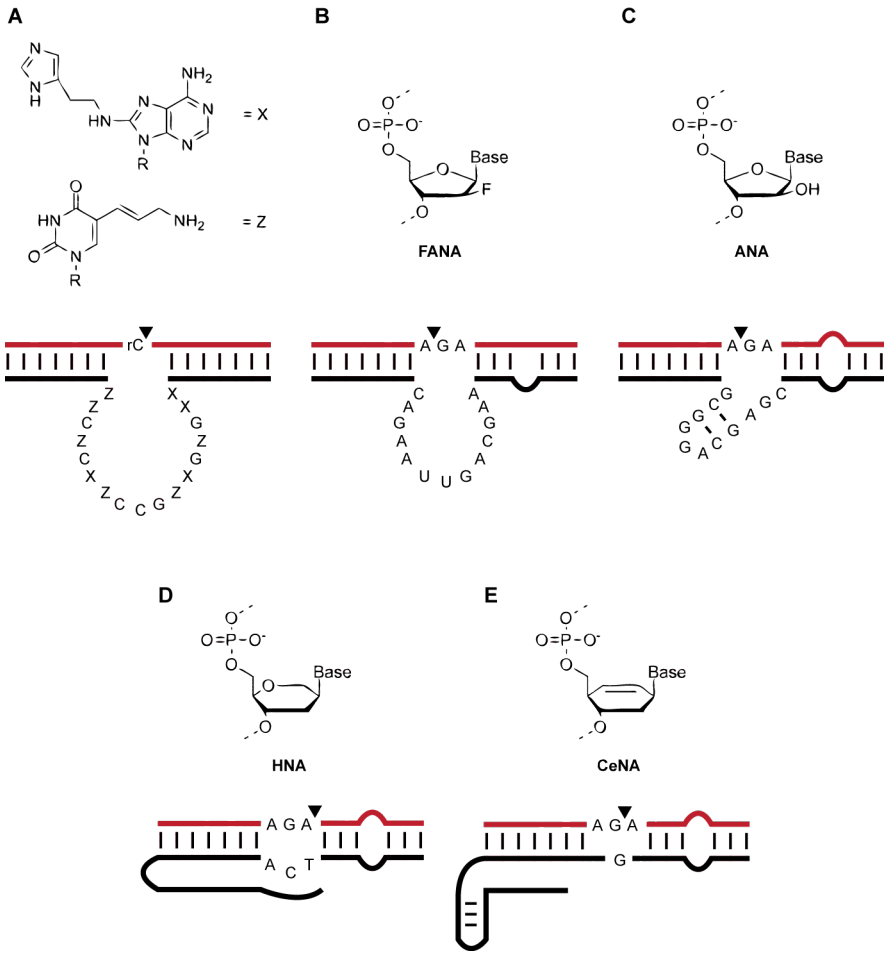

Figure 1-6. Modified RNA-cleaving DNAzymes. Cleavage of RNA using A) covalently bound histidines and amines; B) Fluoro-arabinonucleic acid; C) arabinonucleic acid; D) 1,5 anhydrohexitol nucleic acid; E) cyclohexenyl nucleic acid.

Other areas of interest are to probe the mechanisms of RNA cleavage. Most DNAzymes that cleave RNA follow a common reaction mechanism.[77,82,83] Catalysis is initiated with a nucleophilic attack by the 2′-hydroxyl group of ribose to the neighboring phosphodiester bond. This results in a 2′, 3′-cyclic phosphate and a free 5′-hydroxyl terminus. In an effort to study the mechanisms of RNA cleavage, the Silverman

group selected for a DNAzyme that could cleave RNA through hydrolysis instead of transesterification.[84] Hydrolysis of RNA involves an attack of a water molecule to the phosphodiester bond, creating a 5′-phosphate end and a 3′-OH terminus (Figure 1-7). When compared to the mechanisms of transesterification, RNA hydrolysis is considered a highly unfavorable reaction.[85,86] However, under stringent *in vitro* selection conditions, the 5′-phosphate product generated by hydrolysis can be captured through a ligation reaction. These sequences were then enriched in subsequent rounds, favoring hydrolysis over transesterification. Although DNAzymes that rely on hydrolysis were not as efficient as the ones that underwent transesterification, understanding every aspect of RNA cleavage presents new opportunities for developing biosensors that can operate within its most optimal context. In this case, the result of a 5′-phosphate is unique and can be utilized by enzymes such as T4 DNA ligase. Engineering biosensors that can take advantage of this mechanism could be particularly useful and could extend to any platforms or enzymes that relies on a 5′-phosphorylated DNA.

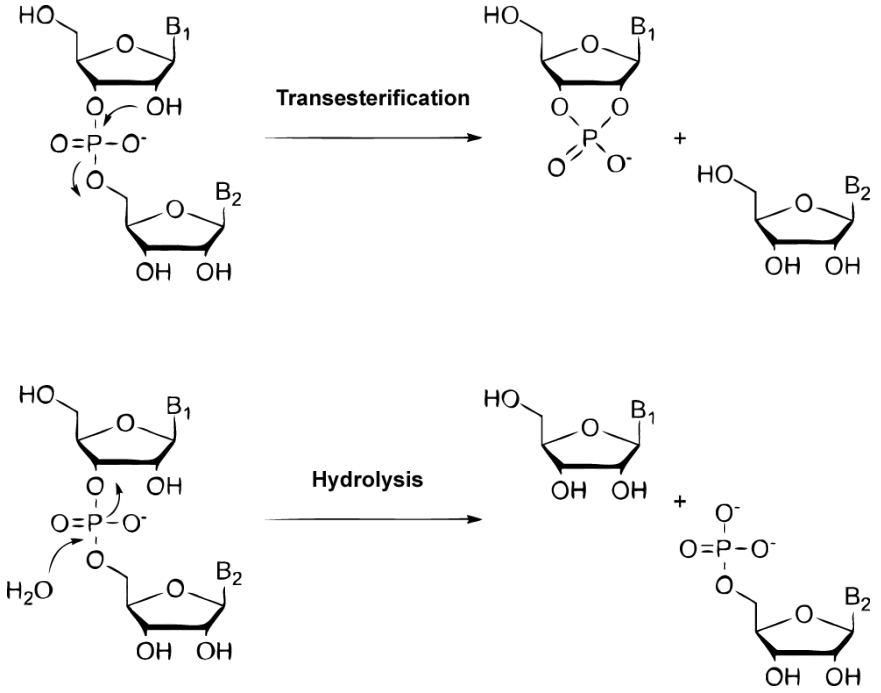

Figure 1-7. Sequence truncation can be catalyzed through a transesterification reaction (top panel) or hydrolysis (bottom panel).

1.3.4 Fluorescent RNA-cleaving DNAzyme biosensors

A typical RNA cleavage reaction is initiated by annealing the DNAzyme to the substrate sequence. In the presence of target, the hybridized substrate is cleaved into two fragments. As a result, the departure of two strands from the DNAzyme provides a unique opportunity to strategically position fluorescent and quencher dyes to create a fluorescent-based biosensor. Fluorescence is an excellent signal transduction mechanism for nucleic acids due to its high sensitivity and ease of chemical incorporation. There are several methods for attaching fluorophore and quencher dyes to maximize fluorescence signal and reduce background noise. In the first example from Figure 1-8A, the

fluorophore and quencher are placed on the opposite end of the substrate.[87-89] Although this arrangement was initially used to replace use of radioisotopes for characterization assays, the distance between the two dyes results in high background fluorescence and poor signal enhancements. Other earlier efforts were to label the 3′-terminus of the substrate and the 5′-terminus of the DNAzyme such that the fluorophore and quencher are closer in proximity to reduce background fluorescence (Figure 1-8B).[68,90-92] However, if the substrate and DNAzyme are not efficiently hybridized, high background fluorescence could still be observed. Liu and Lu attempted to improve on this system by attaching a second quencher to the opposite end of the substrate strand (Figure 1-8C).[93] As a result, even if the two strands dissociate or were not able to anneal correctly, the substrate sequence was partially quenched. This system was successfully utilized for the detection of UO_2^{2+}.[71] To maximize signal enhancement, the fluorophore and quencher could be positioned next to the cleavage site (Figure 1-8D).[70,94,95] However, placing the dyes close to the cleavage site may disrupt catalysis and render the DNAzyme inactive. This limitation could be solved by directly incorporating the two dyes into the *in vitro* selection process. Despite the added steric bulk of the fluorophore and quencher, several DNAzymes have been successfully isolated. The first DNAzyme to cleave an RNA substrate with this specific fluorophore-quencher arrangement was isolated by the Li group. It was characterized to have a catalytic rate of 7 min^{-1}, which placed it among one of the fastest RNA-cleaving DNAzymes known to date. In addition, *in vitro* selection of other DNAzymes that were able to cleave this fluorogenic substrate was isolated to have optimal activity at varying pH values.[96-98]

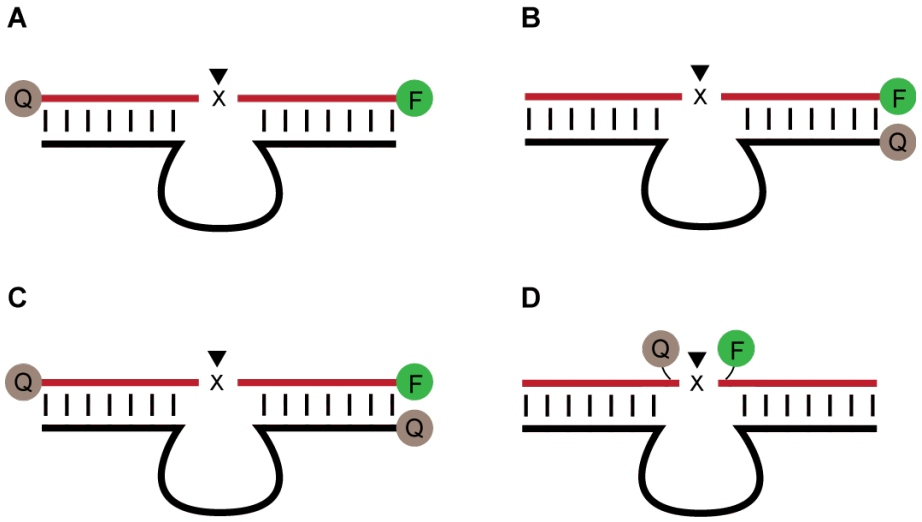

Figure 1-8. Fluorophore (F) and Quencher (Q) dye arrangement. A) The dyes are on opposite ends of the substrate sequences; B) F and Q are on one side of the probe for closer contact quenching effects; C) An improvement to the previous design with an added Q on the opposite side of the substrate to reduce background fluorescence; D) the F/Q flank the cleavage site.

In the previous designs, control of fluorescence was achieved through the use of quencher dyes. The poor placements of dyes can reduce signal enhancement and increase background fluorescence. In recent years, gold nanoparticles (AuNPs) and gold nanorods (GNRs), have been explored as fluorescence quenchers. Chung and co-workers used thiolated DNA to immobilize fluorescein labeled substrates and observed near complete quenching effects of the fluorophore (Figure 1-9A). This strategy was used to detect Pb^{2+} with a detection limit of 5 nM within 20 minutes.[99] An alternative design employed by the Liu group utilized the GR-5 DNAzyme and catalyzed the reaction in *cis* (the cleavage reaction occurs intramolecularly) such that the fluorophore is in even closer contact with the AuNPs (Figure 1-9B).[100] Fluorescence quenching was also demonstrated with the use of GNR and an 8-17 DNAzyme. This sensitive platform developed by Wang and co-

workers was able to detect Pb^{2+} with a detection limit of 62 pM (Figure 1-9C).[101] Another interesting property for these gold nanomaterials is their ability to penetrate cellular membranes.[102] In a study to explore the detection of uranyl ions in living cells, the Lu group immobilized their UO_2^{2+}-dependent DNAzyme onto AuNPs. The substrate strand contained a 5′-Cy3, which is released from the Au surface in the presence of uranyl ions in cells. This simple platform further extends the utility of RNA-cleaving DNAzyme sensors and could theoretically be used for the detection of other metal ions in cells.[103]

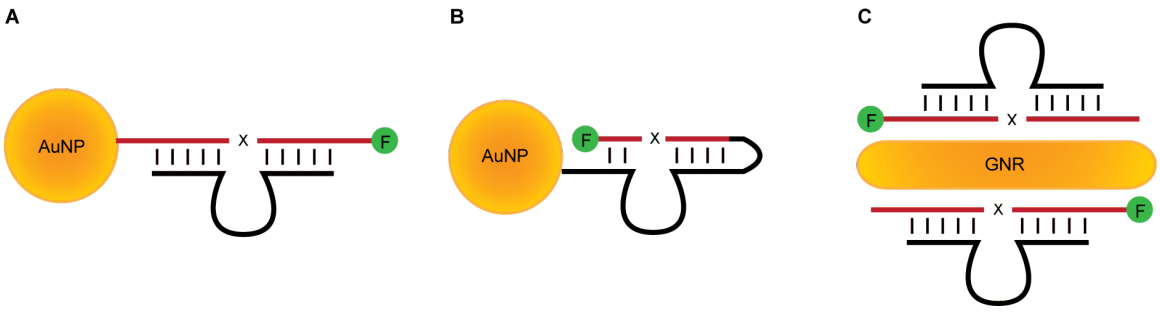

Figure 1-9. Using gold nanoparticle and gold nanorods as quenchers. A) DNA substrates with a fluorophore was immobilized onto AuNPs for quenching; B) A cis-conformation brings the fluorophore closer to the AuNP; C) Many DNAzymes-substrate probes could be adsorbed onto gold nanorods for close contact quenching of the fluorophore.

Other nanomaterials reported for fluorescence quenching properties are graphene oxides (GOs) and carbon nanotubes (CNTs). These platforms have been more recognized in recent years due to their unique interaction between single- versus double-stranded DNA.[104,105] Single-stranded DNA will bind to both CNTs and GO through

electrostatic interactions and π-stacking. However, the more rigid double-stranded DNA with exposing negative charges has limited affinity for CNTs or GOs.[106] Several studies have taken advantage of this property to develop a "turn-off" sensor (Figure 1-10A). When the DNAzyme and substrate are hybridized, the duplex structure allows them to remain free in solution. Upon addition of target, the substrate is cleaved and releases from the DNAzyme and the single-stranded DNA can be captured by the CNTs or GOs. This has been demonstrated with the 8-17 DNAzyme to detect Pb^{2+} with a detection limit of 1 nM.[107] Conversely, the Yu group was able to develop a "turn-on" sensor by minimizing the length of the single-stranded DNA that is released after RNA cleavage.[108] When the cleaved fluorescent sequence was reduced to a length of 5 residues, minimal binding of FAM labeled DNA to GOs was observed. In this case, by introducing a large single-stranded loop on the DNAzyme strand, the whole probe was able to stay immobilized on graphene (Figure 1-10B).

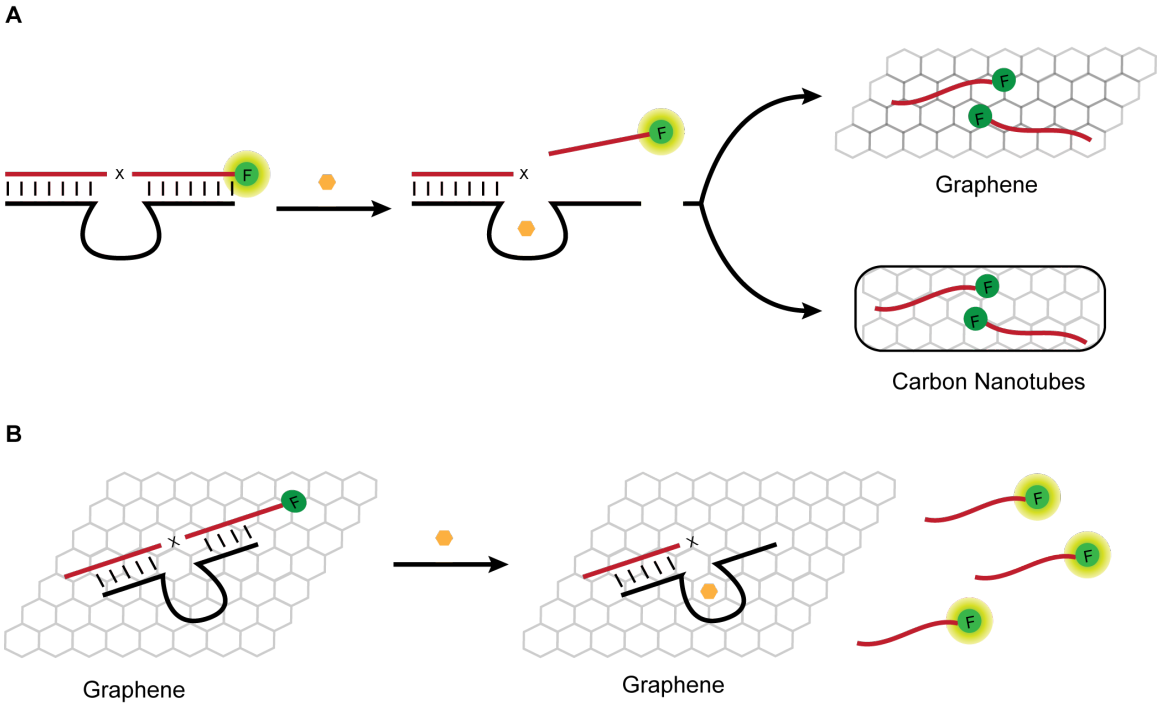

Figure 1-10. Carbon-based nanomaterial as super quenchers. A) Double-stranded DNA has limited affinity for graphene and carbon nanotubes. Upon cleavage, the single-stranded fluorescent piece will be adsorbed onto these nanomaterials and become quenched. B) A large single-stranded loop is introduced to keep the fluorescent probe bound to graphene. By adjusting the length of the cleaved fluorescent strand, it can depart from the graphene and provide a fluorescent signal.

1.3.5 Construction of aptazyme sensors

Given the key role of divalent metal ions in the RNA cleavage reaction, it is no surprise that many sensors have been engineered to detect them. However, if DNAzymes are to compete with protein-based biosensors, their utility must extend beyond the detection of these cofactors. To detect molecules other than metal ions, aptamers are used as the recognition element to synergistically work with the RNA-cleaving DNAzyme. The linked aptamer-DNAyzme systems are often referred to as "allosteric DNAzymes" or

simply "aptazymes". These aptazymes are rationally designed to judiciously integrate the aptamer to the RNA-cleaving DNAzyme such that catalysis is regulated by aptamer domain. The Sen group was the first to design a DNA aptazyme that combined an anti-ATP DNA aptamer to a 10-23 DNAzyme.[109] From Figure 1-11A, two short duplex regions are designed to flank the substrate binding domain and the aptamer domain. These regions have been altered to cause the aptazyme to inefficiently bind with the substrate sequence in the absence of ATP. Upon addition of ATP, it binds to the aptamer domain and reassembles the ATP-aptamer complex to allow additional base-pairing with the substrate. This binding event subsequently facilitates RNA cleavage.

Other approaches to construct aptazymes are through base paring inhibition of either the DNAzyme or substrate sequence.[110,111] From Figure 1-11B, Li and co-workers coupled the same ATP aptamer sequence with a fluorescence-signaling DNAzyme. In the absence of ATP, a regulator sequence was annealed to the DNAzyme's binding arm and part of the ATP domain. This step deters hybridization of the DNAzyme to the substrate and suppresses RNA cleavage. However, the presence of ATP will induce a conformation change in the aptamer domain to facilitate the departure of the regulator sequence. As a result, the DNAzyme's binding arm is free to hybridize with the substrate for catalysis. This fluorescence-generating RNA-cleaving DNAzyme was able to achieve a 30-fold rate enhancement in the presence of ATP. Another similar method was constructed for the detection of ATP in which the aptamer domain is now located on the substrate strand. Part of the aptamer sequence will block the substrate binding arm and is only released upon addition of ATP (Figure 1-11C). Blocking the binding arms is not the

only option to regulate catalysis. In another demonstration by the Li group, sequestering catalytically active residues to base pair with a part of the aptamer domain could also regulate RNA cleavage. In the presence of ATP, the aptamer domain complexes with ATP, thereby releasing the catalytically essential nucleotides for RNA cleavage.[112]

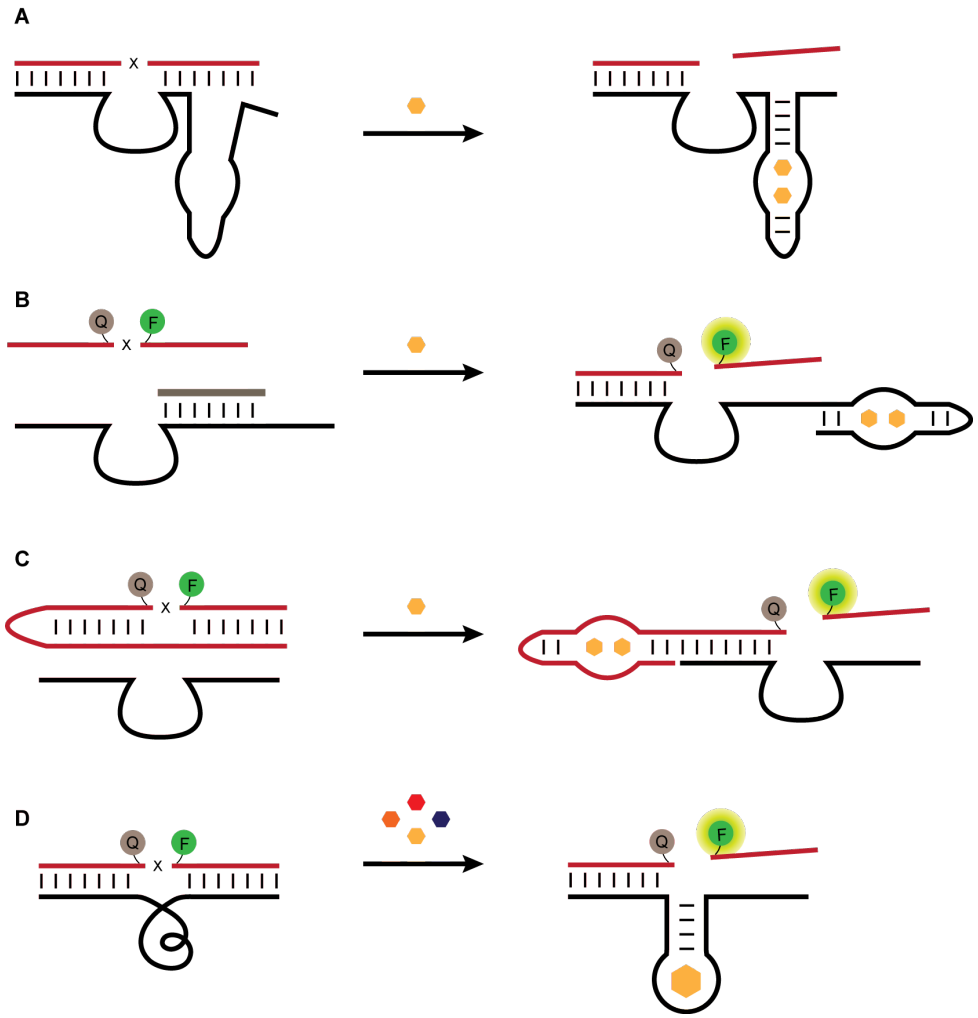

Figure 1-11. Construction of aptazymes. A) The presence of ATP will allow additional base-pairing to the substrate for RNA cleavage; B) A regulator sequence prevents binding of the substrate; C) The substrate sequence prevents binding of the DNAzyme and is only released in the presence of ATP; D) Aptazymes can be isolated through *in vitro* selection.

Rational design of aptazymes is a proven method to take advantage of existing DNAzymes, however, the process of making the aptamer regulate DNAzyme activity can be tedious. Its success depends on the aptamer's size, binding characteristics, and how amenable it is for mutagenesis. These qualities will dictate how well it could function with the DNAzyme. Therefore, an alternative method to obtain an aptazyme is to use *in vitro* selection to directly isolate sequences that will be catalytic in response to a target of interest. The advantage with this strategy is that aptazymes could be developed for targets with no existing aptamers. Furthermore, the specificity could be tuned through the addition of a negative selection step. This is a process where similar or related analytes are used to remove undesired aptazymes. In a study to develop a fluorescent DNAzyme that responds to bacteria, the Li group performed *in vitro* selection using the crude extracellular mixture (CEM) of *Escherichia coli* (*E. coli*).[113] Specificity was attained through counter selection using the CEM of *Bacillus subtilis*. After 20 rounds of selection, an aptazyme that was highly specific for *E. coli* was isolated. The aptazyme was tested against a series of gram-negative and gram-positive bacteria and no cross reactivity was observed. Furthermore, with the use of a culturing step, the *E. coli*-responsive aptazyme was able to detect a single seeding of *E. coli*. The advantage with this method is that the *in vitro* selection process will choose the most optimal target within the crude mixture. This allows researchers to skip the process of finding a suitable target that is unique to a specific bacterium. Even if a target candidate was identified for selection, there is no guarantee that the selection will yield a highly sensitive and selective aptamer.

1.3.6 Colorimetric RNA-cleaving DNAzyme biosensors

A colorimetric sensor will generate a visible color change in the presence of target analytes. They offer many distinct advantages when compared to other reporting systems. First, the observable color change can be detected using the naked eye, which reduces reliance on expensive and bulky equipment. This also makes on-field detection much more manageable and responsive. Second, native nucleic acids do not absorb in the visible region and therefore would not interfere with colorimetric reporting groups such as small organic dyes, conjugated polymers, and metallic nanoparticles. Metallic nanoparticles such as Gold nanoparticles (AuNPs) in particular have gained much attention as a colorimetric platform. They generate an intense red color and possess a much higher extinction coefficient than most organic dyes. AuNPs are characterized to have strong distance-dependent optical properties and will change color from red to purple (and sometimes blue) in response to being dispersed or aggregated, respectively. Following the reports of DNA detection using DNA oligonucleotide conjugated AuNPs by the Mirkin group,[114] a series of RNA-cleaving DNAzyme-AuNP platforms have been constructed.

In the first design by the Lu group, AuNPs were conjugated with short oligonucleotides and a substrate sequence was added for assembling AuNPs into aggregates.[78] A heating and cooling process was used to align the AuNPs-DNA into a 'head-to-tail' manner and the linked aggregates generate a purple color. In the presence of Pb^{2+}, the Pb^{2+}-dependent DNAzyme would cleave the substrate, thereby dispersing the

AuNPs and a red color can be quantified using a spectrophotometer. In a follow-up study to improve on this system, the AuNPs were rearranged into a "tail-to-tail" orientation (Figure 1-12A).[115] The first head-to-tail system suffered from high steric effects that caused the assay to be slow. In addition to the change in AuNP alignment, the Lu group also replaced the 13 nm AuNPs to a 42 nm AuNPs to increase the rate of color change. Using the same Pb^{2+}-dependent DNAzyme, the assay time was reduced from 2 h to 5 min.

In another AuNPs-based system for the detection of Pb^{2+}, the sensor was developed based on salt-induced aggregation.[116] As shown in Figure 1-12B, the substrate and the Pb^{2+}-dependent DNAzyme were assembled on the AuNPs in high salt concentrations. The salt concentrations were optimized to a critical point in which the AuNPs were still stable and remain dispersed. With the addition of Pb^{2+}, the substrate was cleaved and departed from the AuNPs, making the conjugated oligonucleotide shorter. This shorter sequence could no longer aid in the AuNP stability under high salt conditions, and therefore aggregated and turned from red to purple.

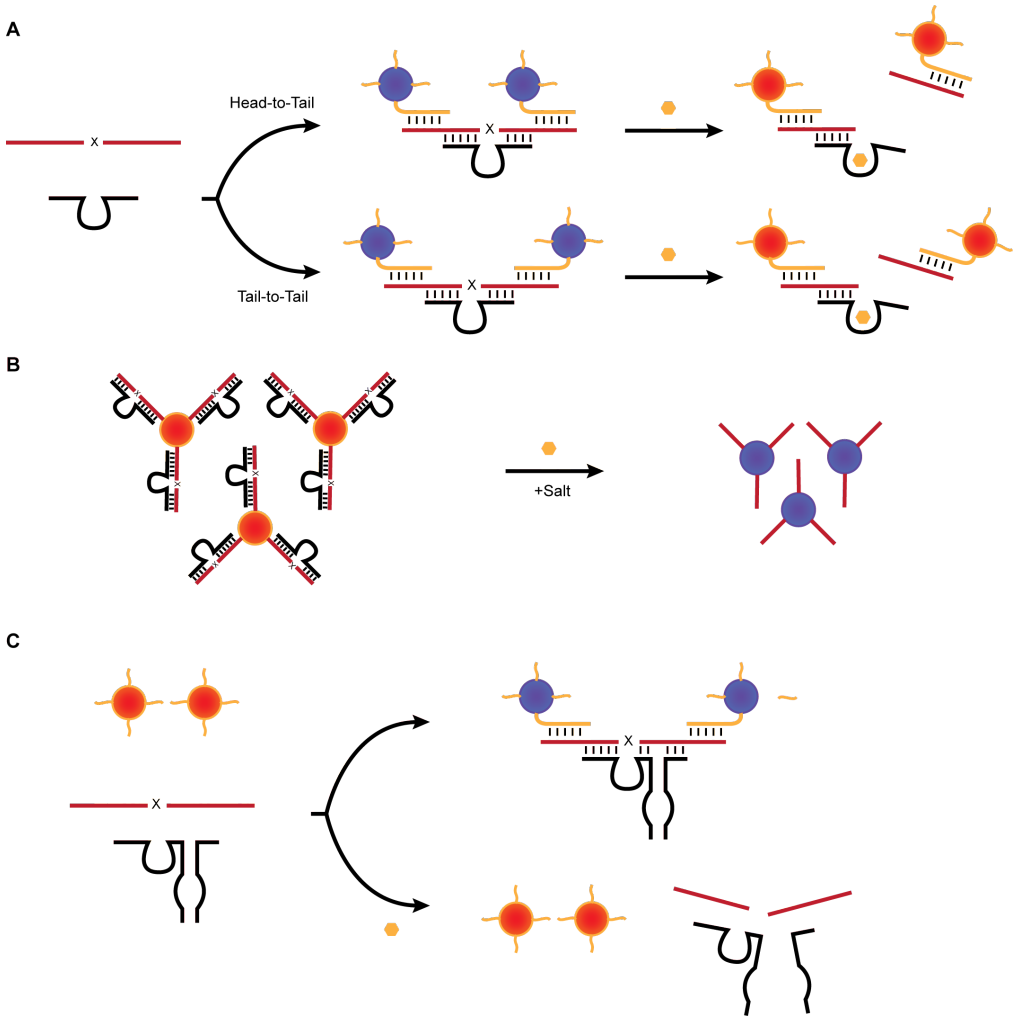

Figure 1-12. Colorimetric RNA-cleaving DNAzyme probes. A) AuNP alignment to induce preassembled AuNP that are blue. After cleavage, the AuNPs become dispersed and turn red; B) Salt-induced aggregation of AuNPs by manipulating the salt concentration in solution and lengths of DNA. Before cleavage, the assembled DNA probe prevents aggregation. Upon cleavage the shorter sequence can no longer stabilize the AuNPs, causing them to aggregate; C) An ATP-dependent aptazyme using AuNP. The absence of ATP will cross-link AuNPs, making them turn blue. Addition of ATP will cleave the substrate and prevent AuNP cross-linking, keeping them dispersed.

Aptazymes have also been explored in conjunction with AuNPs for developing aptzyme-based colorimetric sensors. From Figure 1-12C, an ATP aptamer domain is split into two separate strands. The first strand contains an 8-17 DNAzyme followed by the

first half of an ATP aptamer. A second DNA strand contains the other half of the ATP aptamer. The AuNPs are linked through a bridging oligonucleotide that is hybridized to the short conjugated sequences on the AuNPs. In the absence of ATP, the linked AuNPs are forced to aggregate, resulting in a purple color. Conversely, upon addition of ATP, the DNAzyme becomes activated and cleaves the substrate, which disperses the AuNPs and causes the solution to turn red.[117]

1.3.7 Electrochemical RNA-cleaving DNAzymes

Other reporting systems that employ RNA-cleaving DNAzymes are electrochemical-based sensors. There are several advantages of an electrochemical-based sensor that make this method an attractive alternative to colorimetric or fluorescent sensors. Advances in electronic technology have miniaturized many benchtop equipment to battery powered hand-held devices. Electronic devices can offer greater sensitivity, reproducibility, and faster response time. With the ease of chemically incorporating these electroactive labels to DNA, some efforts have been made to utilize RNA-cleaving DNAzymes for developing electrochemical-based sensors.

The first study to explore electrochemical sensors using RNA-cleaving DNAzymes was carried out by the Plaxco group. A Pb^{2+}-dependent DNAzyme was first modified with a 3′-methylene blue dye and immobilized to a gold electrode.[118] By annealing the substrate to the DNAzyme, the double stranded structure became rigid, causing the methylene blue to be spatially separated from the gold surface, resulting in

low electron transfer. In the presence of Pb^{2+}, the substrate is cleaved and the DNAzyme becomes much more flexible, which brings the methylene blue closer to the surface for enhanced electron transfer (Figure 1-13A). This probe was able to monitor Pb^{2+} with a detection limit of 300 nM and was also capable of detecting Pb^{2+} in soil samples. Recently, this system was slightly altered by Li and co-workers. In search of enhanced sensitivity, the sensing surface was constructed by using gold nanoparticle assembled onto graphene-nanosheets (Figure 1-13B). This design was able to detect L-histidine with a detection limit of 0.1 pM.[119]

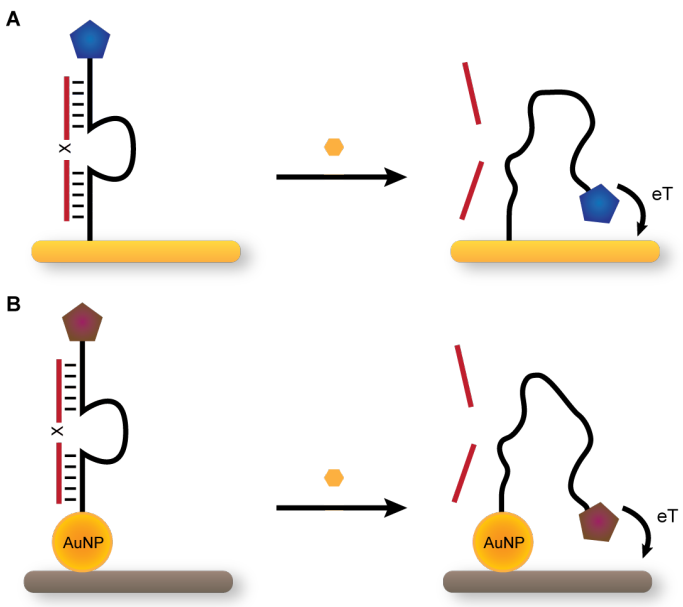

Figure 1-13. Electrochemical probes using RNA-cleaving DNAzymes. A) A methylene blue mediator was distanced from the gold electrode due to the rigid structure of DNA duplex. Addition of Pb^{2+} will make the backbone flexible and electron transfer is observed as the dye moves closer to the electrode; B) A similar mechanism is developed where a graphene-nanosheet was used in place of gold electrode and the methylene blue was replaced with ferrocene.

Other electrochemical designs have taken the label-free approach to develop simpler assays. The Shao group used $Ru(NH_3)_6^{3+}$, a redox mediator, to electrostatically bind to the anionic backbone of DNA to serve as the signal transducer.[120] In the presence of Pb^{2+}, the DNAzyme cleaves the substrate and releases the AuNP-DNA from the electrode. The $Ru(NH_3)_6^{3+}$ that were bound to the DNA were also washed away which results in a reduced signal (Figure 1-14A). Although this study demonstrated the ability to detect 1 nM of Pb^{2+}, this is a "signal off" approach. To design a "signal on" method, Yang and co-workers functionalized AuNP with a Pb^{2+}-dependent DNAzyme. In the presence of Pb^{2+}, the substrate sequence is cleaved, and the DNAzyme's binding arm becomes available for capture. Subsequent addition of $Ru(NH_3)_6^{3+}$ to bind any captured DNAzyme can then be detected to confirm the presence of Pb^{2+} (Figure 1-14B).[121]

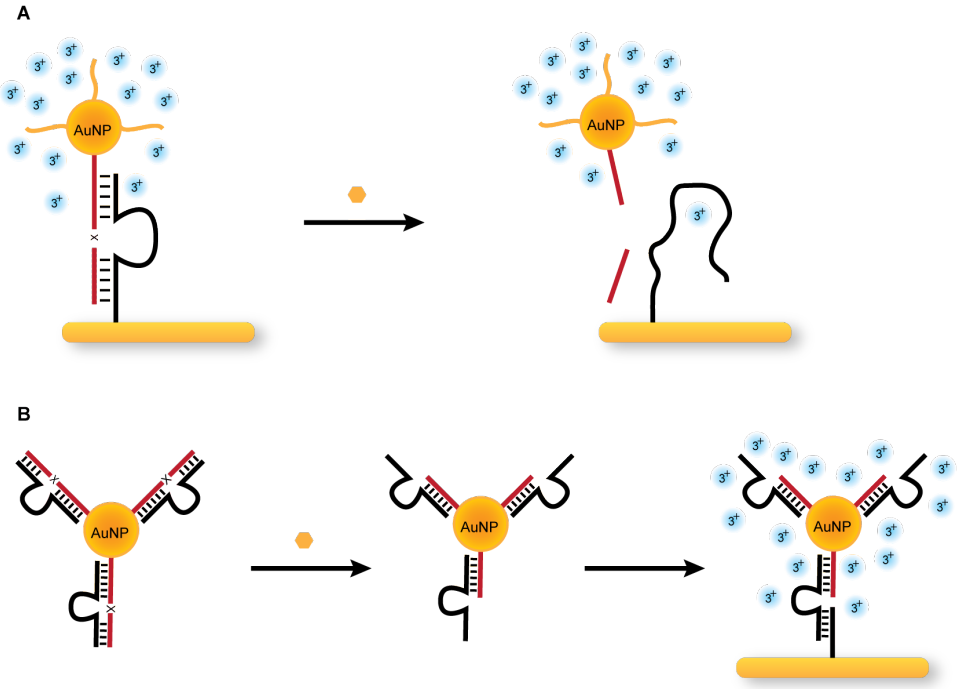

Figure 1-14. Label-free electrochemical design. (A) $Ru(NH_3)_6^{3+}$ was used as the redox mediator to interact with the negative phosphate groups of DNA. The addition of Pb^{2+} will release most of the DNA, which were previously immobilized on AuNP. (B) In a similar mechanism, the cleaved substrate will release a binding arm which can then be captured by the electrode. The DNA-rich surface will then be able to capture more $Ru(NH_3)_6^{3+}$.

1.3.8 Aptamers as recognition elements for biosensor development

Biosensors that rely on DNAzymes are often limited to detecting metal ions and few examples have been made to demonstrate their ability to easily target other analytes. In response to this limitation, aptamers were appended to DNAzymes to extend their functionality. Over the past 25 years, hundreds of aptamers have been isolated through *in vitro* selection to recognize a plethora of unique analytes. They are molecular recognition elements that have played a key role in the growth of FNA-based biosensors. Similar to

antibodies, aptamers can only recognize a specific analyte. However, unlike antibodies, aptamers are able to undergo a major conformational change into well-defined structures in the presence of their cognate ligand. This ability to switch between two states can be utilized to program aptamers to report binding events. There is a substantial amount of studies regarding this topic and many comprehensive reviews are available for aptamer-based sensors.[122-125] To stay within the boundaries of this thesis, I will focus on the current general design and strategies for developing aptamer-based biosensors.

1.3.9 Current design of aptamer-based biosensing reporters

As previously mentioned, the ease of conjugating fluorophores to DNA make fluorescent-based sensor a well-explored area of research. One such design is to incorporate a single fluorescent dye at key sites within the aptamer domain. In the presence of its cognate ligand, the aptamer rearranges into a new conformation, which in turn can induce a change in fluorescence intensity (Figure 1-15A).[126,127] The Ellington group demonstrated this with the detection of ATP down to a concentration of 25 μM.[128] They were able to observe a 2-fold enhancement in fluorescence intensity with this design. Based on the concept of structural rearrangement, two dyes can be positioned at each end of the aptamer to create a FRET-based reporter system (Figure 1-15B).[129] In the presence of target, the aptamer restructures and brings the two dyes closer together. This strategy was successfully used for the detection of ATP[130] and platelet-derived growth factors.[131] In another similar design, an aptamer sequence was

split into two strands where one strand would contain a fluorophore and the other a quencher (Figure 1-15C). Upon addition of target, the two strands would be reassembled, bringing the two fluorophore and quencher closer.[132] In these examples, the relative fluorescent intensities between the presence and absence of target are typically small due to high background noise and inefficient quenching effects.

In order to generate a large fluorescent enhancement in the presence of target, the Li group designed an approach known as "structure switching" aptamers.[110,133] Since aptamers can either be made of RNA or DNA, they have the unique ability to bind not only their cognate ligand, but also other nucleic acids. Aptamers can therefore adopt two distinct structures: Nucleic acid duplexes and ligand-bound aptamer structures. The structure switching method begins with an aptamer that is first labeled with a fluorophore and is annealed to a second strand of DNA (or RNA) with a quencher. In this state, the quencher suppresses fluorescence, however, upon addition of target, the aptamer preferentially binds to the target and displaces the quencher strand. This results in a large increase in fluorescence intensity (Figure 1-15D). This model has also been applied using electrode surfaces with methylene blue[134] and gold nanoparticles[135] in place of fluorescent dyes. Another method to generate a positive fluorescent signal is to use graphene oxide to immobilize single stranded fluorescent aptamers (Figure 1-15E). In the presence of target, the single stranded aptamer folds into a defined tertiary structure and releases the fluorescent aptamer from the graphene oxide in which fluorescence can then be measured.[105]

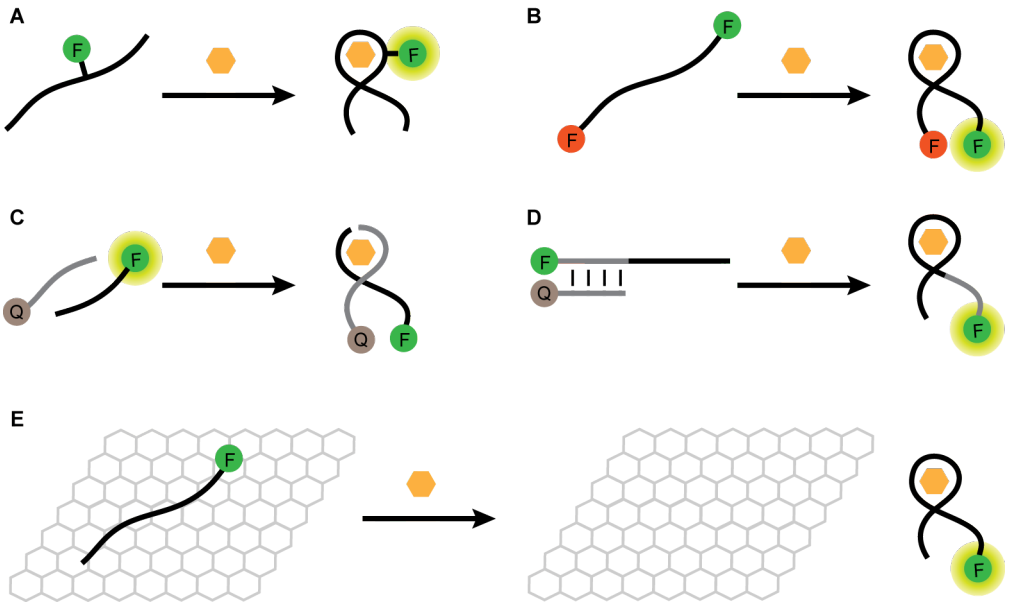

Figure 1-15. Fluorescent-based biosensors using Aptamers. (A) A single fluorophore that will fluoresce upon aptamer rearrangement. (B) A dual labeled aptamer that will induce FRET-based activity as the two dyes come closer after binding to the target. (C) Two separate strands that contain one half of an aptamer. Addition of target will cause them to associate and a quenching effect is observed. (D) Fluorescence enhancement is caused by quencher dissociation due to aptamer-ligand formation. (E) An aptamer with a single fluorophore that is quenched by graphene. The single stranded form will be adsorbed onto graphene and released through the formation of ligand-aptamer complex.

Use of AuNPs is also a common strategy for engineering a colorimetric aptamer-based sensor. Similar to the AuNP-DNAzyme designs above, AuNPs can be regulated to either disperse or aggregate by using aptamers. One strategy is to induce AuNP aggregation by bridging the AuNPs together with an aptamer sequence. The presence of target will release the AuNPs, causing them to disperse and turn red (Figure 1-16A).[136,137] Conversely, the AuNps could begin in a dispersed state and are labeled with one-half of an aptamer. Addition of the target will assemble the complete aptamer

between two halves and aggregate the AuNPs to create a color change to blue (Figure 1-16B).[138]

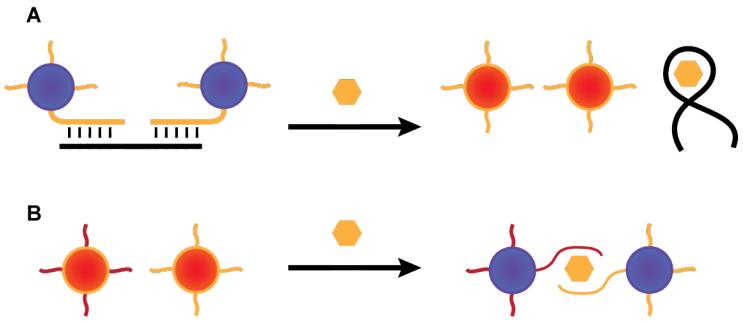

Figure 1-16. Colorimetric Biosensor that use Aptamers. (A) Aggregated AuNPs are cross-linked and can only be released in the presence of a target analyte. (B) Each AuNPs are immobilized with one half of an aptamer. The addition of target will cause these two halves to associate, resulting in AuNP aggregation.

1.4 Thesis objective and outline

The worldwide effort towards developing the next generation of biosensors has set an incredible pace for innovation. The need for biosensors has extended beyond a simple point-of-care device. Many industries are now looking for simple, efficient, and cost-effective biosensing technologies and this need to clearly expressed in the rapidly growing market. One such technology that has the potential to fulfill this need is functional nucleic acid (FNA). In the past few years, substantial progress has been made to enhance their stability, functionality, and effectiveness. However, there are still major deficiencies that FNA has yet to have a clear solution for. The projects described in this thesis were conceived to address these deficiencies.

Chapter 1 of my thesis is intended to provide a broad overview of the current state in FNA-derived biosensors. Its purpose is to illustrate the progress made thus far, and more importantly, reveal the current technology's strengths and weaknesses. I have intentionally emphasized on DNAzymes (specifically RNA-cleaving DNAzymes) and DNA aptamers since these are the two areas in which I believe have the necessary prerequisites for creating the most ideal biosensor.

Chapter 2 – Translating Bacterial Detection into a Litmus Test using DNAzymes. In this chapter, I will describe the use of an *E. coli*-responsive RNA-cleaving DNAzyme to regulate urease activity. Urease is a protein enzyme that is capable of converting urea into carbon dioxide and ammonia. The generation of ammonia in solution will cause the pH of the solution to increase and this change in pH can be monitored by an indicator dye. As described in chapter one, many colorimetric RNA-cleaving DNAzyme reporters heavily rely on gold nanoparticles (AuNPs). There are a limited number of methods for coupling RNA-cleaving DNAzymes to other colorimetric platforms. Therefore, one of the motivations for our work in Chapter 2 is to develop a novel and unconventional method for generating a color change using FNA. By having more options to create colorimetric sensors, it will provide additional flexibility to create devices with features most suited for the task at hand. The advantage of using our urease coupled-FNA platform is that it is not easily affected by salt, pH, temperature, or particulates that would otherwise disrupt the effectiveness of other colorimetric approaches.

Chapter 3 – *In vitro* Selection of an L-RNA-cleaving DNAzyme for Sensor Development. Nearly all biosensors that incorporate RNA-cleaving DNAzymes have been designed to detect analytes in controlled conditions free of undesired contaminants. We have established in Chapter 1 that RNA-cleaving DNAzymes can be a powerful tool for creating biosensors and that the biosensing industry is quickly expanding to various sectors. If RNA-cleaving DNAzymes are to compete within high demand sectors such as disease detection and health related point-of-care devices, it needs to function effectively in these samples matrices. Searching for infectious pathogens and important biomarkers in biologically active samples present a new set of challenges to the RNA-cleaving DNAzyme platform. The RNA moiety in these DNAzymes can be unintentionally cleaved by contaminants such RNases, which are present in biological samples. This cleavage event will cause the system to generate a false positive signal, making our system obsolete. Therefore, the goal of our project in Chapter 3 was to enhance RNase resistance while maintaining the core catalytic RNA cleavage function. To achieve this, we used the enantiomeric L-RNA in place of the common D-RNA and performed *in vitro* selection for a DNAzyme to cleave this unnatural substrate. We chose L-RNA because it is an unrecognizable substrate for RNases while maintaining its ability to undergo the same transesterification reaction similar to D-RNA. This simple modification will significantly enhance the stability of this system and allow for the creation of biosensors that could detect infectious diseases or monitor specific biological analytes in biological sample matrices.

Chapter 4 – Arrest of Rolling Circle Amplification by Protein-binding DNA Aptamers. DNA aptamers have the unique ability to interact with a variety of biomolecules. They are able to bind nucleic acids through Watson-Crick base pairing and form rigid duplex structures or bind small molecules, proteins, and even cells through intricate secondary and tertiary structures. These types of interactions have been exploited for uses in developing biosensors. In Chapter 4, we were able to probe the binding properties of aptamers and use it to regulate a process known as rolling circle amplification (RCA). RCA is used to generate a long single stranded concatemeric DNA molecule from a circular DNA template. This isothermal reaction is carried out using a special polymerase known as phi29 DNA polymerase. This enzyme has one of the highest processivity rates and is able to displace DNA duplexes without any auxiliary proteins. Considering these properties, it is therefore conceivable that phi29 should also be able to disrupt a ligand-bound aptamer complex during polymerization. However, this was not the case. This discovery prompted us to further investigate the aptamer-ligand complex's influence on phi29 and how this feature can be used to engineer a biosensor.

In the final chapter of my thesis, I will summarize the major achievements and provide a brief outlook on the future of FNA-based biosensors.

1.5 References cited

1. Kruger K, Grabowski PJ, Zaug AJ, Sands J, Gottschling DE, et al. (1982) Self-splicing RNA: autoexcision and autocyclization of the ribosomal RNA intervening sequence of Tetrahymena. Cell 31: 147-157.
2. Guerrier-Takada C, Gardiner K, Marsh T, Pace N, Altman S (1983) The RNA moiety of ribonuclease P is the catalytic subunit of the enzyme. Cell 35: 849-857.
3. Breaker RR, Joyce GF (2014) The expanding view of RNA and DNA function. Chem Biol 21: 1059-1065.
4. Ellington AD, Szostak JW (1990) In vitro selection of RNA molecules that bind specific ligands. Nature 346: 818-822.
5. Robertson DL, Joyce GF (1990) Selection in vitro of an RNA enzyme that specifically cleaves single-stranded DNA. Nature 344: 467-468.
6. Tuerk C, Gold L (1990) Systematic evolution of ligands by exponential enrichment: RNA ligands to bacteriophage T4 DNA polymerase. Science 249: 505-510.
7. Mandal M, Breaker RR (2004) Gene regulation by riboswitches. Nat Rev Mol Cell Biol 5: 451-463.
8. Tucker BJ, Breaker RR (2005) Riboswitches as versatile gene control elements. Curr Opin Struct Biol 15: 342-348.
9. Winkler WC, Breaker RR (2005) Regulation of bacterial gene expression by riboswitches. Annu Rev Microbiol 59: 487-517.
10. Wickiser JK, Cheah MT, Breaker RR, Crothers DM (2005) The kinetics of ligand binding by an adenine-sensing riboswitch. Biochemistry 44: 13404-13414.
11. Keefe AD, Pai S, Ellington A (2010) Aptamers as therapeutics. Nat Rev Drug Discov 9: 537-550.
12. Ni X, Castanares M, Mukherjee A, Lupold SE (2011) Nucleic acid aptamers: clinical applications and promising new horizons. Curr Med Chem 18: 4206-4214.
13. Xu Z, Yang L, Sun L, Cao Y (2012) Use of DNAzymes for cancer research and therapy. Chinese Science Bulletin 57: 3404-3408.

14. Burnett JC, Rossi JJ (2012) RNA-based therapeutics: current progress and future prospects. Chem Biol 19: 60-71.
15. Yoo E-H, Lee S-Y (2010) Glucose biosensors: an overview of use in clinical practice. Sensors 10: 4558-4576.
16. Clark LC, Jr., Lyons C (1962) Electrode systems for continuous monitoring in cardiovascular surgery. Ann N Y Acad Sci 102: 29-45.
17. Wang J (2001) Glucose Biosensors: 40 Years of Advances and Challenges. Electroanalysis 13: 983-988.
18. Turner APF (2013) Biosensors: sense and sensibility. Chem Soc Rev 42: 3184-3196.
19. Thusu R (2010) Strong Growth Predicted for Biosensor Market. Sensors Online. http://www.sensorsmag.com: Questex Media Group.
20. Luong JH, Male KB, Glennon JD (2008) Biosensor technology: technology push versus market pull. Biotechnol Adv 26: 492-500.
21. Chames P, Van Regenmortel M, Weiss E, Baty D (2009) Therapeutic antibodies: successes, limitations and hopes for the future. Br J Pharmacol 157: 220-233.
22. Pan T, Uhlenbeck OC (1992) A small metalloribozyme with a two-step mechanism. Nature 358: 560-563.
23. Williams KP, Ciafre S, Tocchini-Valentini GP (1995) Selection of novel Mg(2+)-dependent self-cleaving ribozymes. EMBO J 14: 4551-4557.
24. Jayasena VK, Gold L (1997) In vitro selection of self-cleaving RNAs with a low pH optimum. Proc Natl Acad Sci U S A 94: 10612-10617.
25. Breaker RR, Joyce GF (1994) A DNA enzyme that cleaves RNA. Chem Biol 1: 223-229.
26. Santoro SW, Joyce GF, Sakthivel K, Gramatikova S, Barbas CF, 3rd (2000) RNA cleavage by a DNA enzyme with extended chemical functionality. J Am Chem Soc 122: 2433-2439.

27. Perrin DM, Garestier T, Helene C (2001) Bridging the gap between proteins and nucleic acids: a metal-independent RNAseA mimic with two protein-like functionalities. J Am Chem Soc 123: 1556-1563.
28. Sidorov AV, Grasby JA, Williams DM (2004) Sequence-specific cleavage of RNA in the absence of divalent metal ions by a DNAzyme incorporating imidazolyl and amino functionalities. Nucleic Acids Res 32: 1591-1601.
29. Breaker RR, Joyce GF (1995) A DNA enzyme with Mg^{2+}-dependent RNA phosphoesterase activity. Chem Biol 2: 655-660.
30. Santoro SW, Joyce GF (1997) A general purpose RNA-cleaving DNA enzyme. Proc Natl Acad Sci U S A 94: 4262-4266.
31. Geyer CR, Sen D (1997) Evidence for the metal-cofactor independence of an RNA phosphodiester-cleaving DNA enzyme. Chem Biol 4: 579-593.
32. Bartel DP, Szostak JW (1993) Isolation of new ribozymes from a large pool of random sequences. Science 261: 1411-1418.
33. Teramoto N, Imanishi Y, Ito Y (2000) In vitro selection of a ligase ribozyme carrying alkylamino groups in the side chains. Bioconjug Chem 11: 744-748.
34. Ekland EH, Szostak JW, Bartel DP (1995) Structurally complex and highly active RNA ligases derived from random RNA sequences. Science 269: 364-370.
35. Hager AJ, Szostak JW (1997) Isolation of novel ribozymes that ligate AMP-activated RNA substrates. Chem Biol 4: 607-617.
36. Flynn-Charlebois A, Wang Y, Prior TK, Rashid I, Hoadley KA, et al. (2003) Deoxyribozymes with 2'-5' RNA ligase activity. J Am Chem Soc 125: 2444-2454.
37. Hoadley KA, Purtha WE, Wolf AC, Flynn-Charlebois A, Silverman SK (2005) Zn^{2+}-dependent deoxyribozymes that form natural and unnatural RNA linkages. Biochemistry 44: 9217-9231.
38. Purtha WE, Coppins RL, Smalley MK, Silverman SK (2005) General deoxyribozyme-catalyzed synthesis of native 3'-5' RNA linkages. J Am Chem Soc 127: 13124-13125.

39. Tuschl T, Sharp PA, Bartel DP (1998) Selection in vitro of novel ribozymes from a partially randomized U2 and U6 snRNA library. EMBO J 17: 2637-2650.
40. Wang Y, Silverman SK (2003) Deoxyribozymes that synthesize branched and lariat RNA. J Am Chem Soc 125: 6880-6881.
41. Coppins RL, Silverman SK (2005) A deoxyribozyme that forms a three-helix-junction complex with its RNA substrates and has general RNA branch-forming activity. J Am Chem Soc 127: 2900-2907.
42. Lorsch JR, Szostak JW (1994) In vitro evolution of new ribozymes with polynucleotide kinase activity. Nature 371: 31-36.
43. Curtis EA, Bartel DP (2005) New catalytic structures from an existing ribozyme. Nat Struct Mol Biol 12: 994-1000.
44. Wang W, Billen LP, Li Y (2002) Sequence diversity, metal specificity, and catalytic proficiency of metal-dependent phosphorylating DNA enzymes. Chem Biol 9: 507-517.
45. Chapman KB, Szostak JW (1995) Isolation of a ribozyme with 5'-5' ligase activity. Chem Biol 2: 325-333.
46. Huang F, Yarus M (1997) 5'-RNA self-capping from guanosine diphosphate. Biochemistry 36: 6557-6563.
47. Huang F, Yang Z, Yarus M (1998) RNA enzymes with two small-molecule substrates. Chem Biol 5: 669-678.
48. Li Y, Liu Y, Breaker RR (2000) Capping DNA with DNA. Biochemistry 39: 3106-3114.
49. Ekland EH, Bartel DP (1996) RNA-catalysed RNA polymerization using nucleoside triphosphates. Nature 383: 192.
50. Cuenoud B, Szostak JW (1995) A DNA metalloenzyme with DNA ligase activity. Nature 375: 611-614.
51. Sreedhara A, Li Y, Breaker RR (2004) Ligating DNA with DNA. J Am Chem Soc 126: 3454-3460.

52. Seelig B, Keiper S, Stuhlmann F, Jaschke A (2000) Enantioselective Ribozyme Catalysis of a Bimolecular Cycloaddition Reaction. Angew Chem Int Ed 39: 4576-4579.
53. Tarasow TM, Tarasow SL, Eaton BE (1997) RNA-catalysed carbon-carbon bond formation. Nature 389: 54-57.
54. Tarasow TM, Kellogg E, Holley BL, Nieuwlandt D, Tarasow SL, et al. (2004) The effect of mutation on RNA Diels-Alderases. J Am Chem Soc 126: 11843-11851.
55. Sheppard TL, Ordoukhanian P, Joyce GF (2000) A DNA enzyme with N-glycosylase activity. Proc Natl Acad Sci U S A 97: 7802-7807.
56. Lee N, Bessho Y, Wei K, Szostak JW, Suga H (2000) Ribozyme-catalyzed tRNA aminoacylation. Nat Struct Biol 7: 28-33.
57. Saito H, Kourouklis D, Suga H (2001) An in vitro evolved precursor tRNA with aminoacylation activity. EMBO J 20: 1797-1806.
58. Illangasekare M, Sanchez G, Nickles T, Yarus M (1995) Aminoacyl-RNA synthesis catalyzed by an RNA. Science 267: 643-647.
59. Chinnapen DJ, Sen D (2004) A deoxyribozyme that harnesses light to repair thymine dimers in DNA. Proc Natl Acad Sci U S A 101: 65-69.
60. Zhang B, Cech TR (1997) Peptide bond formation by in vitro selected ribozymes. Nature 390: 96-100.
61. Burmeister J, von Kiedrowski G, Ellington AD (1997) Cofactor-Assisted Self-Cleavage in DNA Libraries with a 3′–5′-Phosphoramidate Bond. Angew Chem Int Ed 36: 1321-1324.
62. Conn MM, Prudent JR, Schultz PG (1996) Porphyrin Metalation Catalyzed by a Small RNA Molecule. J Am Chem Soc 118: 7012-7013.
63. Li Y, Sen D (1996) A catalytic DNA for porphyrin metallation. Nat Struct Biol 3: 743-747.
64. Faulhammer D, Famulok M (1996) The Ca^{2+} Ion as a Cofactor for a Novel RNA-Cleaving Deoxyribozyme. Angew Chem Int Ed 35: 2837-2841.

65. Roth A, Breaker RR (1998) An amino acid as a cofactor for a catalytic polynucleotide. Proc Natl Acad Sci U S A 95: 6027-6031.
66. Feldman AR, Sen D (2001) A new and efficient DNA enzyme for the sequence-specific cleavage of RNA. J Mol Biol 313: 283-294.
67. Cruz RP, Withers JB, Li Y (2004) Dinucleotide junction cleavage versatility of 8-17 deoxyribozyme. Chem Biol 11: 57-67.
68. Li J, Lu Y (2000) A Highly Sensitive and Selective Catalytic DNA Biosensor for Lead Ions. J Am Chem Soc 122: 10466-10467.
69. Bruesehoff PJ, Li J, Augustine AJ, Lu Y (2002) Improving metal ion specificity during in vitro selection of catalytic DNA. Comb Chem High Throughput Screen 5: 327-335.
70. Mei SH, Liu Z, Brennan JD, Li Y (2003) An efficient RNA-cleaving DNA enzyme that synchronizes catalysis with fluorescence signaling. J Am Chem Soc 125: 412-420.
71. Liu J, Brown AK, Meng X, Cropek DM, Istok JD, et al. (2007) A catalytic beacon sensor for uranium with parts-per-trillion sensitivity and millionfold selectivity. Proc Natl Acad Sci U S A 104: 2056-2061.
72. Hollenstein M, Hipolito C, Lam C, Dietrich D, Perrin DM (2008) A highly selective DNAzyme sensor for mercuric ions. Angew Chem Int Ed 47: 4346-4350.
73. Huang PJ, Liu J (2014) Sensing parts-per-trillion Cd^{2+}, Hg^{2+}, and Pb^{2+} collectively and individually using phosphorothioate DNAzymes. Anal Chem 86: 5999-6005.
74. Huang PJ, Lin J, Cao J, Vazin M, Liu J (2014) Ultrasensitive DNAzyme beacon for lanthanides and metal speciation. Anal Chem 86: 1816-1821.
75. Huang PJ, Vazin M, Liu J (2014) In vitro selection of a new lanthanide-dependent DNAzyme for ratiometric sensing lanthanides. Anal Chem 86: 9993-9999.
76. Isaka Y (2007) DNAzymes as potential therapeutic molecules. Curr Opin Mol Ther 9: 132-136.
77. Schlosser K, Li Y (2009) Biologically inspired synthetic enzymes made from DNA. Chem Biol 16: 311-322.

78. Liu J, Lu Y (2003) A colorimetric lead biosensor using DNAzyme-directed assembly of gold nanoparticles. J Am Chem Soc 125: 6642-6643.
79. Lermer L, Roupioz Y, Ting R, Perrin DM (2002) Toward an RNaseA mimic: A DNAzyme with imidazoles and cationic amines. J Am Chem Soc 124: 9960-9961.
80. Taylor AI, Pinheiro VB, Smola MJ, Morgunov AS, Peak-Chew S, et al. (2014) Catalysts from synthetic genetic polymers. Nature.
81. Taylor AI, Arangundy-Franklin S, Holliger P (2014) Towards applications of synthetic genetic polymers in diagnosis and therapy. Curr Opin Chem Biol 22C: 79-84.
82. Doudna JA, Cech TR (2002) The chemical repertoire of natural ribozymes. Nature 418: 222-228.
83. Silverman SK (2010) DNA as a versatile chemical component for catalysis, encoding, and stereocontrol. Angew Chem Int Ed 49: 7180-7201.
84. Parker DJ, Xiao Y, Aguilar JM, Silverman SK (2013) DNA catalysis of a normally disfavored RNA hydrolysis reaction. J Am Chem Soc 135: 8472-8475.
85. Li Y, Breaker RR (1999) Kinetics of RNA Degradation by Specific Base Catalysis of Transesterification Involving the 2‘-Hydroxyl Group. J Am Chem Soc 121: 5364-5372.
86. Schroeder GK, Lad C, Wyman P, Williams NH, Wolfenden R (2006) The time required for water attack at the phosphorus atom of simple phosphodiesters and of DNA. Proc Natl Acad Sci U S A 103: 4052-4055.
87. Jenne A, Gmelin W, Raffler N, Famulok M (1999) Real-Time Characterization of Ribozymes by Fluorecence Resonance Energy Transfer (FRET). Angew Chem Int Ed 38: 1300-1303.
88. Vitiello D, Pecchia DB, Burke JM (2000) Intracellular ribozyme-catalyzed trans-cleavage of RNA monitored by fluorescence resonance energy transfer. RNA 6: 628-637.
89. Stojanovic MN, de Prada P, Landry DW (2000) Homogeneous assays based on deoxyribozyme catalysis. Nucleic Acids Res 28: 2915-2918.

90. Perkins TA, Wolf DE, Goodchild J (1996) Fluorescence resonance energy transfer analysis of ribozyme kinetics reveals the mode of action of a facilitator oligonucleotide. Biochemistry 35: 16370-16377.
91. Walter NG, Burke JM (1997) Real-time monitoring of hairpin ribozyme kinetics through base-specific quenching of fluorescein-labeled substrates. RNA 3: 392-404.
92. Lu Y, Liu J, Li J, Bruesehoff PJ, Pavot CM, et al. (2003) New highly sensitive and selective catalytic DNA biosensors for metal ions. Biosens Bioelectron 18: 529-540.
93. Liu J, Lu Y (2003) Improving fluorescent DNAzyme biosensors by combining inter- and intramolecular quenchers. Anal Chem 75: 6666-6672.
94. Chiuman W, Li Y (2006) Evolution of high-branching deoxyribozymes from a catalytic DNA with a three-way junction. Chem Biol 13: 1061-1069.
95. Chiuman W, Li Y (2007) Efficient signaling platforms built from a small catalytic DNA and doubly labeled fluorogenic substrates. Nucleic Acids Res 35: 401-405.
96. Kandadai SA, Mok WW, Ali MM, Li Y (2009) Characterization of an RNA-cleaving deoxyribozyme with optimal activity at pH 5. Biochemistry 48: 7383-7391.
97. Shen Y, Mackey G, Rupcich N, Gloster D, Chiuman W, et al. (2007) Entrapment of fluorescence signaling DNA enzymes in sol-gel-derived materials for metal ion sensing. Anal Chem 79: 3494-3503.
98. Liu Z, Mei SH, Brennan JD, Li Y (2003) Assemblage of signaling DNA enzymes with intriguing metal-ion specificities and pH dependences. J Am Chem Soc 125: 7539-7545.
99. Kim JH, Han SH, Chung BH (2011) Improving Pb^{2+} detection using DNAzyme-based fluorescence sensors by pairing fluorescence donors with gold nanoparticles. Biosens Bioelectron 26: 2125-2129.
100. Wang H-B, Wang L, Huang K-J, Xu S-P, Wang H-Q, et al. (2013) A highly sensitive and selective biosensing strategy for the detection of Pb^{2+} ions based on GR-5 DNAzyme functionalized AuNPs. New J of Chem 37: 2557-2563.
101. Wang L, Jin Y, Deng J, Chen G (2011) Gold nanorods-based FRET assay for sensitive detection of Pb^{2+} using 8-17DNAzyme. Analyst 136: 5169-5174.

102. Van Lehn RC, Atukorale PU, Carney RP, Yang YS, Stellacci F, et al. (2013) Effect of particle diameter and surface composition on the spontaneous fusion of monolayer-protected gold nanoparticles with lipid bilayers. Nano Lett 13: 4060-4067.
103. Wu P, Hwang K, Lan T, Lu Y (2013) A DNAzyme-gold nanoparticle probe for uranyl ion in living cells. J Am Chem Soc 135: 5254-5257.
104. Yang R, Jin J, Chen Y, Shao N, Kang H, et al. (2008) Carbon nanotube-quenched fluorescent oligonucleotides: probes that fluoresce upon hybridization. J Am Chem Soc 130: 8351-8358.
105. Lu CH, Yang HH, Zhu CL, Chen X, Chen GN (2009) A graphene platform for sensing biomolecules. Angew Chem Int Ed Engl 48: 4785-4787.
106. Zheng M, Jagota A, Semke ED, Diner BA, McLean RS, et al. (2003) DNA-assisted dispersion and separation of carbon nanotubes. Nat Mater 2: 338-342.
107. Yao J, Li J, Owens J, Zhong W (2011) Combing DNAzyme with single-walled carbon nanotubes for detection of Pb(II) in water. Analyst 136: 764-768.
108. Zhao XH, Kong RM, Zhang XB, Meng HM, Liu WN, et al. (2011) Graphene-DNAzyme based biosensor for amplified fluorescence "turn-on" detection of Pb^{2+} with a high selectivity. Anal Chem 83: 5062-5066.
109. Wang DY, Lai BH, Sen D (2002) A general strategy for effector-mediated control of RNA-cleaving ribozymes and DNA enzymes. J Mol Biol 318: 33-43.
110. Nutiu R, Li Y (2003) Structure-Switching Signaling Aptamers. J Am Chem Soc 125: 4771-4778.
111. Achenbach JC, Nutiu R, Li Y (2005) Structure-switching allosteric deoxyribozymes. Anal Chim Acta 534: 41-51.
112. Chiuman W, Li Y (2007) Simple fluorescent sensors engineered with catalytic DNA 'MgZ' based on a non-classic allosteric design. PLoS One 2: e1224.
113. Ali MM, Aguirre SD, Lazim H, Li Y (2011) Fluorogenic DNAzyme probes as bacterial indicators. Angew Chem Int Ed 50: 3751-3754.

114. Elghanian R, Storhoff JJ, Mucic RC, Letsinger RL, Mirkin CA (1997) Selective colorimetric detection of polynucleotides based on the distance-dependent optical properties of gold nanoparticles. Science 277: 1078-1081.
115. Liu J, Lu Y (2004) Accelerated color change of gold nanoparticles assembled by DNAzymes for simple and fast colorimetric Pb^{2+} detection. J Am Chem Soc 126: 12298-12305.
116. Zhao W, Lam JC, Chiuman W, Brook MA, Li Y (2008) Enzymatic cleavage of nucleic acids on gold nanoparticles: a generic platform for facile colorimetric biosensors. Small 4: 810-816.
117. Liu J, Lu Y (2004) Adenosine-dependent assembly of aptazyme-functionalized gold nanoparticles and its application as a colorimetric biosensor. Anal Chem 76: 1627-1632.
118. Xiao Y, Qu X, Plaxco KW, Heeger AJ (2007) Label-free electrochemical detection of DNA in blood serum via target-induced resolution of an electrode-bound DNA pseudoknot. J Am Chem Soc 129: 11896-11897.
119. Liang J, Chen Z, Guo L, Li L (2011) Electrochemical sensing of L-histidine based on structure-switching DNAzymes and gold nanoparticle-graphene nanosheet composites. Chem Commun 47: 5476-5478.
120. Shen L, Chen Z, Li Y, He S, Xie S, et al. (2008) Electrochemical DNAzyme sensor for lead based on amplification of DNA-Au bio-bar codes. Anal Chem 80: 6323-6328.
121. Yang X, Xu J, Tang X, Liu H, Tian D (2010) A novel electrochemical DNAzyme sensor for the amplified detection of Pb^{2+} ions. Chem Commun (Camb) 46: 3107-3109.
122. Song S, Wang L, Li J, Fan C, Zhao J (2008) Aptamer-based biosensors. TrAC Trends in Analytical Chemistry 27: 108-117.
123. Strehlitz B, Nikolaus N, Stoltenburg R (2008) Protein Detection with Aptamer Biosensors. Sensors 8: 4296-4307.

124. Sefah K, Phillips JA, Xiong X, Meng L, Van Simaeys D, et al. (2009) Nucleic acid aptamers for biosensors and bio-analytical applications. Analyst 134: 1765-1775.
125. Lau PS, Li Y (2011) Functional nucleic acids as molecular recognition elements for small organic and biological molecules. Curr Org Chem 15: 557-575.
126. Jhaveri SD, Kirby R, Conrad R, Maglott EJ, Bowser M, et al. (2000) Designed Signaling Aptamers that Transduce Molecular Recognition to Changes in Fluorescence Intensity. J Am Chem Soc 122: 2469-2473.
127. Yamana K, Ohtani Y, Nakano H, Saito I (2003) Bis-pyrene labeled DNA aptamer as an intelligent fluorescent biosensor. Bioorg Med Chem Lett 13: 3429-3431.
128. Jhaveri S, Rajendran M, Ellington AD (2000) In vitro selection of signaling aptamers. Nat Biotechnol 18: 1293-1297.
129. Ueyama H, Takagi M, Takenaka S (2002) A novel potassium sensing in aqueous media with a synthetic oligonucleotide derivative. Fluorescence resonance energy transfer associated with Guanine quartet-potassium ion complex formation. J Am Chem Soc 124: 14286-14287.
130. Urata H, Nomura K, Wada S, Akagi M (2007) Fluorescent-labeled single-strand ATP aptamer DNA: chemo- and enantio-selectivity in sensing adenosine. Biochem Biophys Res Commun 360: 459-463.
131. Yang CJ, Jockusch S, Vicens M, Turro NJ, Tan W (2005) Light-switching excimer probes for rapid protein monitoring in complex biological fluids. Proc Natl Acad Sci U S A 102: 17278-17283.
132. Stojanovic MN, de Prada P, Landry DW (2001) Aptamer-based folding fluorescent sensor for cocaine. J Am Chem Soc 123: 4928-4931.
133. Lau PS, Coombes BK, Li Y (2010) A general approach to the construction of structure-switching reporters from RNA aptamers. Angew Chem Int Ed 49: 7938-7942.
134. Xiao Y, Piorek BD, Plaxco KW, Heeger AJ (2005) A reagentless signal-on architecture for electronic, aptamer-based sensors via target-induced strand displacement. J Am Chem Soc 127: 17990-17991.

135. Liu J, Mazumdar D, Lu Y (2006) A simple and sensitive "dipstick" test in serum based on lateral flow separation of aptamer-linked nanostructures. Angew Chem Int Ed 45: 7955-7959.
136. Zhao W, Brook MA, Li Y (2008) Design of gold nanoparticle-based colorimetric biosensing assays. Chembiochem 9: 2363-2371.
137. Zhao W, Chiuman W, Brook MA, Li Y (2007) Simple and rapid colorimetric biosensors based on DNA aptamer and noncrosslinking gold nanoparticle aggregation. Chembiochem 8: 727-731.
138. Li F, Zhang J, Cao X, Wang L, Li D, et al. (2009) Adenosine detection by using gold nanoparticles and designed aptamer sequences. Analyst 134: 1355-1360.

Chapter 2

Translating Bacterial Detection by DNAzymes into a Litmus Test

2.1 Introduction

Portable sensors are highly desirable for environmental monitoring, food safety control, and medical surveillance, particularly in resource-limited regions.[1-3] Colorimetric sensors represent an attractive option as the change of color can be easily detected by the naked eye. The Litmus test for pH is a well-established and cheap colorimetric sensor that is still being widely used today. Existing litmus dyes and pH papers respond to pH changes by producing a color signal. By devising a method that links a molecular recognition event to the pH change of the sensing solution, we can take advantage of these inexpensive litmus dyes and pH papers to detect other targets.

Urease catalyzes the hydrolysis of urea into carbon dioxide and ammonia.[4-6] The hydrolytic reaction raises the pH value of the solution. Urease is highly efficient, speeding up the hydrolysis of urea by about 10^{14} times. Urease is also a stable enzyme and various forms of ureases are commercially available.[7,8] Thus, we postulate that urease in combination with litmus dyes (or pH papers) are suited for the development of colorimetric biosensors. To do so, a strategy is required to couple a molecular recognition event to the activity of urease.

Functional nucleic acids, particularly DNA aptamers and aptazymes (aptamer-regulated DNAzymes), have been shown to be excellent molecular recognition elements because they offer high affinity and specificity for their cognate targets, and they are stable and cost-effective.[9-31] Many aptazymes have been engineered using RNA-cleaving DNAzymes, where target binding triggers the cleavage of an RNA-containing substrate.[32-38] Some of these aptazymes have been linked to signal-generation modules to produce fluorescent, colorimetric, and electrochemical readouts.[39-41] As we will show herein, the RNA cleavage system also offers a convenient way to link the action of an aptazyme to the activity of urease through the use of magnetic beads. The ease of separation makes magnetic beads (MBs) an attractive option to immobilize biomacromolecules,[42] and thus they have been widely used to set up bioassays.[43-46]

2.2 Results and Discussion

The conceptual framework is illustrated in Figure 2-1. Four components are utilized: streptavidin-coated MBs, an aptazyme, urease conjugated to a DNA oligonucleotide (UrDNA), and a pH-sensitive dye (or pH paper). The aptazyme contains a biotin moiety at its 5' end for streptavidin binding and a sequence extension at its 3' end for hybridization with UrDNA. Thus, simple mixing of the MBs, the aptazyme, and the UrDNA results in functional MBs that can release urease in response to the target of the aptazyme (Figure 2-1A). Upon magnetic separation, the freed urease can be used to hydrolyze urea in the presence of a litmus dye for color generation (Figure 2-1B).

The above design is compatible with any RNA-cleaving aptazyme; however for the current demonstration, we employed a DNAzyme, EC1, previously developed in our laboratory for the specific detection of Escherichia coli (*E. coli*), a model bacterial pathogen.[47,48] Pathogenic bacteria pose a grave threat to public health and safety, and early detection of specific pathogens is an important step towards preventing a potential outbreak. However, laborious and expensive pathogen tests often represent a bottleneck in such efforts, particularly in resource-limited regions. A simple litmus test for pathogen detection offers a very attractive option.

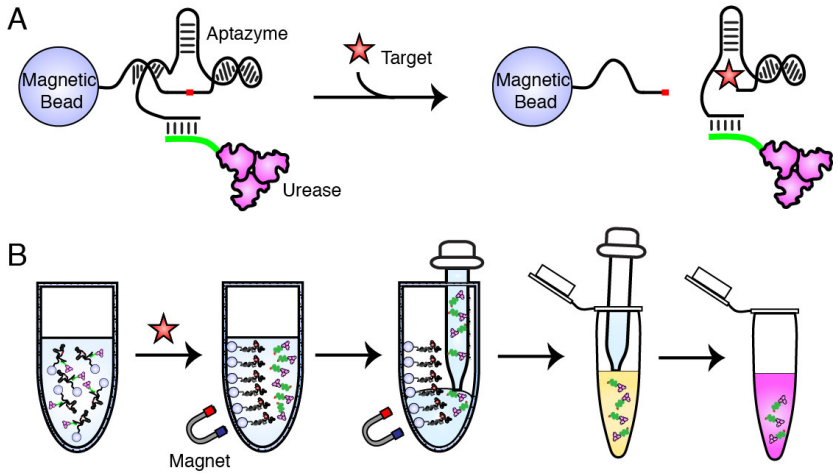

Figure 2-1. Conceptual schematic representation. A) Cleavage reaction. The binding of the cognate target to the aptazyme on the magnetic bead triggers its cleavage activity, thereby resulting in the release of urease. B) Colorimetric reporting assay. Upon target-induced cleavage and magnetic separation, the urease is used to hydrolyze urea in the presence of a litmus dye.

A bifunctional linker, maleimidobenzoic acid N-hydroxysuccinimide ester (MBS), was used to achieve the conjugation of a 5'-amino-modified DNA oligonucleotide (H_2NDNA) to urease (Figure 2-2A). H_2N-DNA was first allowed to react with MBS,

which resulted in maleimidobenzoic DNA amide (MDA). This was followed by the coupling of urease to MDA through the addition of thiol to the double bond of the maleimide. By using a fluorescently labeled DNA, we showed that this method was able to achieve successful coupling of H_2N-DNA to urease (Figure 2-2B).

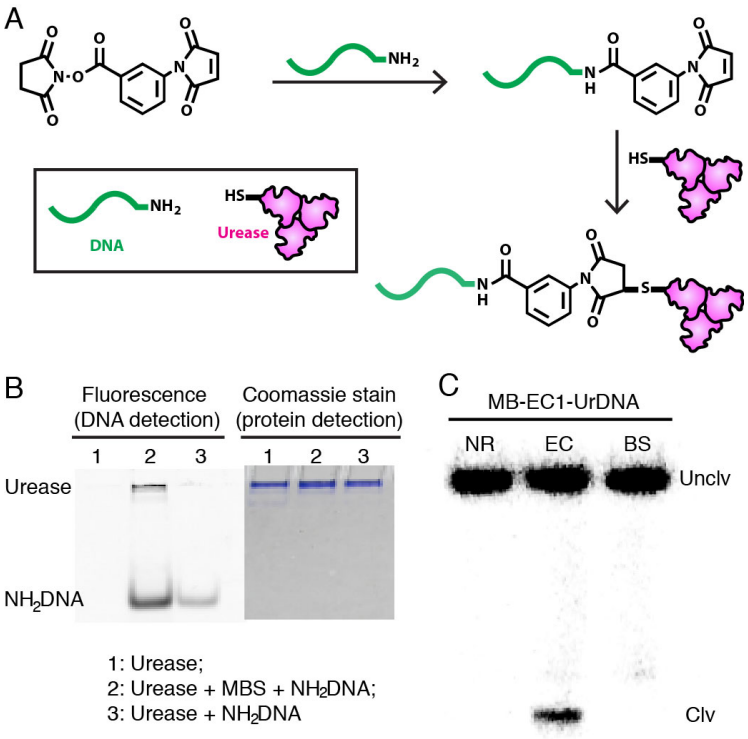

Figure 2-2. Synthesis and functional test of the sensor construct. (A) Conjugation of 5′-amino modified DNA to urease using MBS. (B) Analysis of DNA-urease conjugation mixtures using non-denaturing PAGE. (C) Functional test. Clv: cleavage product; Unclv: uncleaved construct. Note: EC1 was radioactively labeled.

The functionality of the MB-EC1-UrDNA was examined by treating the MB conjugates with the crude cellular extract (CCE) prepared from *E. coli* (EC; intended bacteria) or Bacillus subtilis (BS; a negative control; we have previously shown that EC1

can not be activated by CCEs from a host of bacteria including *B. subtilis*).[47,48] The cleavage activity was analyzed by denaturing polyacrylamide gel electrophoresis (dPAGE); for this reason, EC1 was internally labeled with 32^{P} so that the cleavage of EC1 would result in a DNA fragment that could be detected by dPAGE. We found MB-EC1- UrDNA can indeed be activated by CCE-EC, but not by CCE-BS (Figure 2-2C).

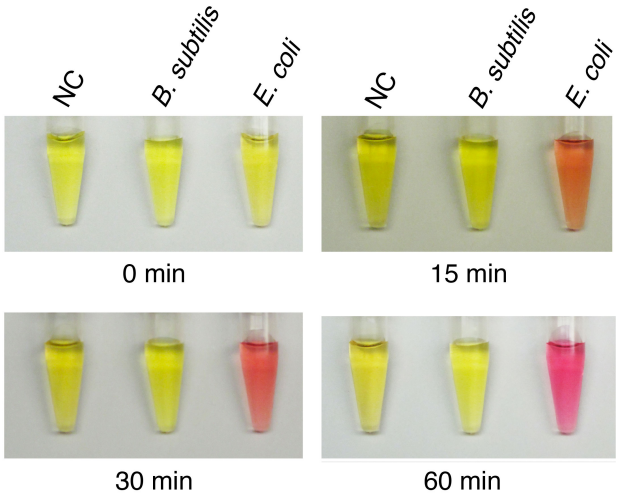

Figure 2-3. Litmus test with reaction buffer alone (left tube of each panel), CCE prepared from 10^{7} of *B. subtilis* cells (middle), or *E. coli* cells (right). The photographs were taken at 0, 15, 30 and 60 minutes.

We next carried out the litmus test for *E. coli* using phenol red as the litmus dye because in our preliminary test it produced a rather sharp, yellow-to-pink transition. The procedure consisted of two separate reactions: *E. coli* induced a probe cleavage reaction and urease mediated a reporting reaction. The cleavage reaction was conducted at room temperature for 60 min in 1 x reaction buffer (1× RB; 1 mM HEPES, pH 7.4, 150 mM NaCl, 15 mM MgCl2, 0.01% tween 20) containing CCE-EC or CCE-BS prepared from

10^7 *E. coli* or *B. subtlis* cells, respectively (total reaction volume was 10 mL). This was followed by a 10-fold dilution with H2O to facilitate the magnetic separation and minimize the impact of the buffering agent on the reporting reaction. After magnetic separation, 70 mL of the diluted cleavage solution were mixed with 100 mL of a urea-containing solution (2 M NaCl, 60 mM MgCl2, 50mM urea, 1 mM HCl) and 10 mL of 0.04% phenol red. This resulted in a new reaction mixture with an initial pH value of approximately 5.5; at this pH value, phenol red exhibits a yellow color. As shown in Figure 2-3 the reaction mixture from CCE-EC changed its color within 15 min from yellow to brownish pink, which continued to intensify into bright pink within 60 min. In sharp contrast, the color of the reaction mixture originating either from RB alone or from CCE-BS remained unchanged.

We then examined the functionality of the litmus test in complex sample matrices represented by apple juice, milk, and lake water (see Figure 2-4). This experiment shows that background materials present in these complex samples do not significantly affect the outcome of the litmus test.

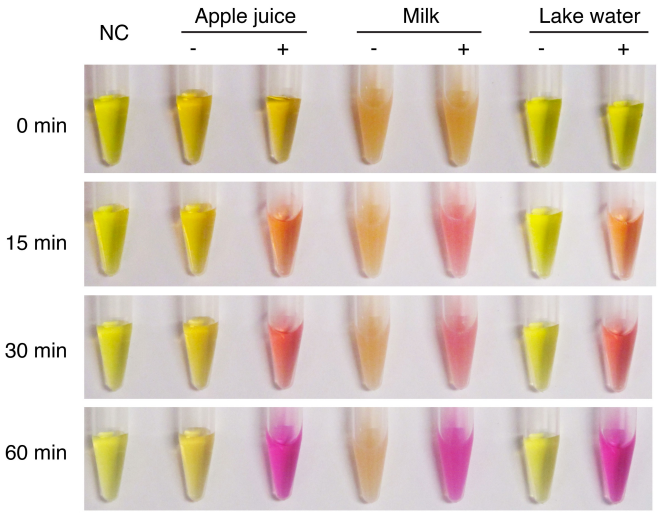

Figure 2-4. Detection of *E. coli* in the presence of complex sample matrices represented by apple juice, milk, and lake water. NC: negative control with pure reaction buffer. "+": 10^7 *E. coli* cells added to a test sample. "-": a test sample without added *E. coli* cells. Photographs were taken after a signal-producing time of 0-60 minutes.

Several other dyes were then examined for the same assay, including bromothymol blue, neutral red, cresol red, m-cresol purple, and o-cresolphthalein complexone (see Figure 2-5). It is apparent from the results that any of these dyes are compatible with our assay.

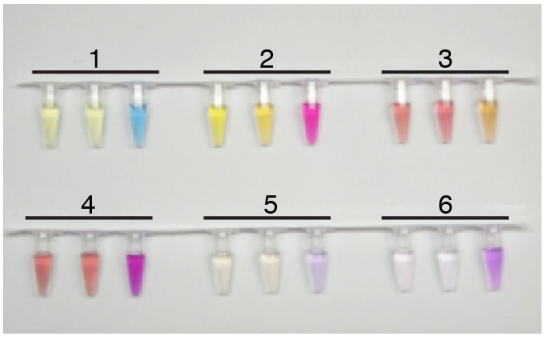

Figure 2-5. Color responses of six pH-sensitive dyes in the hydrolytic reaction of urea by urease. MB-EC1-UrDNA was treated with reaction buffer (RB) only, CCE-BS prepared from 10^7 *Bacillus subtilis* cells, or CCE-EC from 10^7 *E. coli* cells for 2 hours. After magnetic separation, the supernatant from each cleavage reaction (RB, CCE-BS and CCE-EC) was incubated with a urea solution containing one of the following 6 dyes: 1, bromothymol blue; 2, phenol red; 3, neutral red; 4, cresol red; 5, m-cresol purple; 6, o-cresolphthalein complexone. For each dye, the left, middle and right tubes contained RB only, CCE-BS and CCE-EC, respectively. Photographs were taken after a signal-producing time of 60 minutes.

We next measured the time-dependent increase in the pH value of the reporting solution using a hand-held pH meter (Figure 2-6A). The pH value increased nearly 3 pH units for the *E. coli* sample, while the pH value of the control samples (either buffer only or *B. subtilis* samples) remained unchanged.

We also monitored the changes in the pH value of these samples using commercially available pH paper strips (Figure 2-6B). Once again, while the control samples produced no detectable color change on the pH paper, a notable color change can be detected within 10 min with the *E. coli* sample. The results from all the experiments above show that the devised method can indeed be used to achieve target-specific

detection using simple methods that include the color change of litmus dyes in solution, color change of a pH paper, and electronic readings using a hand-held pH meter.

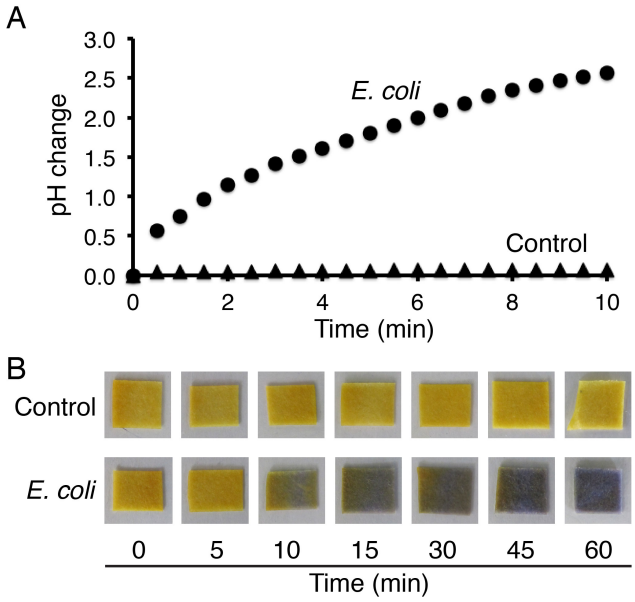

Figure 2-6. Monitoring pH changes caused by the presence of 10^7 *E. coli* cells *via* electronic reading with a hand-held pH meter (A) and pH paper strips (B).

We determined the sensitivity of our assay using phenol red. Eight CCE-EC samples were prepared from serially diluted *E. coli* samples, each of which contained the specific number of cells shown in Figure 2-7. A sharp color transition was observed for the sample containing 5×10^5 cells after color development for both 1 hour (top panel) or 2 hours (bottom panel). A subtle but detectable color transition, in comparison to the two reference samples (5×10^7 *B. subtilis* cells and RB alone), was observed for the sample containing 5000 cells after incubation for 1 hour and 500 cells after incubation for 2 hours. For comparison, polymerase chain reaction (PCR) and sandwich enzyme-linked

immunosorbent assay (ELISA) approaches, two popular pathogen detection methods, offer detection limits of approximately 10^4–10^5 *E. coli* cells.[49-54] Thus, our litmus test offers comparable detection sensitivity.

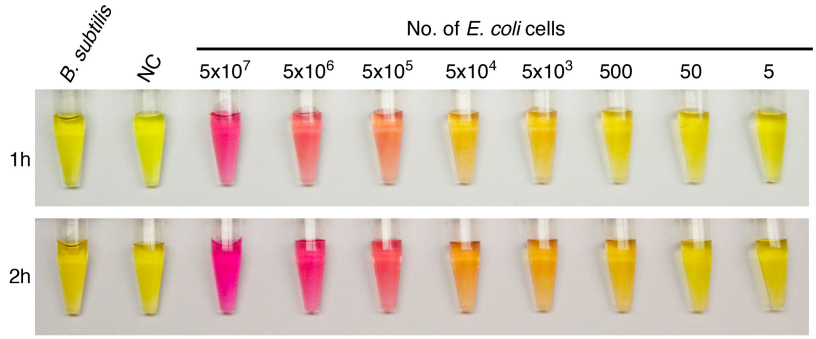

Figure 2-7. Litmus test with CCE-EC prepared from varying numbers of *E. coli* cells. The photograph was taken after a signal-producing time of 1 hour (top panel) or 2 hours (bottom).

Methods for the practical detection of food or waterborne pathogens such as *E. coli* are required to detect as low as 1–100 colony-forming units (CFUs). To achieve this level of detection sensitivity, an enrichment step through culturing is necessary. For this consideration, we also examined the ability of the litmus test to detect a single CFU of *E. col*i with a culturing step. The combined culturing/litmus test can easily detect a single CFU after 7 h of culturing (Figure 2-8), which is comparable to the popular PCR (ca. 10 h) and ELISA (ca. 16 h) methods.[49-54]

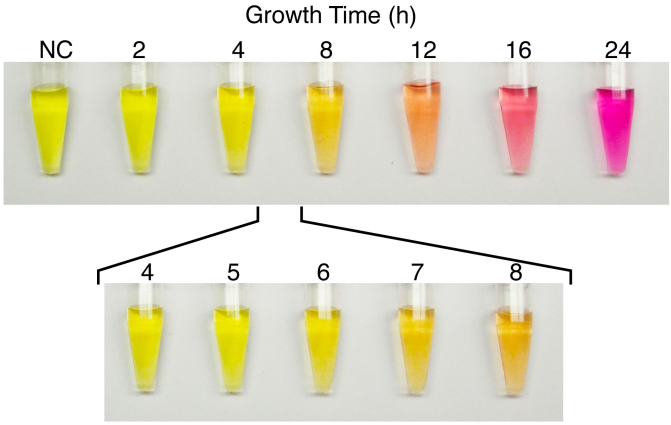

Figure 2-8. Detection of a single colony-forming unit of *E. coli* using the litmus test following varying hours of culturing. Photographs were taken after a signal-producing time of 60 minutes.

In summary, we have developed a litmus test for *E. coli* that uses an RNA-cleaving DNAzyme as the molecular recognition element and protein enzyme urease as the signal transducer. Our sensing system also takes advantage of magnetic separation, which is easy to implement, and pH sensitive dyes or pH paper strips, which are cheap and widely available. To our knowledge, this is the first example where a molecular recognition event of an aptazyme (or any functional nucleic acid) is translated into a pH change. The litmus test exhibits a sensitivity similar to that of the fluorescence-based detection method we published earlier using the same DNAprobe,[47,48] however the colorimetric test is simple to perform and does not require specialized equipment, and therefore is better suited for field applications, particularly in developing countries.

Although an *E. coli*-sensing aptazyme was used in the current study, the sensor design can be easily extended to any RNA-cleaving aptazyme. Similarly, the design principle should be broadly compatible with any system in which a cleavable substrate (for the detection for an enzyme or factors that activate the enzyme) can be coupled to urease.

2.3 Materials and Method

2.3.1 Enzymes, chemicals and other materials.

T4 DNA ligase, T4 polynucleotide kinase (PNK) and ATP were purchased from Thermo Scientific. [γ-32P]dATP were purchased from Perkin Elmer. Streptavidin coated magnetic beads of 1.5 μm (BioMag-SA) was purchased from Bangs Laboratories Inc. Urease powder from *Canavalia ensiformis* (Jack bean), maleimidobenzoic acid N-hydroxy-succinimide ester (MBS), phenol red, bromothymol blue sodium salt, neutral red, cresol red, m-cresol purple, o- cresolphthalein complexone, were obtained from Sigma-Aldrich. All other chemicals were purchased from Bioshop Canada and used without further purification. The water used in this study was double- deionized (ddH_2O) and autoclaved. Milk (Beatrice skim milk) and apple juice (Minute Maid) were purchased from a local supermarket. Lake water was fetched from Lake Ontario.

2.3.2 Synthesis and purification of oligonucleotides.

Five synthetic oligonucleotides were used in this study; their sequences and functions are provided in the table below. The unmodified DNA oligonucleotides were purchased from Integrated DNA Technologies (IDT) and the modified oligonucleotides were obtained from the Keck Facility at Yale University. All DNA oligonucleotides were purified by 10% denaturing (8 M urea) polyacrylamide gel electrophoresis (dPAGE), and their concentrations were determined spectroscopically.

2.3.3 Synthesis of the aptazyme EC1.

DE1 (2 nmol) was phosphorylated (reaction volume: 50 μL) at 37°C with 10 units (U) of PNK in 1× PNK buffer A containing 2 mM ATP (final concentration) for 20 min. The reaction was quenched by heating the mixture at 90°C for 5 min. Upon cooling to room temperature, equimolar BS1 and T1 were added. The resultant DNA mixture was then heated to 90°C for 1 min and cooled to room temperature. Then, 10 μL of 10× DNA ligase buffer and 10 U of T4 DNA Ligase were added, along with enough ddH2O to make the final volume to be 100 μL. This was followed by incubation at room temperature for 2 h. The DNA was then concentrated by ethanol precipitation and the ligated EC1 was purified by 10% dPAGE.

Table 2-1. Sequences used for making the Ur-DNA probe

Name	**Labels**	**Sequence**	**Note**
BS1	5′-Biotin; adenine ribonucleotide (R); fluorescein-dT (F); dabcyl-dT (Q)	5″-TTTTT TTTTT TTACT CTTCC TAGCF RQGGT TCGAT CAAGA-3″	Substrate
DE1	None	5″-GATGT GCGTT GTCGA GACCT GCGAC CGGAA CACTA CACTG TGTGG GGATG GATTT CTTTA CAGTT GTGTG *TTGAA CGCTG TGTCA AAAAA AAAA*-3″	DNAzyme with an extension (italic letters) that can hybridize to LD1
T1	None	5″-GACAA CGCAC ATCTC TTGAT CGAAC C-3″	Template for ligating BS1 to DE1
LD1	5′-NH2	5″-TTTTT T*TTTT TTTTT TGACA CAGCG TTCAA*-3″	DNA for coupling to urease
LD2	5′-NH2 and 3′-FAM	5″-TTTTT T*TTTT TTTTT TGACA CAGCG TTCAA*-3″	FAM-tagged LD1

For the labeling of the same construct with 32P, 2 nmol of DE1 was phosphorylated (reaction volume: 50 μL) at 37°C with 10 U of PNK in 1× PNK buffer A containing 10 μCi [γ-32P]ATP for 20 min. This was followed by addition of 2 μL of 100 mM ATP and further incubation at 37°C for 20 min. The rest of the procedure was identical to the one described above for the synthesis of non-radioactive EC1.

2.3.4 DNA-urease conjugation.

An MBS solution (6.4 mM) was made by dissolving 2 mg MBS (6.4 μmol) in 1 mL of dimethyl sulphoxide (DMSO). Similarly a urease solution was produced by dissolving 1.5 mg urease (3.3 nmol) powder in 1 mL of 1× PBS buffer (pH 7.2). 1 nmol LD1 (or LD2) and 3.2 μL of the MBS solution (20 nmol) were mixed and adjusted to a final reaction volume of 100 μL with 1× PBS buffer, and allowed to react at room temperature. After 1 h, the mixture was passed through a membrane based molecular sizing centrifugal column with a molecular weight cut-off of 3,000 Daltons (NANOSEP OMEGA, Pall Incorporation) in order to remove excess MBS. The column was washed with 50 μL of 1× PBS buffer 3 times and the DNA was resuspended in 100 μL of 1× PBS buffer. The urease solution (1 mL, 3.3 nmol) was then added to the MBS activated DNA. The conjugation reaction was allowed to proceed at room temperature for 1 h. The mixture was filtered through 300,000-Dalton cut-off centrifugal column. The DNA-urease conjugate (UrDNA) was then washed with 50 μL of 1× PBS buffer 3 times, and resuspended in 100 μL of 1× PBS buffer. The concentration of the DNA-urease conjugate was estimated to be 10 μM.

2.3.5 Probe immobilization.

First, 100 μL of MB suspension (particle concentration: 1 mg/mL; 1 mg MB will bind >1000 pmol of a biotinated oligonucleotide, according to the manufacturer) was placed in a magnet holder to separate the supernatant and MB. MB was then washed with

100 μL of binding buffer (20 mM Tris-HCl, pH 8.0, 0.5 M NaCl) twice and resuspended in 100 uL of binding buffer. Then, 100 pmol EC1 was added, followed by incubation with mild shaking at room temperature for 1 h (it was found that more than 95% radioactive EC1 was bound to MB, consistent with the loading capacity of the MB specified by the manufacturer). After removing the supernatant, MB was washed twice with 100 μL of binding buffer. This was followed by the addition of 15 μL of 10 μM UrDNA (150 pmol) and 15 μL of 0.5 M NaCl. The mixture was then heated to 45°C for 2 min and then cooled to room temperature. After incubation at room temperature for 2 h, MB was magnetically separated from the supernatant, washed twice with 100 uL 1× reaction buffer (1× RB; 1 mM HEPES, pH 7.4, 150 mM NaCl, 15 mM MgCl2, 0.01% tween 20). The resultant MB-EC1-UrDNA was then resuspended in 100 μL of 1× RB and stored at 4°C. The EC1-UrDNA concentration of the suspension was estimated to be ~1 μM.

2.3.6 Preparation of bacterial cells.

E. coli K12 MG1655 was used as the intended bacterium and *Bacillus subtilis* 168 was used as the control. A single colony freshly grown on Luria Broth (LB) agar plate was taken and used to inoculate 2 mL of LB. After shaking at 37°C for 14 h, the bacterial culture was serially diluted in 10-fold intervals. 100 μL of each diluted solution were plated on the LB agar plates (5 repeats) and cultured at 37°C for 18 h to obtain the cell counts. For the experiment shown in Figure 2-7, the number of *E. coli* cells used were:

5×10^7, 5×10^6, 5×10^5, 5×10^4, 5×10^3 50^2, 50, and 5; the number of *B. subtilis* cells was 10^7. For the single cell experiment (Figure 2-8), six culture tubes containing 2 mL of LB were set up, each of which was inoculated with 100 μL of 0.005 CFU/μL glycerol stock and then incubated at 37 oC. A 0.3-mL solution was harvested from each tube at 2, 4, 5, 6, 7, 8, 12, 16 and 24 h.

Each cell suspension was centrifuged at 13,000 g for 20 min at 4°C. After the removal of the supernatant, the cells were stored at -20°C prior to the litmus test.

2.3.7 Litmus test.

E. coli and *B. subtilis* cells that were frozen at -20°C were resuspended in 10 μL of 1× RB, sonicated for 1 min, put on the ice for 1 min, and sonicated for 1 more min. The cell suspension was then centrifuged at 13,000 g for 5 min at 4°C. The supernatant (10 μL) was mixed with 10 pmol MB- EC1-UrDNA (10 μL of the 1 μM stock described earlier, washed 3 times with 50 μL of 1× RB) and suspension was incubated at room temperature for 1 h. It is worth noting that 5 pmol MB-EC1-UrDNA was the minimal amount of the conjugate required to achieve consistent experimental results. Then, 90 μL of ddH2O was added to the reaction vial. Following magnetic separation, 70 μL of the supernatant was transferred into a new reaction tube, followed by the addition of 100 μL of substrate solution (2 M NaCl, 60 mM MgCl2, 50 mM urea, 1 mM HCl) and 10 μL of 0.04% phenol red. Note that this reaction solution should have a starting pH of 5.5. A

photograph was taken after a signal-producing time of 0-2 h according to individual experiments for Figures 2-3 and 2-5.

2.3.8 Litmus test in complex matrices.

The milk and the lake water were directly used in this experiment without further treatment while the apple juice was adjusted to pH 7.4 using 0.2 M NaOH. First, 1 mL of each test sample was spiked with 10^7 *E. coli* cells while the control samples was not spiked with *E. coli*. The test and control samples were then centrifuged at 13,000 g for 5 min. The supernatant was removed and 20 µL of 1× RB was added to the pellet. The samples were then subjected to the litmus test as described immediately above. A photograph was taken after a signal-producing time of 0-60 min as specified in Figure 2-4.

2.3.9 Measuring pH changes using a hand-held pH meter.

A portable FiveGo pH meter equipped with an InLab Ultra-Micro electrode from Mettler Toledo was used to measure pH changes (Figure 2-6A). The cleavage reaction was performed using 10^7 *E. coli* cells. Following the litmus test procedure as described above, 70 µL of the supernatant was transferred into a new reaction tube followed by addition of 10 µL of 0.04% phenol red. The pH reaction was initiated by addition of 100 µL of the substrate solution. The pH electrode was placed directly into the vial and measurements were taken every 30 s for 10 min.

2.3.10 Monitoring pH changes using pH paper strips.

A pH sensitive paper, Hydrion MicroFine 5.5-8.0, purchased from MicroEssential Laboratories, was used to test the pH of reaction mixtures (Figure 2-6B). The cleavage reaction was performed using 10^7 *E. coli* cells. Similar to the litmus test outlined above, 70 µL of the supernatant was transferred into a new reaction tube followed by addition of 10 µL of ddH2O. The pH reaction was initiated by adding 100 µL of the substrate solution. The pH strip was cut into smaller square pieces that were dipped into the reaction vial at time points of 0, 5, 10, 15, 30, 45, and 60 min to generate Figure 2-6B.

2.4 References cited

1. Daar AS, Thorsteinsdottir H, Martin DK, Smith AC, Nast S, et al. (2002) Top ten biotechnologies for improving health in developing countries. Nat Genet 32: 229-232.
2. Newman JD, Turner AP (2005) Home blood glucose biosensors: a commercial perspective. Biosens Bioelectron 20: 2435-2453.
3. Turner AP (2013) Biosensors: sense and sensibility. Chem Soc Rev 42: 3184-3196.
4. Sumner JB, Hand DB (1929) Isoelectric point of crystalline urease. J Am Chem Soc 51: 1255-1260.
5. Karplus PA, Pearson M, Hausinger RP (1997) 70 Years of crystalline urease: What have we learned? Acc Chem Res 30: 330-337.
6. Dunn BE, Campbell GP, Perez-Perez GI, Blaser MJ (1990) Purification and characterization of urease from Helicobacter pylori. J Biol Chem 265: 9464-9469.

7. Stemke GW, Robertson JA, Nhan M (1987) Purification of urease from Ureaplasma urealyticum. Can J Microbiol 33: 857-862.
8. Clemens DL, Lee BY, Horwitz MA (1995) Purification, characterization, and genetic analysis of Mycobacterium tuberculosis urease, a potentially critical determinant of host-pathogen interaction. J Bacteriol 177: 5644-5652.
9. Bock LC, Griffin LC, Latham JA, Vermaas EH, Toole JJ (1992) Selection of single-stranded DNA molecules that bind and inhibit human thrombin. Nature 355: 564-566.
10. Ellington AD, Szostak JW (1990) In vitro selection of RNA molecules that bind specific ligands. Nature 346: 818-822.
11. Ellington AD, Szostak JW (1992) Selection in vitro of single-stranded DNA molecules that fold into specific ligand-binding structures. Nature 355: 850-852.
12. Tuerk C, Gold L (1990) Systematic evolution of ligands by exponential enrichment: RNA ligands to bacteriophage T4 DNA polymerase. Science 249: 505-510.
13. oyce GF (2004) Directed evolution of nucleic acid enzymes. Ann Rev Biochem 73: 791-836.
14. Famulok M, Hartig JS, Mayer G (2007) Functional aptamers and aptazymes in biotechnology, diagnostics, and therapy. Chem Rev 107: 3715-3743.
15. Brody EN, Gold L (2000) Aptamers as therapeutic and diagnostic agents. Rev Mol Biotechnol 74: 5-13.
16. Hermann T, Patel DJ (2000) Adaptive recognition by nucleic acid aptamers. Science 287: 820-825.
17. Famulok M, Mayer G, Blind M (2000) Nucleic acid aptamers - From selection in vitro to applications in vivo. Acc Chem Res 33: 591-599.
18. Mayer G (2009) The Chemical Biology of Aptamers. Angew Chem Int Ed 48: 2672-2689.
19. Li Y, Breaker RR (1999) Deoxyribozymes: new players in the ancient game of biocatalysis. Curr Opin Struct Biol 9: 315-323.

20. Baum DA, Silverman SK (2008) Deoxyribozymes: useful DNA catalysts in vitro and in vivo. Cell Mol Life Sci 65: 2156-2174.
21. Silverman SK (2010) DNA as a versatile chemical component for catalysis, encoding, and stereocontrol. Angew Chem Int Ed 49: 7180-7201.
22. Lee JH, Wang ZD, Liu JW, Lu Y (2008) Highly sensitive and selective colorimetric sensors for uranyl UO_2^{2+} : development and comparison of labeled and label-Free DNAzyme-Gold nanoparticle systems. J Am Chem Soc 130: 14217-14226.
23. Liu J, Lu Y (2007) Rational design of "Turn-On" allosteric DNAzyme catalytic beacons for aqueous mercury ions with ultrahigh sensitivity and selectivity. Angew Chem Int Ed 46: 7587-7590.
24. Wu PW, Hwang KV, Lan T, Lu Y (2013) A DNAzyme-Gold Nanoparticle Probe for Uranyl Ion in Living Cells. J Am Chem Soc 135: 5254-5257.
25. Xiang Y, Lu Y (2011) Using personal glucose meters and functional DNA sensors to quantify a variety of analytical targets. Nat Chem 3: 697-703.
26. Huang P-JJ, Liu J (2014) Sensing Parts-per-Trillion Cd^{2+}, Hg^{2+}, and Pb^{2+} Collectively and Individually Using Phosphorothioate DNAzymes. Anal Chem 86: 5999-6005.
27. Tang YT, Ge BX, Sen D, Yu HZ (2014) Functional DNA switches: rational design and electrochemical signaling. Chem Soc Rev 43: 518-529.
28. Navani NK, Li Y (2006) Nucleic acid aptamers and enzymes as sensors. Curr Opin Chem Biol 10: 272-281.
29. Liu JW, Cao ZH, Lu Y (2009) Functional Nucleic Acid Sensors. Chem Rev 109: 1948-1998.
30. Zhang HQ, Li F, Dever B, Li XF, Le XC (2013) DNA-Mediated Homogeneous Binding Assays for Nucleic Acids and Proteins. Chem Rev 113: 2812-2841.
31. Huang YC, Ge BX, Sen D, Yu HZ (2008) Immobilized DNA switches as electronic sensors for picomolar detection of plasma proteins. J Am Chem Soc 130: 8023-8029.

32. Breaker RR, Joyce GF (1994) A DNA enzyme that cleaves RNA. Chem Biol 1: 223-229.
33. Santoro SW, Joyce GF (1998) Mechanism and utility of an RNA-cleaving DNA enzyme. Biochemistry 37: 13330-13342.
34. Wang DY, Lai BHY, Sen D (2002) A general strategy for effector-mediated control of RNA-cleaving ribozymes and DNA enzymes. J Mol Biol 318: 33-43.
35. Ali MM, Li YF (2009) Colorimetric sensing by using allosteric-DNAzyme-coupled rolling circle amplification and a peptide nucleic acid-organic dye probe. Angew Chem Int Ed 48: 3512-3515.
36. Mei SH, Liu Z, Brennan JD, Li Y (2003) An efficient RNA-cleaving DNA enzyme that synchronizes catalysis with fluorescence signaling. J Am Chem Soc 125: 412-420.
37. Silverman SK (2005) In vitro selection, characterization, and application of deoxyribozymes that cleave RNA. Nucleic Acids Res 33: 6151-6163.
38. Schlosser K, Li Y (2009) Biologically inspired synthetic enzymes made from DNA. Chem Biol 16: 311-322.
39. Xiang Y, Tong AJ, Lu Y (2009) Abasic site-containing DNAzyme and aptamer for label-free fluorescent detection of Pb^{2+} and adenosine with high sensitivity, selectivity, and tunable dynamic range. J Am Chem Soc 131: 15352-15357.
40. Xiao Y, Rowe AA, Plaxco KW (2007) Electrochemical detection of parts-per-billion lead via an electrode-bound DNAzyme assembly. J Am Chem Soc 129: 262-263.
41. Liu J, Lu Y (2003) A colorimetric lead biosensor using DNAzyme-directed assembly of gold nanoparticles. J Am Chem Soc 125: 6642-6643.
42. Haukanes BI, Kvam C (1993) Application of magnetic beads in bioassays. Nature: Biotechnology 11: 60-63.
43. Johansen L, Nustad K, Orstavik TB, Ugelstad J, Berge A, et al. (1983) Excess antibody immunoassay for rat glandular kallikrein. Monosized polymer particles as the preferred solid phase material. J Immunol Methods 59: 255-264.

44. Gabrielsen OS, Hornes E, Korsnes L, Ruet A, Oyen TB (1989) Magnetic DNA affinity purification of yeast transcription factor tau - a new purification principle for the ultrarapid isolation of near homogeneous factor. Nucleic Acids Res 17: 6253-6267.
45. Brinchmann JE, Vartdal F, Gaudernack G, Markussen G, Funderud S, et al. (1988) Direct immunomagnetic quantification of lymphocyte subsets in blood. Clin Exp Immunol 71: 182-186.
46. Albretsen C, Kalland KH, Haukanes BI, Havarstein LS, Kleppe K (1990) Applications of magnetic beads with covalently attached oligonucleotides in hybridization: isolation and detection of specific measles virus mRNA from a crude cell lysate. Anal Biochem 189: 40-50.
47. Ali MM, Aguirre SD, Lazim H, Li Y (2011) Fluorogenic DNAzyme probes as bacterial indicators. Angew Chem Int Ed 50: 3751-3754.
48. Aguirre SD, Ali MM, Salena BJ, Li Y (2013) A sensitive DNA enzyme-based fluorescent assay for bacterial detection. Biomolecules 3: 563-577.
49. Omiccioli E, Amagliani G, Brandi G, Magnani M (2009) A new platform for Real-Time PCR detection of Salmonella, Listeria monocytogenes and Escherichia coli O157 in milk. Food Microbiol 26: 615-622.
50. Cui S, Schroeder CM, Zhang DY, Meng J (2003) Rapid sample preparation method for PCR-based detection of Escherichia coli O157:H7 in ground beef. J Appl Microbiol 95: 129-134.
51. Ibekwe AM, Watt PM, Grieve CM, Sharma VK, Lyons SR (2002) Multiplex fluorogenic real-time PCR for detection and quantification of Escherichia coli O157:H7 in dairy wastewater wetlands. Appl Environ Microbiol 68: 4853-4862.
52. Strachan NJ, Ogden ID (2000) A sensitive microsphere coagulation ELISA for Escherichia coli O157:H7 using Russell's viper venom. FEMS Microbiol Lett 186: 79-84.
53. de Boer E, Beumer RR (1999) Methodology for detection and typing of foodborne microorganisms. Int J Food Microbiol 50: 119-130.

54. Gracias KS, McKillip JL (2004) A review of conventional detection and enumeration methods for pathogenic bacteria in food. Can J Microbiol 50: 883-890.

Chapter 3

In vitro selection of an Efficient L-RNA Cleaving DNAzyme for Sensor Development

3.1 Introduction

Catalytic DNAs or DNAzymes are single-stranded DNA molecules that enhance the rate of chemical reactions. They are isolated from a random-sequence DNA library using an established technique known as *in vitro* selection.[1,2] The process of enriching for DNA sequences that can catalyze a chemical reaction was first demonstrated in by Breaker and Joyce in 1994 with a lead-ion dependent RNA-cleaving DNAzyme.[3] Since then, many DNAzymes have been discovered for catalyzing an impressive range of chemical reactions.[4-10] However, RNA-cleaving DNAzymes have been extensively studied for several reasons. First, the transesterification reaction involving RNA is well known in biology. Many protein enzymes and ribozymes rely on this chemistry to cleave RNA.[11-14] This creates a unique opportunity to compare catalytic abilities of DNA, RNA and protein. Second, the historical precedence of RNA-cleaving DNAzymes has directed the research community to use RNA cleavage as a model reaction to study DNA-based catalysis. In addition, many RNA cleaving DNAzymes are highly efficient, making them suitable candidates for therapeutic and biosensing applications.[15,16] For example, many biosensors have been created from RNA-cleaving DNAzymes to target a wide

range of analytes[17-24] using colorimetric, electrochemical, and fluorescence signal transduction mechanisms.[25-34]

Although research on RNA-cleaving DNAzyme biosensors has been fruitful, most of them have been designed to be responsive in clean and simple sample matrices. Very few examples have demonstrated the utility of such sensors in complex biological samples. This is because RNases are ubiquitous in biological samples and can cleave RNA with an efficiency that is often much higher than DNAzymes. Therefore, biosensors built with RNA-cleaving DNAzymes are prone to producing false-positive signals with biological samples. For this reason, there is a great need to develop RNase-resistant RNA-cleaving DNAzymes that are both efficient and compatible with biological samples.

With this motivation in mind, we set out to develop DNAzymes that cleave L-RNA, enantiomer of the natural D-RNA. L-RNA is known to be highly resistant to RNase degradation.[35] Since natural RNases cannot recognize L-RNA as a substrate, replacing D-RNA with L-RNA offers an attractive solution that productively utilizes RNA-cleaving DNAzymes for biosensing applications.

It has been previously shown that the enantiomeric difference between L- and D-isomers prevents extensive Watson-Crick interactions.[36,37] Thus it is possible that the use L-RNA as the cleavage site may post a challenge for DNAzyme isolation. However, it has also been shown that these stereoisomers are still capable of engaging each other through alternative structures.[38] The Joyce group set a precedency in 2002 by successfully isolating an L-RNA-cleaving DNAzyme from a random-sequence DNA

pool.[39] However, the reported DNAzyme exhibits a catalytic rate constant of 0.001 min^{-1}, which is several orders of magnitude inferior than best D-RNA-cleaving DNAzymes (with a rate constant up 10 min^{-1}).[34] The reduced catalytic rate makes this DNAzyme less desirable unsuited for biosensor engineering. Therefore, the key objective of our study is to develop a significantly more active L-RNA-cleaving DNAzyme.

Herein we report an L-RNA-cleaving DNAzyme that exhibits a catalytic rate constant of ~3 min^{-1}. We have also used this DNAzyme and a well-known ATP-binding DNA aptamer to construct a ligand-responsive biosensor. Finally we demonstrate that this biosensor can achieve ATP detection in biological samples that contain RNases.

3.2 Results

3.2.1 In vitro selection

A pool of 10^{14} molecules, denoted L1 and made of 60-nt (nt: nucleotide) random domain flanked by two 20-nt primer-binding sites, was used for the *in vitro* selection experiment (L1; Figure 3-1A). The in vitro selection scheme is shown in Figure 3-1A. L1 was first phosphorylated and ligated to a chimeric DNA/RNA substrate S1 that contains a single L-riboguanosine nucleotide (LrG) as the cleavage site (Figure 3-1B). Upon pufification using denaturing gel electrophoresis (dPAGE), the ligated construct was incubated for 60 minutes in the selection buffer that contains Mg^{2+} and Mn^{2+} as divalent metal ion cofactors (for the consideration that most RNA-cleaving DNAzymes require

divalent metal ions for high catalytic activity). The cleavage product was purified by dPAGE and subjected to two polymerase chain reactions (PCR1 and PCR2). PCR1 used two standard DNA primers, forward primer FP1 and reverse primer RP1; however PCR2 used FP1 and RP2, which contains an A20 tail separated by a non-amplifiable linker. Therefore, PCR2 produced two DNA strands with unequal sizes, which permits the separation of the coding strand by dPAGE. The purified DNA amplicon was used as the DNA pool for the next cycle of selective enrichment. After 5 rounds, a weak cleavage signal was observed. In order to isolate an efficient DNAzyme, the reaction time was reduced to 1 min for rounds 6 and 7, and then to 5 sec for rounds 8-10 (Figure 3-1C). The round-10 DNA pool was cloned and sequenced.

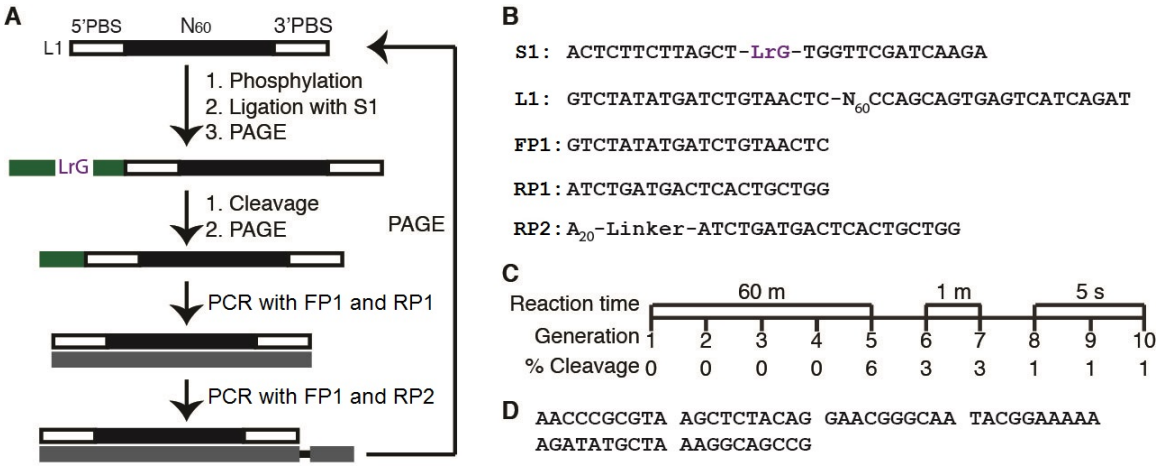

Figure 3-1. In vitro selection of L-RNA-cleaving DNAzymes. (A) *In vitro* selection scheme. (B) The sequences of the substrate (S1), DNA library (L1) and PCR primers (FP1, RP1 and RP2) used during *in vitro* selection. (C) The reaction time and percentage cleavage for each selection cycle. D) The sequence of LRD-B, which is featured in this study.

The top three clones are denoted LRD-A, LRD-B, and LRD-C (Figure 3-2). All three classes were capable of cleaving the attached S1 substrate. It was found that LRD-B (0.34 min^{-1}) was slightly more active than LRD-A (0.33 min^{-1}) whereas the catalytic rate of LRD-C was much smaller (0.04 min^{-1}, Figure 3-3). We chose LRD-B for further study.

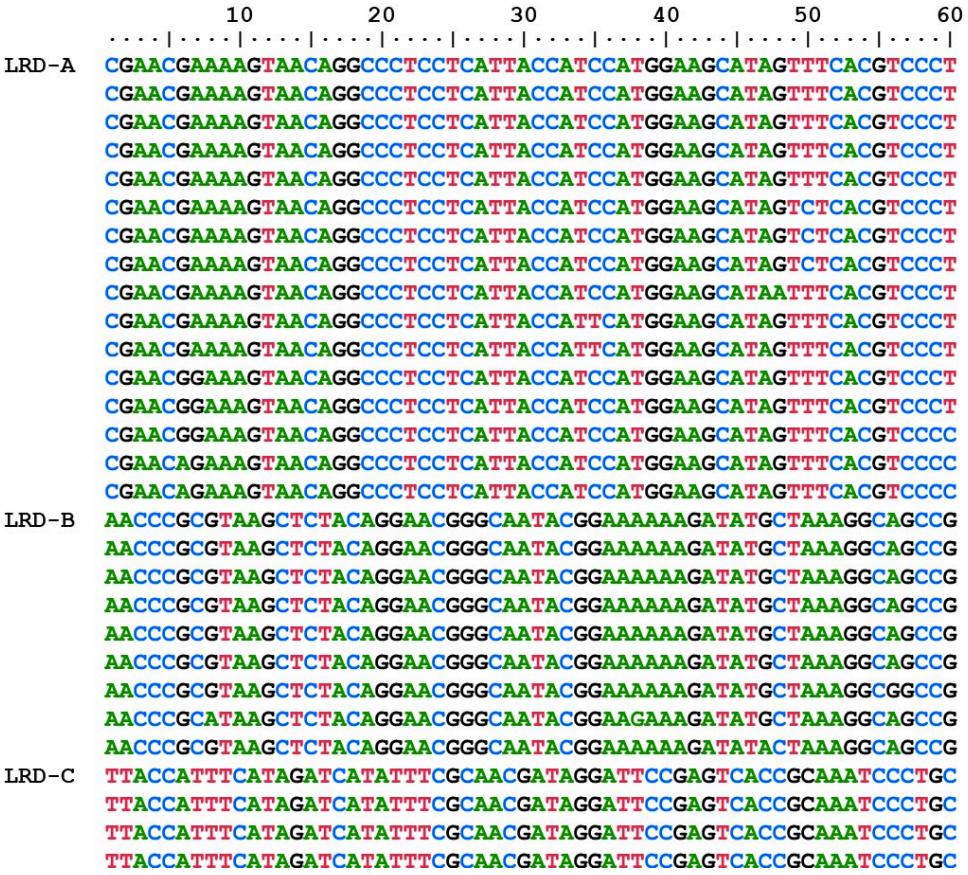

Figure 3-2. Sequencing Results with the round 10 DNA pool. 29 clones were sequenced and they belong to three sequence classes denoted LRD-A (16 copies), LRD-B (9 copies), and LRD-C (4 copies). Note that only the nucleotides located in the random domain of the library L1 are shown.

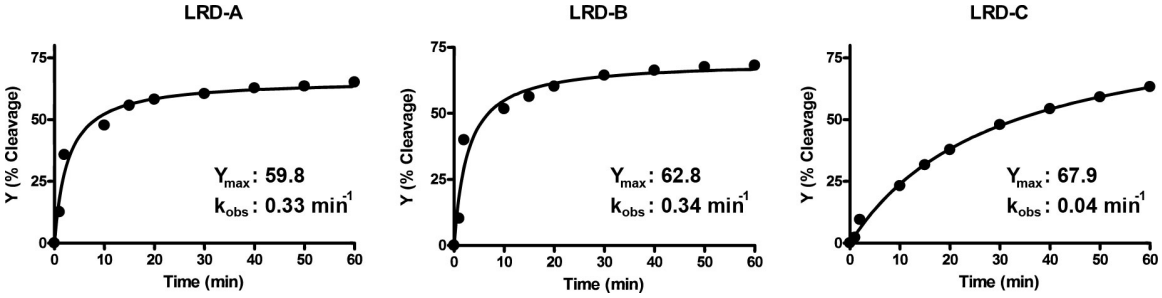

Figure 3-3 Kinetic Analysis of LRD-A, LRD-B, and LRD-C. The *cis*-acting LRD-A, LRD-B and LRD-C were examined for the cleavage activity by measuring % cleavage (Y) at 1, 2, 5, 10, 20, 30, 40, 50, and 60 min. The data were then fitted with the equation $Y = Y_{max}[1-e^{-kt}]$ to obtain the first-order rate constant *k* and maximal cleavage Y_{max}, which are shown in the graph.

3.2.2 Identification of catalytically important nucleotides

To identify the catalytic core of LRD-B, a deletion walking experiment was conducted where sets of three nucleotides were sequentially removed from the full-length sequence starting at the 3′-end. These mutants were then probed for their activities. Loss of important residues is expected to affect catalysis and the severity of disruption is measured through the reduction of activity. The deletion walking experiment identified several potential sites of importance. The results indicate that many nucleotides near the 5′-end of the LRD-B were critical for catalysis. Conversely, deleted residues near the 3′-end had very little effect on L-RNA cleavage (Figure 3-4A).

Along with the deletion walking experiment, a reselection experiment was conducted with a partially randomized library of LRD-B in which each nucleotide in the original random-sequence domain was chemical synthesized to have a degeneracy of 30% (10% exchange to other nucleotides while 70% remained as wild-type). After six

rounds of reselection, the DNA pool was sequenced and individual sequences were analyzed to identify conserved nucleotides. Each individual nucleotide was organized using a variation index (VI) using a method we developed previously.[33] Nucleotides that were absolutely conserved were coded in red (VI = 0), important residues in blue (VI < 0.25) and not important in grey (VI > 0.25) (Figure 3-4B).[33] Residues that had a VI of 0 indicated no tolerance for mutations; these nucleotides either participate in catalysis, or are essential for structural formation. Blue-coded nucleotides can tolerate some level of mutation; it is possible that these nucleotides play a significant role in structural organization rather than catalysis. In contrast, nucleotides coded in grey were not important because its variability remains close to the initial frequency of mutagenesis at 30%. Initial assessment of LRD-B's secondary structure reveals a simple internal stem-loop that may be highly important since many residues in the loop are highly conserved (Figure 3-4C).

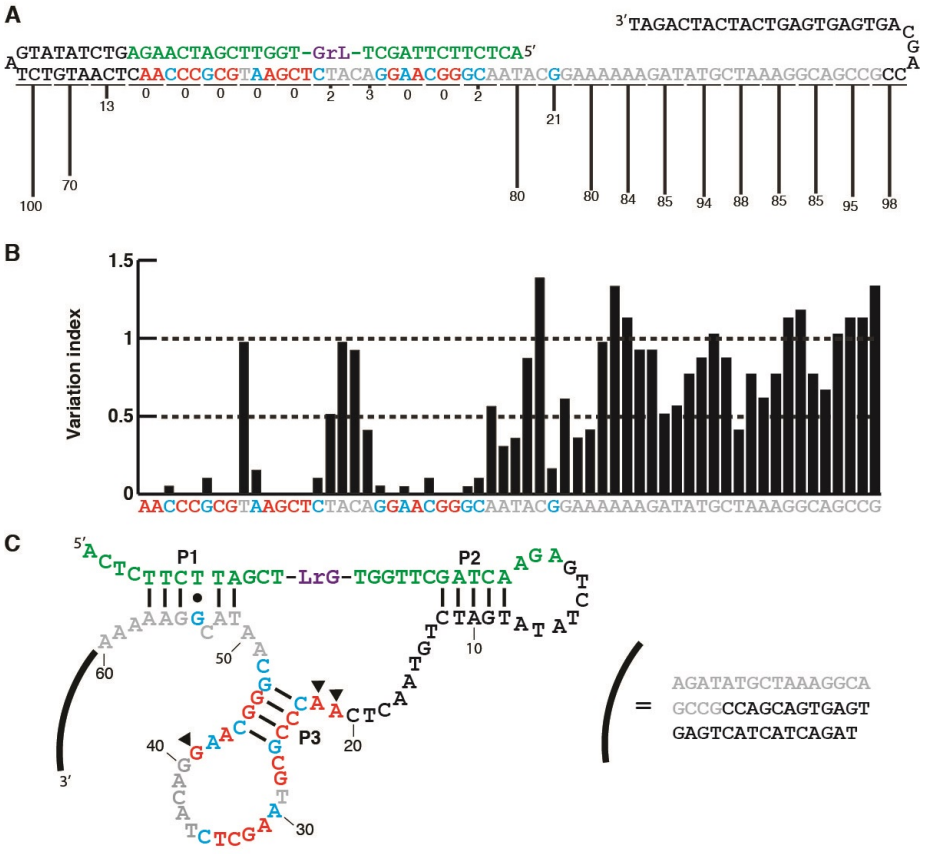

Figure 3-4. (A) Deletion walking experiment. Starting from the 3′-end of LRD-B, sets of three-nucleotide were sequentially removed to determine sites that could contain important structural and catalytic residues. The numbers represent the normal activity against untruncated sequence (taken as 100). (B) Reselection of LRD-B sequence with a 30% degeneracy rate. Nucleotides labeled in red are absolutely conserved, blue are important residues, and grey are nucleotides that are non-conserved. (C) The proposed secondary structure of LRD-B. Most of the functionally important residues are located within the hairpin element of the structure. DMS methylation interfered residues are denoted as solid triangles.

Several adenine and guanine residues are found to be highly conserved. Methylation assay was then carried out to further probe their importance to the function of the DNAzyme. Dimethyl sulfate can methylate N-7 of guanine and N-3 of adenine and

placing a methyl group on nitrogen atoms can interfere the catalytic function of the DNAzyme. These nucleobases will appear as undermethylated (protected against methylation in this assay).[40] As revealed in Figure 3-5, A21, A22, and G41 were observed to have the most significant interference.

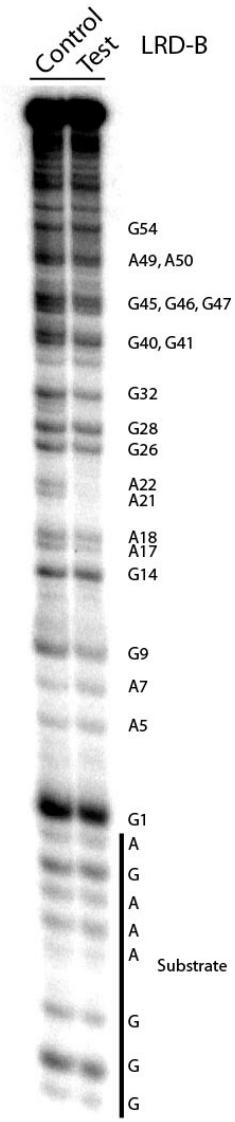

Figure 3-5. Methylation interference of nucleotides in *cis*-acting LRD-B**.** Control: cleavage reaction first and DMS treatment second; min this case every G and A residue can be freely methylated. Test: DMS methylation first and cleavage reaction second; in this case the G and A residues that are important to the catalytic function may not be able to accommodate a methyl group. The reduced intensity of the DNA band in the test lane corresponding to A21, A22, and G41, in comparison to the same DNA band in the control lane, reflects strong methylation interference of these nucleotides, suggesting these three residues are important to the function of the DNAzyme. For nucleotide numbering, see Figure 3-2C.

3.2.3 Design of a trans-acting LRD construct

Once we have identified the key nucleotides that are important to the function of LRD-B, we sought to convert the *cis*-acting catalyst into a *trans*-acting enzyme. The primer binding sites and some non-conserved nucleotides were first removed from the sequence of LRD-B. Additional nucleotides were also introduced to create stronger binding arms between the substrate strand and the DNAzyme strand. The final *trans*-acting LRD-B (denoted LRD-BT1) is shown in Figure 3-6A. The catalytic activity of LRD-BT1 was assessed under multiple turnover conditions. LRD-BT1 was found to have k_{cat} of 2.6 ± 0.2 min^{-1} and a K_M of 280 ± 40 nM (Figure 3-6B).

3.2.4 Identification of a kissing loop in the DNAzyme structure

The secondary structure model for LRD-BT1 places four absolutely conserved motif AGCT in the loop of the hairpin which is located far away from the cleavage site. Our mutational analysis indicates that base alteration to any nucleotide in this motif results in complete loss of the catalytic activity. Upon close inspection, we noticed another ACGT motif located immediately upstream of LrG cleavage site. This observation led us to speculate that two motifs form a kissing loop, which might be important for the function of LRD-B. We believe that this would bring catalytically important nucleotides from the stem-loop closer to the cleavage site (Figure 3-6C).

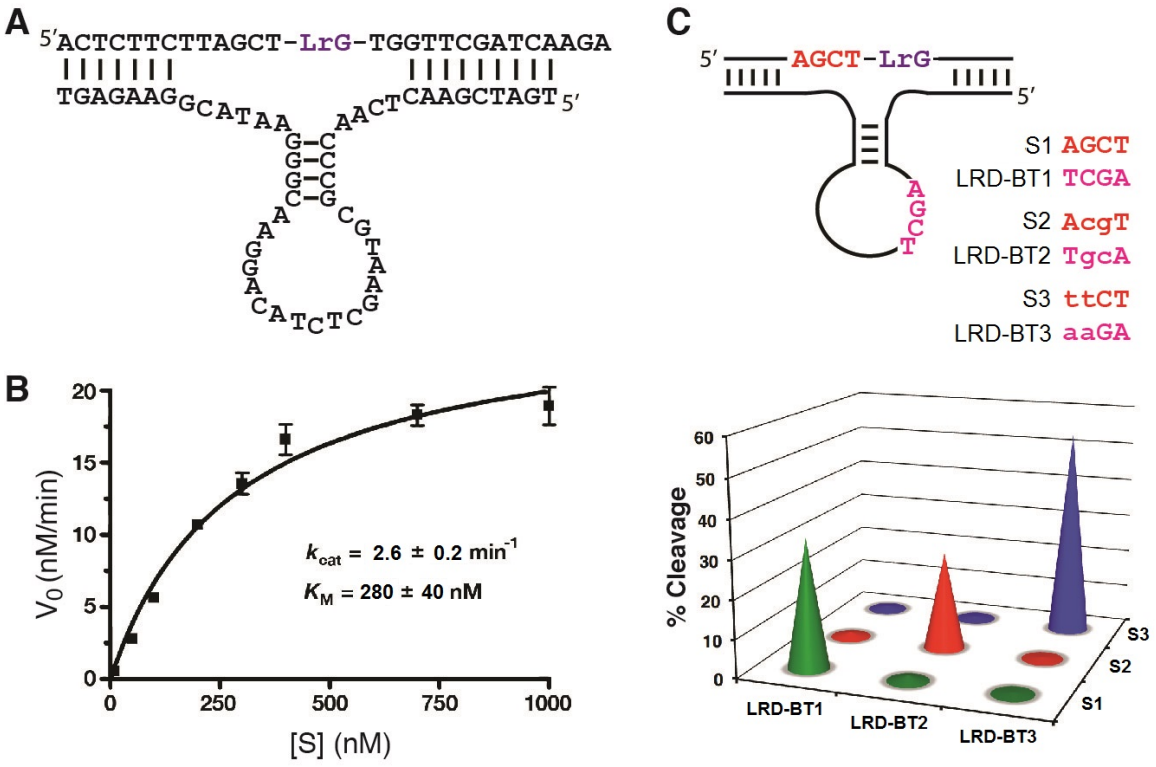

Figure 3-6. A *trans*-acting DNAzyme construct. (A) Optimized *trans*-acting sequence denoted as LRD-BT1. (B) Multiple turnover kinetic analysis of LRD-BT1. The initial velocity is plotted against substrate concentrations and the data is fitted to the Michaelis-Menten equation $v = k_{cat}[S]/(K_M + [S])$. (C) Identification and confirmation of a kissing loop. Three substrates (S1, S2 and, S3) and their matched DNAzymes (LRD-BT1, LRD-BT2, and LRD-BT3) were tested for the cleavage activity. The lowercase letters denote altered nucleotides.

To confirm the existence of the kissing loop and its importance to the function of LRD-BT1, we carried out compensation mutagenesis analysis. In this experiment, the introduction of base mutations to disrupt the kissing loop formation is expected to significantly diminish the catalytic activity while co-variations to restore the base-pairing interactions should also revive the catalyst. Two new enzyme-substrate pairs, LRD-BT2/S2 and LRD-BT3/S3, were constructed and all 9 enzyme-substrate combinations

were examined for cleavage activity (Figure 3-6C). The results show that each enzyme can only cleave its matching substrate, indicating that the kissing loop between the enzyme and the substrate strands does exist and is essential to the function of the DNAzyme.

3.2.5 Substrate specificity and metal ion dependency

As the in vitro selection experiment used the substrate containing guanine L-ribonucleotide (LrG) as the cleavage site, we were interested to see if LRD-BT1 can cleave other L-ribonucleotdes including LrA, LrC, and LrU. The data in Figure 3-7A indicates that LRD-BT1 has extremely weak activity towards these L-ribonucleotides.

We also evaluated the divalent metal ion requirement of LRD-B. We found that this DNAzyme exhibits robust activity in the presence of Mn^{2+}, Cd^{2+}, and Co^{2+}, reduced activity with Ni^{2+}, but is inactive in the presence Mg^{2+} (Figure 3-7B). Even though the original selection buffer contained both Mg^{2+} and Mn^{2+}, LRD-B recruited Mn^{2+} as the divalent metal ion cofactors over Mg^{2+}. This finding is not surprising given the fact that many previous studies have also shown that these divalent transition metal ions are often the preferred metal ions for DNAzyme mediated catalysis.[3,19,41-44]

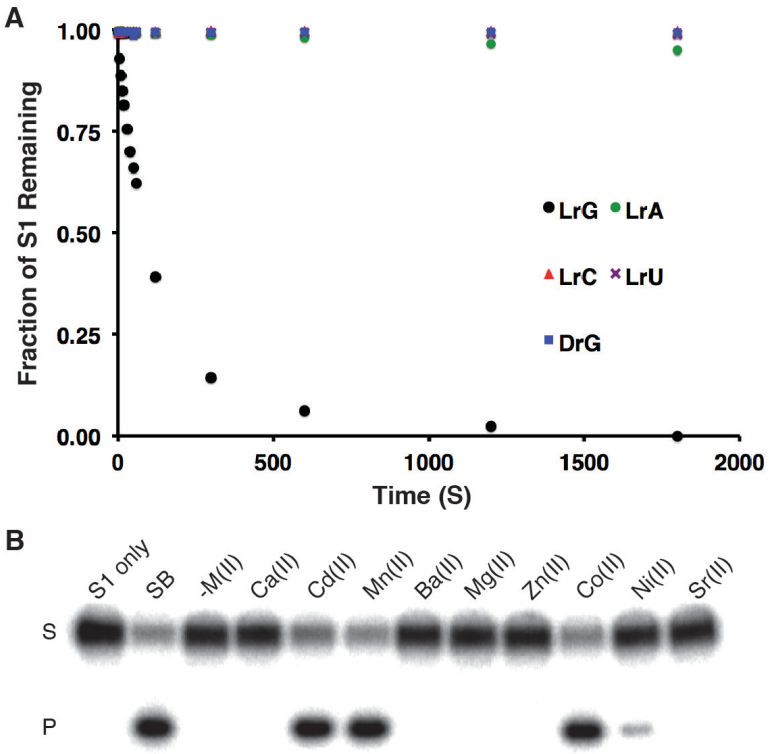

Figure 3-7. Further characterization of LRD-BT1. (A) Cleavage site selectivity. Cleavage profile (fraction of the substrate remaining vs. reaction time) of LRD-BT1 towards four substrates differing only at the cleavage site (LrG, LrA, LrC or LrU). (B) Metal ion dependency. Reaction buffers contain 60 mM HEPES, pH 7.5, 300 mM NaCl, and 100 mM KCl, in addition to a divalent metal ion (15 mM) specified in the figure.

3.2.6 Engineering a ligand-responsive LRD

RNA-cleaving DNAzymes can be combined with aptamers for the engineering of allosteric DNAzymes or aptazymes.[42,45-47] To derive an aptazyme from LRD-B, we adopted a non-classical design previously reported by our group.[33] This approach uses an aptamer-containing substrate strand (S1-Apt1) with a sequence design in which part of the aptamer engages part of the substrate into a hairpin structure that prevents the access of the substrate by the DNAzyme. However, in the presence of the cognate ligand for the

aptamer, the hairpin structure gives the way to the formation of a ligand-aptamer complex, making the substrate fully accessible to the DNAzyme. We used the widely examined ATP-binding DNA aptamer in the design of the aptazyme;[48] the sequence design and the switching mechanism are illustrated in Figure 3-8A. As shown in Figure 3-8B, the cleavage of S1-Apt1 by a modified LRD-BT1 (denoted LRD-Apt1) was found to be dependent on the presence of ATP in a time-dependent manner (also see Figure 3-9).

3.2.7 Stability and functionality in serum

Our key motivation to develop an L-RNA-cleaving DNAzyme system is to develop an RNA-cleaving DNAzyme system that enables biosensing applications with RNase-containing biological samples. To demonstrate the advantage of L-RNA-cleaving DNAzymes over the D-RNA-cleaving counterparts, we compared the stability of LRD-BT1 and 8-17 (a representative D-RNA-cleaving DNAzyme [49]) in human serum. As shown in Figure 3-8C, although in the clean reaction buffer the cleavage of D-RNA substrate was dependent on the presence of 8-17, in serum this dependence vanished. Therefore, it is clear that any biosensor built with 8-17 will unavoidably lead to a false-positive signal in RNase-containing biological samples. In sharp contrast, the cleavage of L-RNA substrate is totally dependent on LRD-BT1 regardless of whether the reaction was performed in the pure reaction buffer or in human serum (Figure 3-8C). Similarly, the biosensor designed with LRD-Apt1 for ATP detection was indeed able to detect ATP in complex sample matrix like human serum (Figure 3-8D).

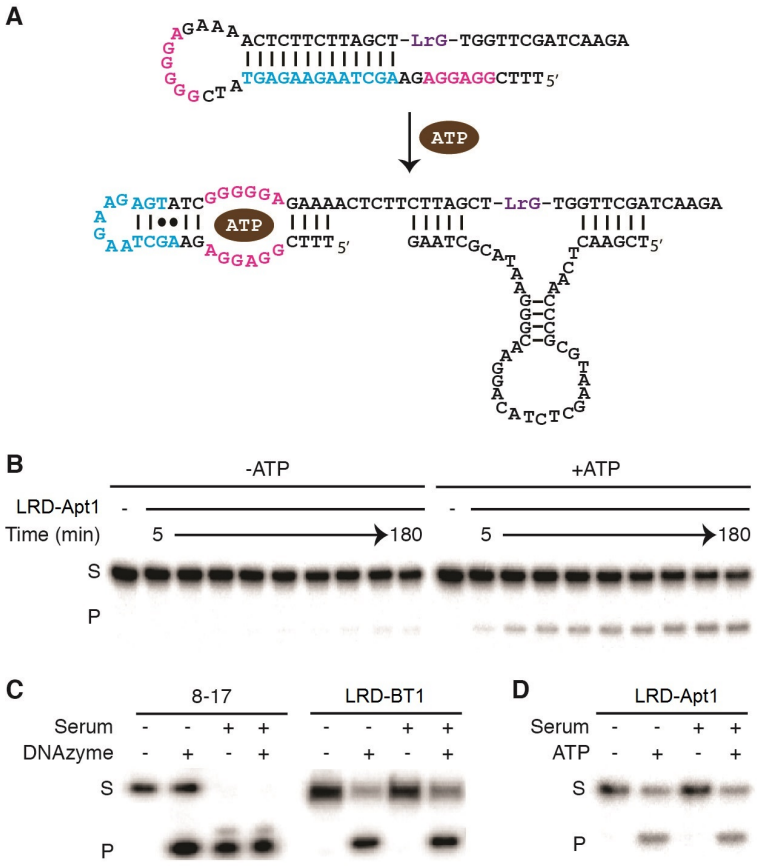

Figure 3-8. An ATP-responsive aptazyme constructed from LRD-BT1. (A) Sequence design and detection mechanism. Residues highlighted in red is the binding site for ATP, blue are DNAzyme-blocking nucleotides. (B) Time-dependent cleavage of S1-Apt1 by LRD-Apt1 in the absence and presence of 1 mM ATP. (C) Activity comparison of D-RNA and L-RNA cleaving systems in human serum. (D) The functionality of the ATP-responsive aptazyme constructed with LRD-Apt1 in human serum. S: substrate; P: cleavage product.

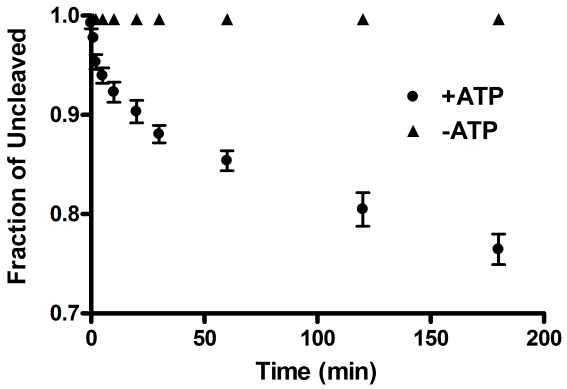

Figure 3-9. Activation of the S1-Apt1/LRD-Apt1 aptazyme system by ATP. The cleavage of the substrate S1-Apt1 by the DNAzyme LRD-Apt1 in the presence and absence of 1 mM ATP was monitored at the following time points: 1, 2, 5, 10, 20, 30, 60, 120, 180 min. The fraction of the substrate that remained uncleaved is determined and plotted vs. the reaction time.

2.4 Discussion

Developing biosensors with enhanced stability toward RNases is important for maintaining their functionality in biological samples and extending their shelf-life. We have chosen L-RNA as the substrate for DNAzyme development for the consideration that L-RNA has identical chemical properties to D-RNA [50] (and can therefore undergo the same transesterification reaction as D-RNA) but natural RNases cannot recognize L-RNA as the substrate.

Compared to the first L-RNA cleaving DNAzyme isolated by the Joyce group [39], our current LRD exhibits >2500-fold enhancement in catalytic activity. The original design by Joyce used an immobilized DNA library, while our approach was to have the DNAzyme cleave the L-RNA in solution. We suspect that immobilizing DNA sequences on a solid support may present structural hindrances and reduce the conformational space that is necessary to accommodate efficient L-RNA cleavage. Due to the conformational

differences between the L- and D- isomers, the use of an L-RNA in a DNA substrate introduces alternative structures. By performing the cleavage reaction in solution, the DNA sequences are free to adopt any structural configuration.

Interestingly the featured DNAzyme has a kissing loop that is important to the catalytic function. If we assume that the kissing loop is a structural requirement for L-RNA cleavage, then the remaining conserved nucleotides must play a vital role in catalysis. From the methylation data, A21, A22, and G41 show significant methylation interference, suggesting they may function as candidate nucleotides mediating catalysis. This speculation is also supported by the reselection data showing these nucleotides positions are absolutely conserved. It is possible that the kissing loop configuration brings these catalytically important residues closer to the cleavage site.

We have successfully converted the featured L-RNA-cleaving DNAzyme to a ligand-responsive sensor, taking advantage of an existing DNA aptamer that binds ATP [48]. More importantly, we have shown that this aptazyme is functional in biological samples that contain RNases. Taken together, the current work lays the foundation for exploring RNA-cleaving DNAzymes for engineering biosensors that are compatible with complex biological samples.

2.5 Materials and Methods

2.5.1 Enzyme, chemicals, and other materials

Triethylamine trihydrofluoride (TEA-THF), dimethyl sulfate (DMS), piperidine, anhydrous dimethyl sulfoxide (DMSO) were purchased from Sigma-Aldrich (Oakville, Ontario). T4 DNA ligase, T4 polynucleotide kinase (PNK), ATP, and dNTPs were obtained from Thermo Scientific. DNA polymerase was purchased from Biotools B & M Labs (Madrid, Spain). [γ-^{32}P]ATP and [α-^{32}P]dGTP were from Perkin Elmer (Woodbridge, Ontario). All other chemicals were purchased from BioBasic Inc. (Markham, Ontario) and used without further purification. Water used in this study was double deionized and autoclaved. Standard oligonucleotides were synthesized by solid-phase synthesis from Integrated DNA Technologies (Coralville, Iowa) while modified L-RNA oligonucleotides were obtained from Keck Biotechnology Resource Laboratory, Yale University (New Haven, Connecticut). All oligonucleotides were purified by 10% denaturing polyacrylamide gel electrophoresis (dPAGE) prior to use. The 2′-O-TBDMS (tert-butyldimethylsilyl) protecting group of L-RNA was deprotected by dissolving the dry pellet in 100 μL of anhydrous DMSO and 125 μL of TEA-THF. This was followed by an overnight incubation at 60 °C. To this mixture, 25 μL of NaOAc (3 M, pH 5.2) and 1 mL of butanol were added. The solution was stored at -20 °C for 30 min and then centrifuged for 20 min at 15,000 g. The pellet was washed 3× with 70% ethanol and purified by 10% dPAGE.

2.5.2 In vitro selection

1 nmol L1 (its sequence is provided in Figure 1) was used as the initial library. L1 was first ^{32}P-labeled at the 5′-end in the presence of 10 units (U) of T4 PNK, 10 μCi [γ-^{32}P]ATP, and 1× T4 PNK buffer A (using the 10× buffer supplied by the vendor) for 20 min at 37°C in a reaction volume of 100 μL. Addition of non-radioactive ATP to a final concentration of 1 mM and further incubation at 37 °C were carried out to ensure complete phosphorylation. The reaction was then stopped by heating at 90 °C for 5 min. Upon cooling to room temperature, 1 nmol of S1 (sequence in Figure 1) and 1 nmol of T1 (the template for ligation: 5′-TCATATAGACTCTTGATCGA) were added. The reaction mixture was then heated to 90 °C for 1 min and cooled to room temperature. 10 units of T4 DNA ligase and 25 μL of 10× T4 DNA ligase buffer (supplied by the vendor) was added to the reaction mixture (total reaction volume: 250 μL). The ligation reaction was carried out at 23 °C for 2 h. The DNA was precipitated by ethanol and the ligated product was purified by 10% dPAGE.

The purified DNA above was suspended in 50 μL of H_2O and heated to 90 °C for 30 s and cooled to 23 °C over 15 min. The cleavage reaction was initiated by addition of 50 μL of 2× selection buffer (120 mM HEPES, pH 7.5, 600 mM NaCl, 200 mM KCl, 30 mM $MgCl_2$, and 30 mM $MnCl_2$). For the first cycle of selection, the reaction was incubated at room temperature for 1 h. The reaction was quenched by addition of EDTA (0.5 M, pH 8.0) to a final concentration of 30 mM. The DNA was precipitated with ethanol and the cleavage fragment was purified by 10% dPAGE. A DNA marker that has the identical size to the cleavage fragment was used to guide the separation.

The isolated DNA above was amplified by polymerase chain reaction (PCR) in a volume of 50 μL containing 1× PCR buffer (supplied by the vendor as the 10× buffer), 0.2 mM each of the standard dNTPs, 1.25 U of DNA polymerase, 0.5 μM of FP1 (the primer sequences can be found in Figure 3-1) and 0.5 μM RP1. 12 thermocycles was carried out with the following parameters: 94 °C, 30 s (2 min for the first cycle); 52 °C, 40 s; 72 °C, 45 s. A 1/100-fold dilution of the PCR product was used for the second PCR using the same condition described above with the exception that RP2 was used instead of RP1. Another PCR2 was performed for internal labeling of ^{32}P. This was achieved by following the PCR2 protocol except that 10 μCi [α-^{32}P]dGTP and 0.02 mM non-radioactive dGTP were used to substitute 0.2 mM dGTP. The non-radiolabeled and ^{32}P-labeled PCR products were combined and the DNA in the mixture was precipitated by ethanol. The desired DNA molecules were purified by 10% dPAGE.

The purified DNA was used to carry out the second selection using the same procedure. The cleavage time for individual selection cycles are: 1 h for rounds 1-5, 1 min for rounds 6-7, and 5 s for round 8-10. The cleavage fragment from round 10 was amplified, cloned and sequenced using a protocol we published previously.[41]

2.5.3 Reselection

Each of the random-sequence position of LRD-B was subjected to 30% random mutagenesis during chemical synthesis (70% chance for a wild-type nucleotide and 10% each for the remaining three nucleotides). 1 nmol of the partially randomized library was used to initiate the reselection experiment following the selection scheme as described

above. The cleavage time was 1 h for round 1, 10 min for round 2, 1 min for rounds 3 and 4, and 5 s for rounds 5 and 6. After the 6th cycle of selection, the population was cloned and sequenced.

2.5.4 Kinetic analysis of cis-acting constructs

Radioactively labeled candidate DNAzymes were prepared by phosphorylation of the DNAzyme strand with 10 μCi [γ-^{32}P]ATP, ligation to S1 and purification by dPAGE as described above. The cleavage reaction was conducted in a 100 μL mixture containing 1 μM ligated construct in 1× SB. A 10 μL aliquot was withdrawn from the reaction mixture at the following time points: 1, 2, 5, 10, 20, 30, 40, 50, and 60 min. These DNA samples were then subjected to 10% dPAGE for DNA separation. The image of cleaved and uncleaved DNA bands was obtained with a Typhoon Trio+ Imager and the radioactivity of each DNA band was quantified with ImageQuant software (Molecular Dynamics). The percent cleavage of the *cis*-acting DNAzyme was then calculated using Microsoft Excel. Rate constants were obtained by curve fitting using $Y = Y_m [1-e^{-kt}]$, where Y represents cleavage yield at the time t, Y_m is maximal cleavage yield, and k is the first-order rate constant.

2.5.5 Kinetic analysis of trans-acting constructs

Single turnover conditions: radioactive S1 was prepared through phosphorylation with [γ-^{32}P]ATP/T4 PNK and purified by 10% dPAGE as described above. The cleavage reaction was conducted using the same procedure described for the *cis*-acting constructs

other than the use of the S1/LRD-BT1 *trans* construct ([S1] = 10 nM; [LRD-BT1] = 200 nM). Rate constants were also obtained through curve fitting using $Y = Y_m [1-e^{-kt}]$.

Multiple turnover conditions: The cleavage reaction was performed using a constant [LRD-BT1] at 5 nM. The initial rates were determined for each of the following [S1]: 10, 50, 100, 200, 300, 400, 700, and 1000 nM. The parameters k_{cat} and K_M were derived using Michaelis-Menten equation.

2.5.6 Metal Ion Dependency

Modified 2× selection buffers were used for this experiment, each of which contained 120 mM HEPES, pH 7.5, 600 mM NaCl, 200 mM KCl, 30 mM M^{2+} (M^{2+} = Ca^{2+}, Cd^{2+}, Mn^{2+}, Ba^{2+}, Mg^{2+}, Zn^{2+}, Co^{2+}, Ni^{2+}, and Sr^{2+}). Each reaction mixture had 10 nM of radioactive S1 and 200 nM LRD-BT1 in a reaction volume of 20 µL. After incubation for 30 min, the cleavage reaction mixture was analyzed by dPAGE to obtain percent cleavage as described above.

2.5.7 Truncation of LRD-B

All truncated sequences were prepared through DNA phosphorylation and ligation with S1 as described above. The cleavage reaction was conducted in a 20 µL mixture containing 1 µM ligated construct in 1× SB. The reaction time was 30 min. The percent cleavage was determined for each construct through dPAGE analysis. The relative activity of each truncation was normalized against the full-length construct by 100 ×

Y_C/Y_F, where Y_C and Y_F represent the percent cleavage of each truncated sequence and full-length sequence, respectively.

2.5.8 ATP detection using aptazyme

The aptazyme detection mixture was prepared by incubating 1 mM ATP with 50 nM S1-Apt1 for 5 min in the presence of 1× SB (60 mM HEPES, pH 7.5, 300 mM NaCl, 100 mM KCl, 15 mM $MgCl_2$, and 15 mM $MnCl_2$). The reaction was initiated by addition of 50 nM LRD-Apt1. Aliquots were taken out and quenched with EDTA at specific time points over the course of 3 h. The products were precipitated with ethanol, separated by 10% dPAGE and analyzed with a Typhoon Trio+ Imager.

2.5.9 DNA methylation

100 pmol LRD-B was used for a self-cleavage reaction in 400 μL of 1× SB. After 30 min, the DNA was precipitated with ethanol and resuspended in 200 μL of H_2O. The reaction was then heated to 90 °C for 1 min and cooled to room temperature for 10 min. Subsequently, 200 μL of 0.4% DMS in H_2O was added and the mixture was incubated at room temperature for 35 min. This methylation experiment was denoted as the "control". Another reaction was carried out using 100 pmol of LRD-B but in a reverse order (DMS methylation first and then self-cleavage reaction); this reaction was denoted as the "test". The DNA in both the control and the test was precipitated by ethanol and radioactively labeled at the 5′-end with 10 μCi [γ-^{32}P]ATP and 10 units of PNK. The cleavage fragment was purified by 10% dPAGE, resuspended in 100 μL of 10% piperidine, and

heated at 90 °C for 30 min. Each reaction mixture was dried in a speedvac. The DNA molecules in each sample were separated by 10% dPAGE. The gel image was taken using Typhoon Trio Imager.

2.6 References Cited

1. Ellington AD, Szostak JW (1990) In vitro selection of RNA molecules that bind specific ligands. Nature 346: 818-822.
2. Tuerk C, Gold L (1990) Systematic evolution of ligands by exponential enrichment: RNA ligands to bacteriophage T4 DNA polymerase. Science 249: 505-510.
3. Breaker RR, Joyce GF (1994) A DNA enzyme that cleaves RNA. Chem Biol 1: 223-229.
4. Flynn-Charlebois A, Wang Y, Prior TK, Rashid I, Hoadley KA, et al. (2003) Deoxyribozymes with 2'-5' RNA ligase activity. J Am Chem Soc 125: 2444-2454.
5. Purtha WE, Coppins RL, Smalley MK, Silverman SK (2005) General deoxyribozyme-catalyzed synthesis of native 3'-5' RNA linkages. J Am Chem Soc 127: 13124-13125.
6. Wang Y, Silverman SK (2003) Deoxyribozymes that synthesize branched and lariat RNA. J Am Chem Soc 125: 6880-6881.
7. Cuenoud B, Szostak JW (1995) A DNA metalloenzyme with DNA ligase activity. Nature 375: 611-614.
8. Li Y, Breaker RR (1999) Phosphorylating DNA with DNA. Proc Natl Acad Sci USA 96: 2746-2751.
9. Carmi N, Balkhi SR, Breaker RR (1998) Cleaving DNA with DNA. Proc Natl Acad Sci USA 95: 2233-2237.

10. Chandra M, Silverman SK (2008) DNA and RNA can be equally efficient catalysts for carbon-carbon bond formation. J Am Chem Soc 130: 2936-2937.
11. Berget SM, Moore C, Sharp PA (1977) Spliced segments at the 5' terminus of adenovirus 2 late mRNA. Proc Natl Acad Sci USA 74: 3171-3175.
12. Chow LT, Roberts JM, Lewis JB, Broker TR (1977) A map of cytoplasmic RNA transcripts from lytic adenovirus type 2, determined by electron microscopy of RNA:DNA hybrids. Cell 11: 819-836.
13. Guerrier-Takada C, Gardiner K, Marsh T, Pace N, Altman S (1983) The RNA moiety of ribonuclease P is the catalytic subunit of the enzyme. Cell 35: 849-857.
14. Kruger K, Grabowski PJ, Zaug AJ, Sands J, Gottschling DE, et al. (1982) Self-splicing RNA: autoexcision and autocyclization of the ribosomal RNA intervening sequence of Tetrahymena. Cell 31: 147-157.
15. Schlosser K, Li Y (2010) A versatile endoribonuclease mimic made of DNA: characteristics and applications of the 8-17 RNA-cleaving DNAzyme. Chembiochem 11: 866-879.
16. Silverman SK (2005) In vitro selection, characterization, and application of deoxyribozymes that cleave RNA. Nucleic Acids Res 33: 6151-6163.
17. Breaker RR, Joyce GF (1995) A DNA enzyme with Mg^{2+}-dependent RNA phosphoesterase activity. Chem Biol 2: 655-660.
18. Faulhammer D, Famulok M (1996) The Ca^{2+} Ion as a cofactor for a novel RNA-cleaving deoxyribozyme. Angew Chem Int Ed 35: 2837-2841.
19. Li J, Zheng W, Kwon AH, Lu Y (2000) In vitro selection and characterization of a highly efficient Zn(II)-dependent RNA-cleaving deoxyribozyme. Nucleic Acids Res 28: 481-488.
20. Liu J, Brown AK, Meng X, Cropek DM, Istok JD, et al. (2007) A catalytic beacon sensor for uranium with parts-per-trillion sensitivity and millionfold selectivity. Proc Natl Acad Sci USA 104: 2056-2061.
21. Huang PJ, Vazin M, Liu J (2014) In vitro selection of a new lanthanide-dependent DNAzyme for ratiometric sensing lanthanides. Anal Chem 86: 9993-9999.

22. Li J, Lu Y (2000) A highly sensitive and selective catalytic DNA biosensor for lead ions. J Am Chem Soc 122: 10466-10467.
23. Lu LM, Zhang XB, Kong RM, Yang B, Tan W (2011) A ligation-triggered DNAzyme cascade for amplified fluorescence detection of biological small molecules with zero-background signal. J Am Chem Soc 133: 11686-11691.
24. Ali MM, Aguirre SD, Lazim H, Li Y (2011) Fluorogenic DNAzyme probes as bacterial indicators. Angew Chem Int Ed 50: 3751-3754.
25. Zhang XB, Kong RM, Lu Y (2011) Metal ion sensors based on DNAzymes and related DNA molecules. Annu Rev Anal Chem 4: 105-128.
26. Liu J, Lu Y (2003) A colorimetric lead biosensor using DNAzyme-directed assembly of gold nanoparticles. J Am Chem Soc 125: 6642-6643.
27. Liu J, Lu Y (2005) Stimuli-responsive disassembly of nanoparticle aggregates for light-up colorimetric sensing. J Am Chem Soc 127: 12677-12683.
28. Zhao W, Lam JC, Chiuman W, Brook MA, Li Y (2008) Enzymatic cleavage of nucleic acids on gold nanoparticles: a generic platform for facile colorimetric biosensors. Small 4: 810-816.
29. Liu J, Lu Y (2004) Adenosine-dependent assembly of aptazyme-functionalized gold nanoparticles and its application as a colorimetric biosensor. Anal Chem 76: 1627-1632.
30. Xiao Y, Qu X, Plaxco KW, Heeger AJ (2007) Label-free electrochemical detection of DNA in blood serum via target-induced resolution of an electrode-bound DNA pseudoknot. J Am Chem Soc 129: 11896-11897.
31. Yang X, Xu J, Tang X, Liu H, Tian D (2010) A novel electrochemical DNAzyme sensor for the amplified detection of Pb^{2+} ions. Chem Commun 46: 3107-3109.
32. Lan T, Furuya K, Lu Y (2010) A highly selective lead sensor based on a classic lead DNAzyme. Chem Commun 46: 3896-3898.
33. Chiuman W, Li Y (2007) Simple fluorescent sensors engineered with catalytic DNA 'MgZ' based on a non-classic allosteric design. PLoS One 2: e1224.

34. Mei SH, Liu Z, Brennan JD, Li Y (2003) An efficient RNA-cleaving DNA enzyme that synchronizes catalysis with fluorescence signaling. J Am Chem Soc 125: 412-420.
35. Klussmann S, Nolte A, Bald R, Erdmann VA, Furste JP (1996) Mirror-image RNA that binds D-adenosine. Nat Biotechnol 14: 1112-1115.
36. Ashley GW (1992) Modeling, synthesis, and hybridization properties of (L)-ribonucleic acid. J Am Chem Soc 114: 9731-9736.
37. Garbesi A, Capobianco ML, Colonna FP, Tondelli L, Arcamone F, et al. (1993) L-DNAs as potential antimessenger oligonucleotides: a reassessment. Nucleic Acids Res 21: 4159-4165.
38. Sczepanski JT, Joyce GF (2013) Binding of a structured D-RNA molecule by an L-RNA aptamer. J Am Chem Soc 135: 13290-13293.
39. Ordoukhanian P, Joyce GF (2002) RNA-cleaving DNA enzymes with altered regio- or enantioselectivity. J Am Chem Soc 124: 12499-12506.
40. Achenbach JC, Jeffries GA, McManus SA, Billen LP, Li Y (2005) Secondary-structure characterization of two proficient kinase deoxyribozymes. Biochemistry 44: 3765-3774.
41. Wang W, Billen LP, Li Y (2002) Sequence diversity, metal specificity, and catalytic proficiency of metal-dependent phosphorylating DNA enzymes. Chem Biol 9: 507-517.
42. Liu Z, Mei SH, Brennan JD, Li Y (2003) Assemblage of signaling DNA enzymes with intriguing metal-ion specificities and pH dependences. J Am Chem Soc 125: 7539-7545.
43. Cruz RP, Withers JB, Li Y (2004) Dinucleotide junction cleavage versatility of 8-17 deoxyribozyme. Chem Biol 11: 57-67.
44. Xiao Y, Allen EC, Silverman SK (2011) Merely two mutations switch a DNA-hydrolyzing deoxyribozyme from heterobimetallic (Zn^{2+}/Mn^{2+}) to monometallic (Zn^{2+}-only) behavior. Chem Commun 47: 1749-1751.

45. Tang J, Breaker RR (1997) Rational design of allosteric ribozymes. Chem Biol 4: 453-459.
46. Tang J, Breaker RR (1998) Mechanism for allosteric inhibition of an ATP-sensitive ribozyme. Nucleic Acids Res 26: 4214-4221.
47. Wang DY, Lai BH, Sen D (2002) A general strategy for effector-mediated control of RNA-cleaving ribozymes and DNA enzymes. J Mol Biol 318: 33-43.
48. Huizenga DE, Szostak JW (1995) A DNA aptamer that binds adenosine and ATP. Biochemistry 34: 656-665.
49. Santoro SW, Joyce GF (1997) A general purpose RNA-cleaving DNA enzyme. Proc Natl Acad Sci USA 94: 4262-4266.
50. Vallazza M, Perbandt M, Klussmann S, Rypniewski W, Einspahr HM, et al. (2004) First look at RNA in L-configuration. Acta Crystallogr D Biol Crystallogr 60: 1-7.
51. Schlosser K, Gu J, Sule L, Li YF (2008) Sequence-function relationships provide new insight into the cleavage site selectivity of the 817 RNA-cleaving deoxyribozyme. Nucleic Acids Res 36: 1472-1481.
52. Schlosser K, Gu J, Lam JCF, Li YF (2008) In vitro selection of small RNA-cleaving deoxyribozymes that cleave pyrimidine-pyrimidine junctions. Nucleic Acids Res 36: 4768-4777.

Chapter 4

Arrest of Rolling Circle Amplification by Protein-binding DNA Aptamers

4.1 Introduction

Rolling circle amplification (RCA) is an isothermal DNA amplification process that generates extremely long DNA molecules from a single-stranded (ss) DNA circle.[1,2] In this unique DNA synthesis reaction, a special DNA polymerase (such as φ29 DNA polymerase, φ29DNAP) makes repetitive rounds of DNA copying over a circular ssDNA template using a short DNA strand as the primer and deoxyribonucleotide 5'-triphosphates (dNTPs) as the building blocks. RCA is widely exploited as a powerful signal amplification technique for bioanalysis as it converts a single primer–template recognition event into thousands of tandem DNA repeats that can be easily detected.[3-14] The power of this technique reflects the high processivity and the strand-displacement ability of φ29DNAP: this enzyme is able to make more than 70000 nucleotide additions before its dissociation from the DNA template,[15,16] and unwind double-stranded DNA on its own without requiring the assistance of any DNA helicases.[17-22] It has also been reported that φ29DNAP is able to unwind stable secondary structures in the circular template.[15,16,23] It is interesting to ask if φ29DNAP can read through a ligand-bound aptamer domain that is incorporated into a circular template. In other words, can ligand–aptamer interaction arrest RCA over an aptameric circular template?

Aptamers are ligand-binding single-stranded DNA or RNA sequences that can be isolated from random-sequence libraries using in vitro selection techniques.[24,25] It has been well documented that aptamers can be evolved to possess high affinity and specificity towards their targets[26-32] because aptamers and their cognate targets can form well-defined tertiary structures.[33-36] Thus, the formation of a tight tertiary structure might make a target-bound aptameric circle unsuitable as the template for φ29DNAP (Figure 4-1A).

4.2 Results and Discussion

To test the above hypothesis, we designed an aptameric circular template (named ACT1) that contains a well-characterised aptamer known to bind human thrombin (Figure 4-1B).[26] In addition to the aptamer domain, ACT1 also has a primer binding site required for the RCA reaction, a TaqI restriction enzyme recognition site to be used for the analysis of the RCA product (RCAP), and a peptide nucleic acid (PNA) binding site to be used later for colorimetric reporting of the RCAP. A mutant ACT (ACT1M) was also designed in which several guanine residues in the aptamer domain critical to the target recognition were mutated into adenines. RCA reactions with ACT1 and ACT1M were carried out in the presence of [α-^{32}P]dGTP to allow the incorporation of radioactive phosphorus into the RCAP so that it can be identified through partial digestion with TaqI, followed by denaturing polyacrylamide gel electrophoresis (dPAGE) analysis. The TaqI/dPAGE procedure was expected to produce a characteristic DNA banding pattern,

which is made of monomeric, dimeric and other higher-ordered DNA repeats (Figure 4-1C), as a measurement of a successful RCA reaction.

First, we examined the RCA reaction with ACT1. In the absence of thrombin, ACT1 was able to function as a regular circular template for φ29DNAP, based on the appearance of the expected characteristic DNA banding pattern (ACT1-Th, Figure 4-1C). This indicates that the inclusion of an aptamer sequence in circular template did not disrupt the RCA reaction. In sharp contrast, the addition of thrombin (2 μm) completely arrested the RCA reaction, as the DNA banding signature was now absent (ACT1 + Th, Figure 4-1C). This observation strongly suggests that thrombin engaged the aptamer domain into a rather stable complex so that φ29DNAP was unable to read through. To provide further evidence to support the notion that the lack of RCA reaction was a result of specific binding between thrombin and the DNA aptamer, we carried out two control experiments. First, ACT1 was replaced by ACT1M. Since several nucleotides crucial for target recognition were mutated in ACT1M, it was expected that the inhibition on the RCA reaction by thrombin would be completely eliminated. This was confirmed by the experimental observations (ACT1M-Th and +Th, Figure 4-1C): the presence and absence of thrombin had no effect on the outcome of the RCA reaction. In the second experiment, bovine serum albumin (BSA) was used to substitute thrombin. Since BSA has been shown to have no affinity for the anti-thrombin aptamer, it was anticipated that the RCA reaction would proceed as usual. The observation of the characteristic DNA banding signature (ACT1-BSA, Figure 4-1C) verified this prediction. Taken together, our data

indicate that the anti-thrombin aptamer forms a highly stable complex with thrombin, which is able to block φ29DNAP from copying the circular DNA template.

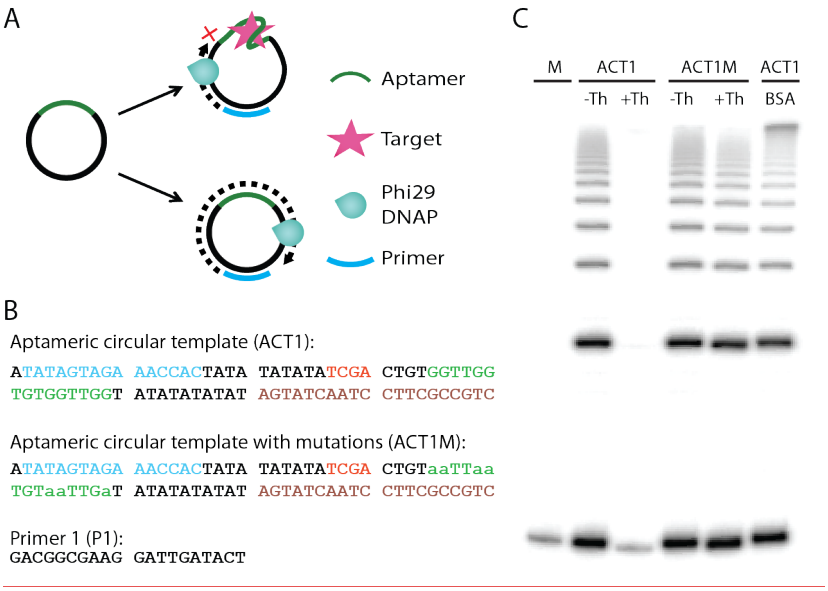

Figure 4-1. A) Schematics of arresting RCA reactions by aptamer–target interactions. B) Sequences of the aptameric circular template (ACT1), ACT1 with mutations in the aptamer domain (ACT1M), and primer 1 (P1). The segments shown in bold, underlined, italic and italic-bold letters are the aptamer for thrombin (Th), the TaqI recognition sequence, the primer binding site and the PNA binding site, respectively. C) Analysis of TaqI-digested RCA product by denaturing polyacrylamide gel electrophoresis (dPAGE). M: marker (linear ACT1).

To rule out the possibility that the observed inhibition might also be dependent on the other non-aptameric sequence elements in ACT1, we tested a new ACT, ACT2, in which 15 nucleotides (nt) before the aptameric domain and five nucleotides after it were chosen for substitution (Figure 4-2A). The same RCA arrest was observed with ACT2 (Figure 4-2C), suggesting that the inhibition was solely linked to the presence of the aptameric sequence in the ACT.

We next examined if the RCA arrest required a specific size of ACT. Using ACT2, which contained 80 nt, as the reference, we progressively removed 10, 20, and 30 nt, resulting in ACT3-5 that contained 70, 60 and 50 nt, respectively (Figure 4-2A). Similar RCA arrests were observed for each shortened ACT (Figure 4-2C), indicating the observed inhibition is not restricted to a given size of ACT.

We also investigated whether the location of the primer-binding site can influence the outcome of RCA arresting. ACT1 was chosen as the aptameric circle for this experiment. ACT1 was broken down into four 20 nt elements labelled as S-I to S-IV (Figure 4-2B); matching primers, P1 to P4, were then designed and used for the individual RCA reactions in the absence and presence of thrombin (Figure 4-2D). The RCA arrest was observed for each primer, indicating that the location of the primer binding site does not interfere with the target-promoted inhibition of RCA.

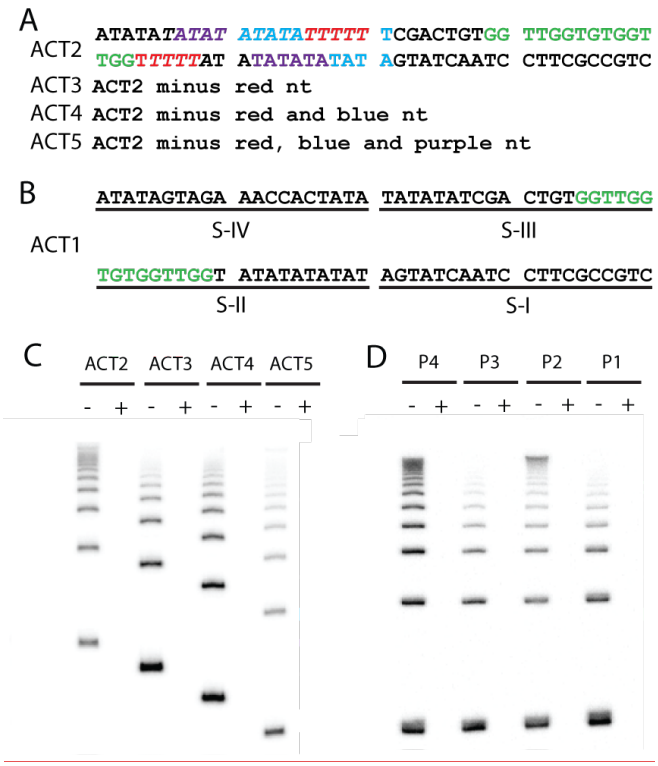

Figure 4-2. RCA reactions with various templates containing anti-thrombin DNA aptamer. A) Sequences of ACT2-5. The aptamer sequence is shown in bold letters. The "-" signs in the sequences of ACT3-5 indicate the nucleotides removed from ACT2. B) The sequence of ACT1 with four 20 nt sequence elements labelled as S-I to S-IV. Four primers, P1 to P4, were designed to bind each of these elements. C) PAGE analysis of TaqI-digested RCA products obtained with ACT2-5. D) PAGE analysis of TaqI-digested RCA products obtained with P1 to P4; -Th: without thrombin; +Th: with thrombin.

We investigated whether the ligand-promoted RCA arresting was a general property of an aptameric DNA circle; a DNA aptamer that binds human platelet-derived growth factor (PDGF)[29] was thus chosen as the second test case. The 35 nt PDGF aptamer was incorporated into an 80nt circular template (named ACT6, Figure 4-3A), which was then subjected to RCA reactions in the absence and presence of PDGF. As expected, in the absence of PDGF, ACT6 can be copied by φ29DNAP; however, the

RCA reaction was arrested by the addition of PDGF (0.4 μM, Figure 4-3B). Control experiments with a mutant circular template (ACT6M, Figure 4-3A, in which several guanosines were mutated into thymidines) and BSA demonstrated that the inhibition of RCA was dependent on the specific aptamer sequence as well as the matching target for the aptamer (Figure 4-3B). These results strongly suggest that the observed RCA arresting appears to be a general phenomenon with, at least, protein-binding DNA aptamers. Future experiments will be directed at investigating if the same inhibition can be achieved with aptamers that bind small molecules.

Next, we examined the possibility of exploiting RCA arresting for biosensing applications. We chose a colorimetric reporting platform that can report the presence or absence of RCA products through the use of a peptide nucleic acid (PNA) and an organic dye known as $DiSC_2(5)$ (diethylthiadicarbocyanine).[9,37-39] It has been shown that $DiSC_2(5)$ can bind to a PNA– DNA duplex and change its colour from blue to purple (Figure 4-4A). When the RCA reaction is carried out in the absence of the target for the aptamer, the production of the RCAP and subsequent hybridisation of the PNA and binding of $DiSC_2(5)$ are expected to produce a purple solution. In the presence of the target, however, RCAP will not be produced and thus, the reaction mixture will be blue.

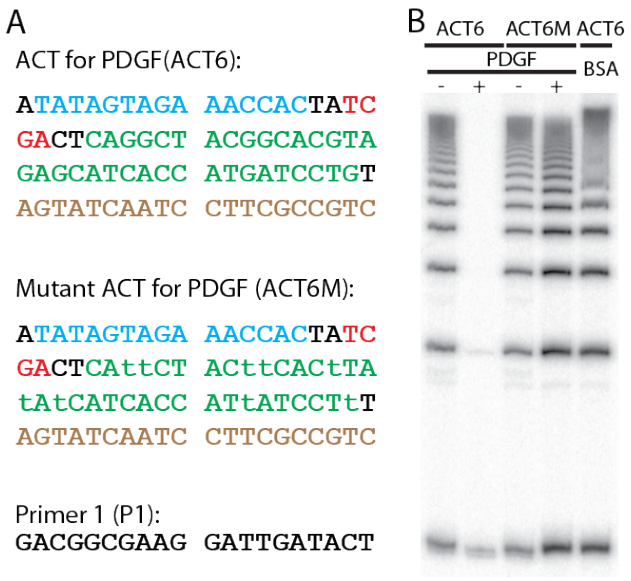

Figure 4-3. Arresting RCA using PDGF binding aptamer. (A) Sequences of the aptameric circular template (ACT6), ACT6 with mutations in the aptamer domain (ACT6M), and primer 1 (P1). The sequence portions in green, red, brown and blue are the aptamer for PDGF, the TaqI recognition sequence, the primer binding site and the PNA binding site, respectively. (B) Analysis of TaqI-digested RCA product via dPAGE.

As shown in Figure 4-3B, the RCA reaction mixture obtained with ACT1 in the presence of thrombin produced a blue colour, whereas the reaction mixture in the absence of thrombin showed a purple colour (Figure 4-4B). In addition, the control reaction mixtures (ACT1M with and without thrombin as well ACT1 with BSA) also produced the expected purple colour (Figure 4-4B).

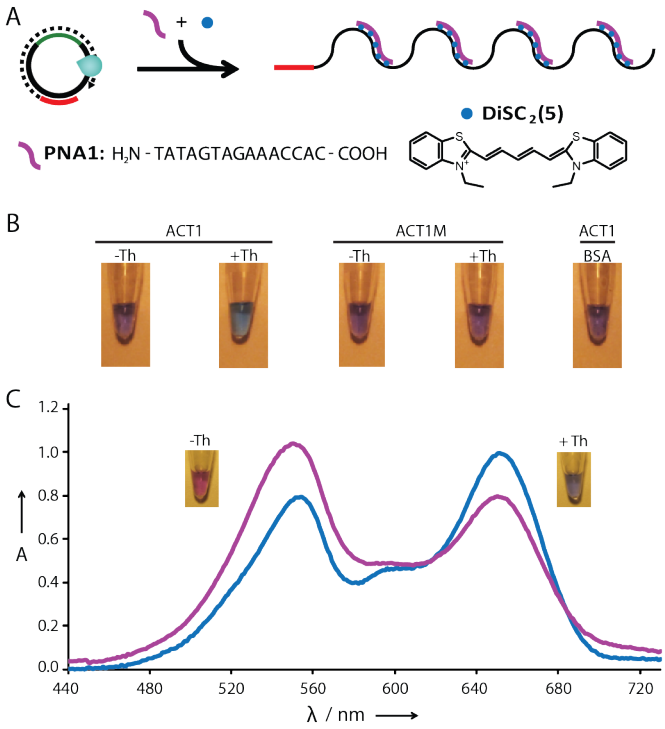

Figure 4-4. Biosensing based on RCA arrest. A) Schematic for colorimetric detection of RCA product using peptide nucleic acid (PNA) and DiSC2(5). B) Photographs of various RCA reaction mixtures after the addition of PNA and DiSC2(5); Th: thrombin. C) Absorption spectra of the RCA reactions of ACT1 in the absence (purple) and presence (blue) of thrombin.

Finally, we investigated the feasibility of performing quantitative analysis of protein targets using the above colorimetric detection method. For this reason, we obtained the absorption spectra of the sensing reaction mixtures, which are provided in Figure 4-4C. In the presence of thrombin, the sensing mixture had the highest absorption peak at 650 nm and the second highest peak at 550 nm. In the absence of thrombin, the magnitude of both peaks registered significant changes: A550 became more prominent than A650. Based on this observation, we examined the A650/A550 ratio when the concentration of thrombin was varied between 0–2000 nm (Figure 4-5A). A linear

empirical correlation is observed when A650/A550 is plotted as a function of the thrombin concentration on a logarithmic scale (Figure 4-5B). The data analysis establishes a detection limit of 15 nm for thrombin (3s of blank). These results suggest that the colorimetric detection method can be used as a quantitative method to measure the concentration of the protein target.

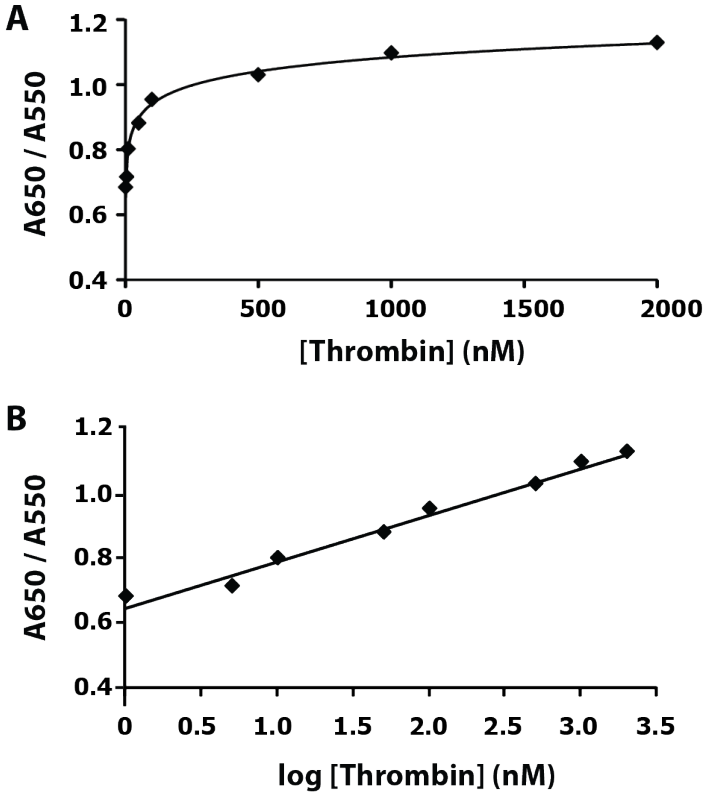

Figure 4-5. Quantitative analysis of thrombin. Colorimetric assay was carried out at the following concentrations of thrombin: 0, 10, 25, 50, 100, 250, 500, 1000 and 2000 nM. The absorption spectrum was then recorded for each reaction, from which A650/A550 (ratio of absorbance at 650 nm and 550 nm) was calculated and plotted against the concentration of thrombin in either normal scale (A) or logarithmic scale (B).

In summary, we have made a novel observation that the binding of a protein target to an aptamer in a circular DNA template can arrest RCA reactions by φ29DNAP. This

observation was demonstrated twice with different protein–aptamer pairs. Our findings indicate that protein-binding aptamers can form highly stable complexes with their targets in solution, consistent with results from many structural analyses showing that aptamers form very defined tertiary structures with their targets.[33,34,36] Both the thrombin and PDGF aptamers exhibit a K_d of approximately 25 and 0.1 nM, respectively. Therefore, the observation of the complete arrest of RCA at saturated target concentration illustrates that both of the tested aptamers appear to fold uniformly into functional (ligand-binding) structures (i.e., these aptamers do not appear to produce misfolded or alternative structures) under the tested conditions. Thus, the RCA arrest can be used as a strategy to examine the folding ability of such aptamers or to search for improved aptamers with uniform folding characteristics.

We have also shown that the arrest of RCA by aptamer–target interactions can be formulated into a colorimetric assay for the detection of the target of the aptamer. The translation of RCA arrest into a simple and convenient assay continues to showcase the versatility of using aptamers as molecular recognition elements for biosensing applications.

Control of the accessibility to DNA by polymerases is a common mechanism used by both eukaryotic and prokaryotic cells as a way to regulate gene expression. For example, in eukaryotic cells, histones bind and organise DNA into compact structures making DNA inaccessible to RNA polymerases;[40,41] post-translational modifications of histones alter their interaction with DNA, freeing it for RNA transcription.[42,43] In

prokaryotic cells, the transcription of many metabolic enzymes is controlled by repressor proteins that bind DNA tightly and prevent its access by RNA polymerases until the metabolic enzymes are in demand.[44-46] In this study, we have shown that the accessibility of φ29DNAP to a circular template can be controlled simply by the incorporation of a protein-binding aptameric domain into the circular template. We hope this finding can lead to the development of more advanced artificial systems that can accurately mimic the more intricate biological mechanisms that regulate the accessibility of DNA.

Finally, we are tempted to speculate that the inability of φ29DNAP to read through aptamer–target complexes in a circular aptameric template might simply reflect the fact that DNA polymerases have never had an opportunity to evolve a coping mechanism to access the DNA sequence in such settings, given that DNA aptamers are man-made structures and are not known to exist in nature.

4.3 Materials and Method

4.3.1 Enzymes, chemicals, and other materials

DNA oligonucleotides were prepared by automated DNA synthesis using standard phosphoramidite chemistry (Integrated DNA Technologies, Coralville, IA) and were purified by 10% denaturing polyacrylamide gel electrophoresis (dPAGE). Peptide nucleic acid (PNA) was purchased from BioSynthesis Inc (Lewisville, TX) and used without

further purification. T4 DNA ligase, φ29 DNA polymerase, T4 polynucleotide kinase (PNK), TaqI and BSA (bovine serum albumin) were purchased from MBI Fermentas (Burlington, ON, Canada). [α-^{32}P]-dGTP was acquired from Perkin Elmer (Woodbridge, ON, Canada). Human thrombin was obtained from Haematologic Technologies Inc (Essex Jct., VT). Recombinant Human PDGF was purchased from R&D Systems (Minneapolis, MN). Water used in this work was double deionized. The autoradiogram and fluorescent images of gels were obtained using Typhoon 9200 variable mode imager (GE healthcare) and analyzed using Image Quant software (Molecular Dynamics). All other materials were purchased from Sigma (Oakville, ON, Canada) and used without further purification.

4.3.2 Preparation of DNA circles

DNA circles were prepared from 5′-phosphorylated linear DNA oligonucleotides through template-assisted ligation with T4 DNA ligase. Each linear DNA oligonucleotide was phosphorylated as follows: a reaction mixture (50 μL) was made to contain 1 nM linear oligonucleotide, 0.2 unit/μL PNK, 1× PNK buffer A (50 mM Tris-HCl, pH7.6 at 25°C, 10 mM MgCl2, 5 mM DTT, 0.1 mM spermidine), and 4 mM ATP. The mixture was incubated at 37 °C for 30 min, followed by heating at 90°C for 5 min. The circularization reaction was conducted in a volume of 400 μL, produced by adding 306.3 μL of H_2O and 2.2 μL of a DNA template (500 μM) to the phosphorylation reaction mixture above. After heating at 90°C for 2 min and cooling down at room temperature

(RT) for 10 min, 40 μL of 10× T4 DNA ligase buffer (400 mM Tris-HCl, 100 mM MgCl2, 100 mM DTT, 5 mM ATP, pH7.8 at 25°C) and 1.5 μL of T4 DNA ligase (10 u/μL) were then added. This mixture was incubated at RT for 1.5 h. The DNA circle were then purified by dPAGE and stored at -20°C until use.

4.3.3 RCA reaction

Each RCA reaction was conducted in a volume of 50 μL made from 1 μL of aptameric circular template (ACT; 1 μM), 36 μL of H_2O, 5 μL of 10× RCA buffer (330 mM Tris acetate, pH 7.9 at 37°C, 100 mM magnesium acetate, 660 mM potassium acetate, 1% (v/v) Tween 20, 10 mM DTT, provided by MBI Fermentas) and 1 μL of thrombin (100 μM) or PDGF (20 μM). Following incubation at RT for 15 min, 1 μL of primer (1 μM), 5 μL of dNTPs (5 mM for each of dATP, dCTP, dGTP and dTTP; the final concentration of each dNTP was 500 μM), and 1 μL of φ29 DNA polymerase (3 U/μL) was added to each sample. The reaction mixture was incubated at 30°C for 30 min, and then heated at 90°C for 2 min to stop the reaction. This reaction mixture was used either for the TaqI/PAGE analysis or for colorimetric detection assay to be described below.

4.3.4 Analysis of RCA products by Taq1/PAGE analysis

To the RCA reaction mixture above, 1 μL of TaqI template (500 μM), TT1 (5′TATATCGACTGT3′ for anti-thrombin aptamer) or TT2 (5′ACTATCGACTCA3′ for anti-PDGF aptamer) was introduced. The mixture was heated at 90°C for 2 min and cooled at RT for 5 min, followed by the addition of 6 μL of 10× Tango buffer (100 mM Tris-HCl, pH 8.0, 50 mM MgCl2, 1 M NaCl, 1 mg/mL BSA) and 1 μL of TaqI (10 U/μL). The reaction mixture was then incubated at 65°C for 15 min before the addition of 60 μL of 2× denaturing loading gel buffer. A 10 μL aliquot was then subjected to PAGE analysis.

4.3.5 Colorimetric assay

To the RCA reaction mixture (50 μL), 2 μL of PNA1 (100 μM) was added. Each sample was heated to 90°C for 90 s and cooled at RT for 10 min. Thereafter, 1 μL of $DiSC_2(5)$ (1 mM stock, dissolved in methanol) was added and the mixture was heated at 90°C for 2 min and allowed to cool to RT. The color images were captured during the cooling process (at ~90 s) by digital camera (Panasonic, LUMIX). The absorbance was taken with Cary 300UV/Vis spectrophotometer. For UV measurement, each sample was diluted to 200 μL with the water before heating and cooling.

4.3.6 Quantitative detection of thrombin

This was carried out similarly as above for the colorimetric assay except that a series of RCA reactions were carried out when the concentration of thrombin was varied between 0-2000 nM.

4.4 References Cited

1. Fire A, Xu SQ (1995) Rolling replication of short DNA circles. Proc Natl Acad Sci U S A 92: 4641-4645.
2. Liu D, Daubendiek SL, Zillman MA, Ryan K, Kool ET (1996) Rolling circle DNA synthesis: small circular oligonucleotides as efficient templates for DNA polymerases. J Am Chem Soc 118: 1587-1594.
3. Larsson C, Koch J, Nygren A, Janssen G, Raap AK, et al. (2004) In situ genotyping individual DNA molecules by target-primed rolling-circle amplification of padlock probes. Nat Methods 1: 227-232.
4. Lizardi PM, Huang X, Zhu Z, Bray-Ward P, Thomas DC, et al. (1998) Mutation detection and single-molecule counting using isothermal rolling-circle amplification. Nat Genet 19: 225-232.
5. Weizmann Y, Beissenhirtz MK, Cheglakov Z, Nowarski R, Kotler M, et al. (2006) A virus spotlighted by an autonomous DNA machine. Angew Chem Int Ed 45: 7384-7388.
6. Di Giusto DA, Wlassoff WA, Gooding JJ, Messerle BA, King GC (2005) Proximity extension of circular DNA aptamers with real-time protein detection. Nucleic Acids Res 33: e64.
7. Yang L, Fung CW, Cho EJ, Ellington AD (2007) Real-time rolling circle amplification for protein detection. Anal Chem 79: 3320-3329.

8. Zhou L, Ou LJ, Chu X, Shen GL, Yu RQ (2007) Aptamer-based rolling circle amplification: a platform for electrochemical detection of protein. Anal Chem 79: 7492-7500.
9. Ali MM, Li Y (2009) Colorimetric sensing by using allosteric-DNAzyme-coupled rolling circle amplification and a peptide nucleic acid-organic dye probe. Angew Chem Int Ed 48: 3512-3515.
10. Cheglakov Z, Weizmann Y, Basnar B, Willner I (2007) Diagnosing viruses by the rolling circle amplified synthesis of DNAzymes. Org Biomol Chem 5: 223-225.
11. Cho EJ, Yang L, Levy M, Ellington AD (2005) Using a deoxyribozyme ligase and rolling circle amplification to detect a non-nucleic acid analyte, ATP. J Am Chem Soc 127: 2022-2023.
12. Tang L, Liu Y, Ali MM, Kang DK, Zhao W, et al. (2012) Colorimetric and ultrasensitive bioassay based on a dual-amplification system using aptamer and DNAzyme. Anal Chem 84: 4711-4717.
13. Tian Y, He Y, Mao C (2006) Cascade signal amplification for DNA detection. Chembiochem 7: 1862-1864.
14. Zhao W, Ali MM, Brook MA, Li Y (2008) Rolling circle amplification: applications in nanotechnology and biodetection with functional nucleic acids. Angew Chem Int Ed 47: 6330-6337.
15. Blanco L, Bernad A, Lazaro JM, Martin G, Garmendia C, et al. (1989) Highly efficient DNA synthesis by the phage ϕ29 DNA polymerase. Symmetrical mode of DNA replication. J Biol Chem 264: 8935-8940.
16. Canceill D, Viguera E, Ehrlich SD (1999) Replication slippage of different DNA polymerases is inversely related to their strand displacement efficiency. J Biol Chem 274: 27481-27490.
17. Berman AJ, Kamtekar S, Goodman JL, Lazaro JM, de VM, et al. (2007) Structures of phi29 DNA polymerase complexed with substrate: the mechanism of translocation in B-family polymerases. EMBO J 26: 3494-3505.

18. Kamtekar S, Berman AJ, Wang J, Lazaro JM, de VM, et al. (2004) Insights into strand displacement and processivity from the crystal structure of the protein-primed DNA polymerase of bacteriophage φ29. Mol Cell 16: 609-618.
19. Kamtekar S, Berman AJ, Wang J, Lazaro JM, de VM, et al. (2006) The φ29 DNA polymerase:protein-primer structure suggests a model for the initiation to elongation transition. EMBO J 25: 1335-1343.
20. Morin JA, Cao FJ, Lazaro JM, Arias-Gonzalez JR, Valpuesta JM, et al. (2012) Active DNA unwinding dynamics during processive DNA replication. Proc Natl Acad Sci U S A 109: 8115-8120.
21. Rodriguez I, Lazaro JM, Blanco L, Kamtekar S, Berman AJ, et al. (2005) A specific subdomain in φ29 DNA polymerase confers both processivity and strand-displacement capacity. Proc Natl Acad Sci U S A 102: 6407-6412.
22. Soengas MS, Esteban JA, Lazaro JM, Bernad A, Blasco MA, et al. (1992) Site-directed mutagenesis at the Exo III motif of ϕ29 DNA polymerase; overlapping structural domains for the 3'-5' exonuclease and strand-displacement activities. EMBO J 11: 4227-4237.
23. Lin C, Wang X, Liu Y, Seeman NC, Yan H (2007) Rolling circle enzymatic replication of a complex multi-crossover DNA nanostructure. J Am Chem Soc 129: 14475-14481.
24. Ellington AD, Szostak JW (1990) In vitro selection of RNA molecules that bind specific ligands. Nature 346: 818-822.
25. Tuerk C, Gold L (1990) Systematic evolution of ligands by exponential enrichment: RNA ligands to bacteriophage T4 DNA polymerase. Science 249: 505-510.
26. Bock LC, Griffin LC, Latham JA, Vermaas EH, Toole JJ (1992) Selection of single-stranded-DNA molecules that bind and inhibit human thrombin. Nature 355: 564-566.
27. Famulok M, Mayer G (2011) Aptamer modules as sensors and detectors. Acc Chem Res 44: 1349-1358.

28. Green LS, Jellinek D, Jenison R, Ostman A, Heldin CH, et al. (1996) Inhibitory DNA ligands to platelet-derived growth factor B-chain. Biochemistry 35: 14413-14424.
29. Jenison RD, Gill SC, Pardi A, Polisky B (1994) High-resolution molecular discrimination by RNA. Science 263: 1425-1429.
30. Nimjee SM, Rusconi CP, Sullenger BA (2005) Aptamers: an emerging class of therapeutics. Annu Rev Med 56: 555-583.
31. Osborne SE, Matsumura I, Ellington AD (1997) Aptamers as therapeutic and diagnostic reagents: problems and prospects. Curr Opin Chem Biol 1: 5-9.
32. Wilson DS, Szostak JW (1999) In vitro selection of functional nucleic acids. Annu Rev Biochem 68: 611-647.
33. Feigon J, Dieckmann T, Smith FW (1996) Aptamer structures from A to zeta. Chem Biol 3: 611-617.
34. Hermann T, Patel DJ (2000) Adaptive recognition by nucleic acid aptamers. Science 287: 820-825.
35. Montange RK, Batey RT (2008) Riboswitches: emerging themes in RNA structure and function. Annu Rev Biophys 37: 117-133.
36. Patel DJ (1997) Structural analysis of nucleic acid aptamers. Curr Opin Chem Biol 1: 32-46.
37. Dilek I, Madrid M, Singh R, Urrea CP, Armitage BA (2005) Effect of PNA backbone modifications on cyanine dye binding to PNA-DNA duplexes investigated by optical spectroscopy and molecular dynamics simulations. J Am Chem Soc 127: 3339-3345.
38. Komiyama M, Ye S, Liang X, Yamamoto Y, Tomita T, et al. (2003) PNA for one-base differentiating protection of DNA from nuclease and its use for SNPs detection. J Am Chem Soc 125: 3758-3762.
39. Wilhelmsson LM, Norden B, Mukherjee K, Dulay MT, Zare RN (2002) Genetic screening using the colour change of a PNA-DNA hybrid-binding cyanine dye. Nucleic Acids Res 30: E3.

40. Luger K, Mader AW, Richmond RK, Sargent DF, Richmond TJ (1997) Crystal structure of the nucleosome core particle at 2.8 A resolution. Nature 389: 251-260.
41. Rhodes D (1997) Chromatin structure. The nucleosome core all wrapped up. Nature 389: 231, 233.
42. Jenuwein T, Allis CD (2001) Translating the histone code. Science 293: 1074-1080.
43. Strahl BD, Allis CD (2000) The language of covalent histone modifications. Nature 403: 41-45.
44. Gilbert W, Muller-Hill B (1966) Isolation of the lac repressor. Proc Natl Acad Sci U S A 56: 1891-1898.
45. Jacob F, Monod J (1961) Genetic regulatory mechanisms in the synthesis of proteins. J Mol Biol 3: 318-356.
46. Schleif R (1992) DNA looping. Annu Rev Biochem 61: 199-223.

Chapter 5

Conclusion and Outlook

In this thesis, I have examined the potential of DNAzymes and DNA aptamers for the development of biosensors. At the beginning of my thesis study, I set up a goal of developing innovative approaches that can uniquely take advantage of DNAzymes and aptamers in biosensor engineering. Along the way I become more and more appreciative of DNA as a functional polymer and the versatility of DNA aptamers and DNAzymes for biosensor development.

In Chapter 2, I devised a novel method that can translate the activity of RNA-cleaving DNAzyme into a colourimetric signal through the use of urease. The approach links the RNA-cleaving activity to the release of urease, which mediates a change in pH that can be conveniently monitored using conventional pH papers or pH-sensitive dyes. Many colorimetric sensors that use RNA-cleaving DNAzymes often rely on gold nanoparticles (AuNPs) for generating a color change. The new method that we have developed has several distinct advantages. First, our method has a built-in amplification mechanism. Each cleavage event releases a single urease protein enzyme that can then hydrolyze many urea molecules. This amplified process results in greater sensitivity towards low concentrations of targets. Second, the urease sensing system can function effectively in complex matrices that may not be compatible with AuNPs. Real-life samples such as juices and milk contain an abundance of proteins, salts, cofactors, and

other small molecules that can disrupt the function of AuNPs. Therefore, our method is more attractive for engineering future biosensors to detect targets within complex matrices. Lastly, the modular nature of the urease system allows easy modification of each component within the system. The current design uses an *E. coli*-responsive DNAzyme; this 'module' could be replaced with any other RNA-cleaving DNAzyme (or aptazyme) that is responsive to a different analyte.

Although we have demonstrated the functionality of the coupling urease to an RNA-cleaving DNAzyme, there are still areas in which the system could be improved. Currently, there is one urease enzyme per DNA sequence immobilized on the magnetic bead. By extending the substrate sequence we should be able to hybridize more than one urease enzyme per DNA sequence, thus, effectively enhancing the sensitivity of the system. Another component for optimization is the streptavidin-coated magnetic beads. The use of magnetic beads eliminates the use of electrical equipment; however, this approach has also increased the cost. Alternative solid supports or methods that are more cost-effective should be investigated in the future.

Overall, relying on a colorimetric approach simplifies the detection process since the presence or absence of an analyte is interpreted using the naked eye. This removes the burden of using expensive equipment and technical procedures that only a trained worker can operate. By coupling the functionality of DNAzymes and protein enzymes to a color change through pH indicators, this platform can be used to create an equipment-free field test kit for the detection of a wide range of targets.

In Chapter 3, I examined the possibility of isolating a highly efficient L-RNA-cleaving DNAzyme using in vitro selection. D-RNA cleaving DNAzymes have been used in many biosensing studies to detect a wide range of targets. These investigations have illustrated the usefulness of these synthetic DNA-based enzymes as analytical tools. However, biosensors based on DNAzymes that cleave natural RNA (D-RNA) substrates may generate false-positive signals due to the widespread existence of RNases in biological and environmental samples. Therefore, I was interested in solving this issue by developing a DNAzyme that can cleave L-RNA - the unnatural isomer of D-RNA, which is well known to resist RNase degradation. Although an L-RNA-cleaving DNAzyme was previously isolated by the Joyce group, its catalytic efficiency is rather poor, making it less useful for creating biosensors. The in vitro selection experiment that I performed under more stringent conditions has led to the isolation of several highly efficient L-RNA-cleaving DNAzymes (LRD). I have further converted one of the LRDs into an ATP-responsive biosensor that was capable of functioning in serum.

A very important quality that all biosensors should have is high stability. A sensor may be sensitive and accurate, but if it has a poor shelf-life or falsely identifies the presence of the target due to poor stability, its usefulness becomes severely limited. This can be the case for sensors relying on D-RNA-cleaving DNAzymes. Since most biological samples are contaminated with RNases, biosensors built with D-RNA-cleaving DNAzymes are prone to false positive signals. The isolation of efficient L-RNA-cleaving DNAzymes that are resistant to RNase degradation represents a significant step forward towards developing practically useful RNA-cleaving DNAzyme biosensors. It is worth

noting that sequencing the DNA pool at the 10th cycle reveals that there are thousands of different DNA sequences capable of cleaving L-RNA. This suggests that there are abundant DNAzyme sequences for L-RNA cleavage. The next milestone for this project is to expand our approach to isolate L- RNA-cleaving aptazymes for important biological targets including disease biomarkers. The ability to successfully create highly stable biosensors for diagnosing medically relevant diseases will be a hot research topic within the biosensor field.

In Chapter 4, I developed a unique bioassay that links DNA aptamers to rolling circle amplification mediated by phi29 DNA polymerase. Phi29 DNA polymerase has high processivity and strand displacement capability. It is also known to break secondary structures during polymerization. Surprisingly, we have found that incorporating a protein-binding DNA aptamer in the circular DNA template can result in the arrest of RCA in the presence of the target for the aptamer. Although the precise mechanism for this arrest is yet to be investigated, we speculate that the aptamer and target form a highly stable structure that cannot be "taken down" by the polymerase. It is also likely that the aptamer-ligand complex is completely foreign to the DNA polymerase. Considering that DNA aptamers are synthetic structures not known in Nature, it is reasonable to suggest that phi29 DNA polymerase has yet to evolve a mechanism to disrupt DNA aptamer structures. Furthermore, I was able to show that the novel observation above can be utilized for the development of a bioassay for the detection of the target of the aptamer, based on the fact that the level of RCA arrest (and thus the amount of RCA product) is dependent on the concentration of the target.

The arrest of protein enzyme activity using aptamers can be conceivably extended beyond phi29 DNA polymerase and RCA as the same concept can be applied for other nucleic acid modifying enzymes, such as nucleases and ligases. Several FNA-based biosensor methods incorporate auxiliary protein enzymes and exploration of DNA aptamers to regulate the activity of these enzymes could further expand the utility of these biosensors.

Although there have been substantial progress made in the last 20 years, the field of FNA-based biosensors are still in its infancy. The projects within this thesis have taken some unconventional approaches with hopes of best utilizing functional nucleic acids for bioanalytical applications. I hope my work serves as a stepping stone towards developing highly versatile and practical FNA-based biosensors that can be used to monitor our health, safeguard our food and water, and protect our environment.